FOURTH INTERNATIONAL WORKSHOP ON FRP BARS FOR CONCRETE STRUCTURES

"Advances in concrete reinforcement"

August 8-9, 2024 - Toronto, Ontario

Development and Lap-Splice Lengths for a New Generation GFRP Bars in Flexural Concrete Bridge and Structural Members

Seyed Arman Hosseini

PhD Candidate at University of Sherbrooke

SPONSORED BY:

PULTRALL · V-ROD · FIBERGLASS Innovations · ALTAIR · MST BAR MAXIMUM STRENGTH GFRP · SFTec · ACMA American Composites Manufacturers Association FRP Rebar Manufacturers Council

Université de Sherbrooke · NSERC CRSNG · University of Miami · Center for Integration of Composites into Infrastructure · FDOT

< Introduction >

- **Steel bar corrosion in reinforced concrete is a significant problem, leading to structural failure and costly repairs.**
- **GFRP bars is a promising solution with exceptional corrosion resistance.**
- **Greener solution than steel bars, offers high stiffness-to-weight ratio, promoting sustainability and durability.**
- **GFRP bars have lower modulus of elasticity and weaker bond strength than steel bars.**
- **Lap splicing is the most common and economic method to connect bars in flexural concrete bridge and structural members.**
- **Staggering of lap splices and its effect on splice strength is not well studied.**

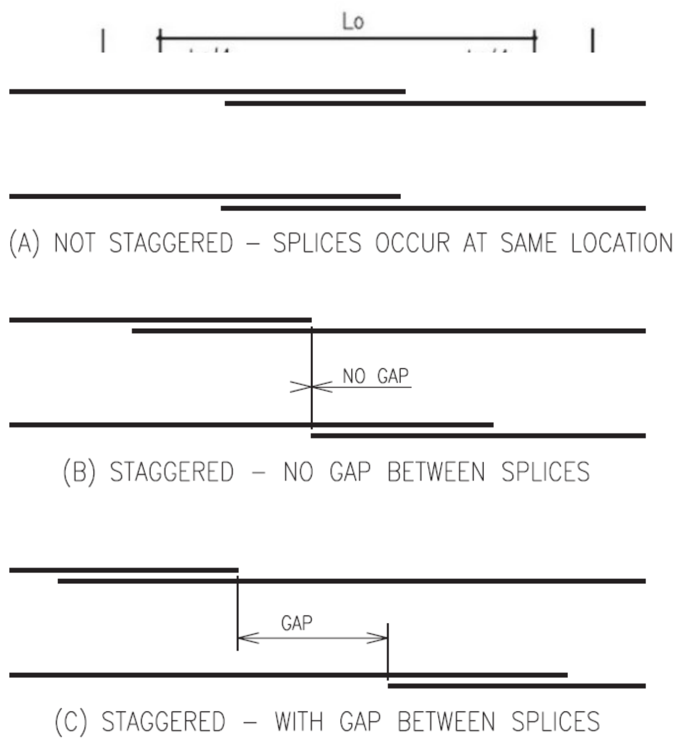

< Problem Statement >

- Need for understanding bond strength of GFRP bars which governs serviceability, cracking behavior, and structural integrity.
- Current design standards rely on test results using old generation GFRP bars, and there is a lack of recent experimental studies on available GFRP bars in the market.
- Study aims to update experimental data on bond strength and minimum splice length of new generation high-modulus GFRP bars.

Ultimate Tensile Strength > 1400 Mpa

Modulus of Elasticity > 65 GPa

< Research Objectives >

- Acquire **experimental data** on bond strength and minimum splice length of high-modulus GFRP bars.
- Investigate the effect of varying **embedment lengths** and **staggering conditions** on bond strength through large-scale splice beam tests.
- Assess load-deflection relationship, failure mode, crack width of spliced beams, and bond strength of lap spliced bars.
- Evaluate current **North American design codes** and propose a new equation for the minimum development and splice length of GFRP bars.

< Experimental Program >

- **Nine (9) large-scale splice beams, with rectangular cross-section: 300 × 450 mm, and length: 5200 mm.**
- **Designed to prevent flexural failure before lap splice failure (minimum splice length to reach flexural capacity: $103d_b$).**
- **Splice lengths: 28, 38, and 45 times the bar diameter.**
- **Three different staggering conditions for each splice length: non-, partial, and full staggered.**

Full staggered

#	Specimen reference	Provided splice length (mm)	Recommended development length by ACI 440.11-22 (mm)	f_{fe} (Mpa)	f_{FRP} (Mpa)
1	L38-S100-D0	610	1577	508	1031
2	L38-S50-D1.0	610	1577	508	1031
3	L38-S50-D1.3	610	1577	508	1031
4	L28-S100-D0	450	1577	422	1031
5	L28-S50-D1.0	450	1577	422	1031
6	L28-S50-D1.3	450	1577	422	1031
7	L45-S100-D0	720	1577	568	1031
8	L45-S50-D1.0	720	1577	568	1031
9	L45-S50-D1.3	720	1577	568	1031

$$f_{fe,\ ACI\ 440.11-22} = \frac{0.083\sqrt{f_c'}}{\alpha}\left(13.6\frac{l_e}{d_b} + \frac{c}{d_b}\frac{l_e}{d_b} + 340\right)$$

$<$

f_{FRP} **at flexural failure with adequate splice length**

(9) L45-S50-D1.3

< Material Properties>

- **Beams cast with ready-mix concrete (max aggregate size 16 mm) and moist cured for 7 days.**
- **Measured compressive strengths (at testing day): 39 to 42 MPa.**
- **GFRP reinforcing bars: No.5 sand-coated grade III, with nominal 15.9 mm diameter, 200 mm² area.**
- **Average tensile strength: 1428 MPa, modulus of elasticity: 65.4 GPa.**
- **GFRP M13 (No.4) stirrups used as transverse reinforcement.**

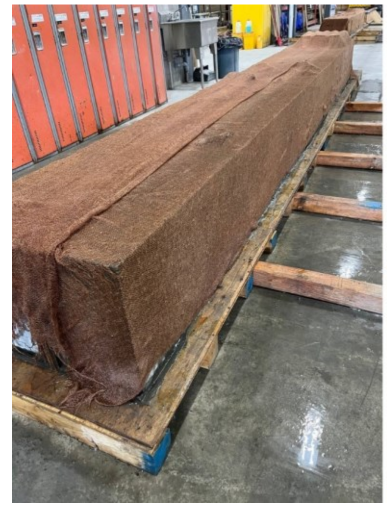

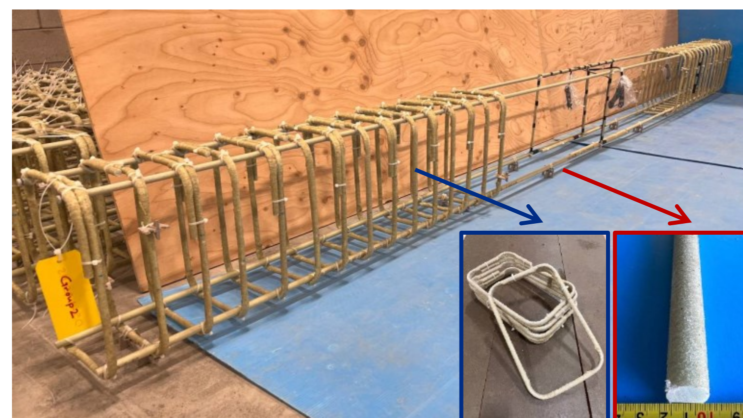

< Instrumentation and Test Setup >

- Four-point bending test using 1000 kN MTS actuator (2,500 mm constant-moment span).
- Load applied at 1.2 mm/min (displacement control) up to failure.
- Recorded mid-span deflection, crack width evolution and strain in bars and concrete using LVDTs and strain gauges (SGs).

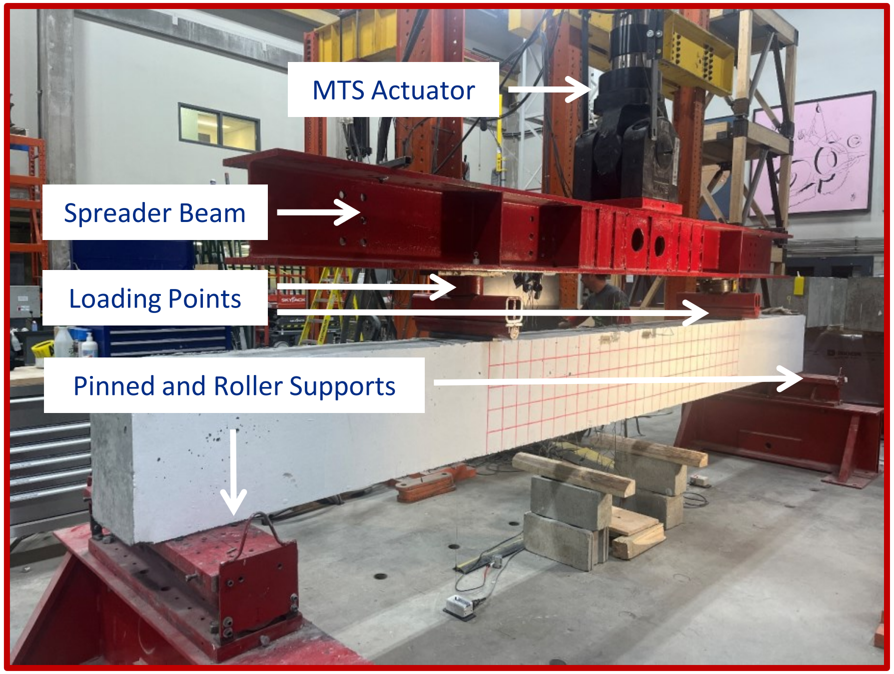

< Load-Deflection Behaviour>

- Load-deflection response: bilinear pattern – reduction in flexural stiffness (concrete cracking)
- Load-carrying capacity: slightly increased by 4% and 8% from beams with non-staggered to partial and full staggered splices.
- Increasing splice length: 36% increase led to 14% rise in splice capacity; 60% increase led to 28% rise (regardless of staggering condition).
- Full staggering of splices led to more ductile failure showing multi-stage failure of splices. (70% residual strength).

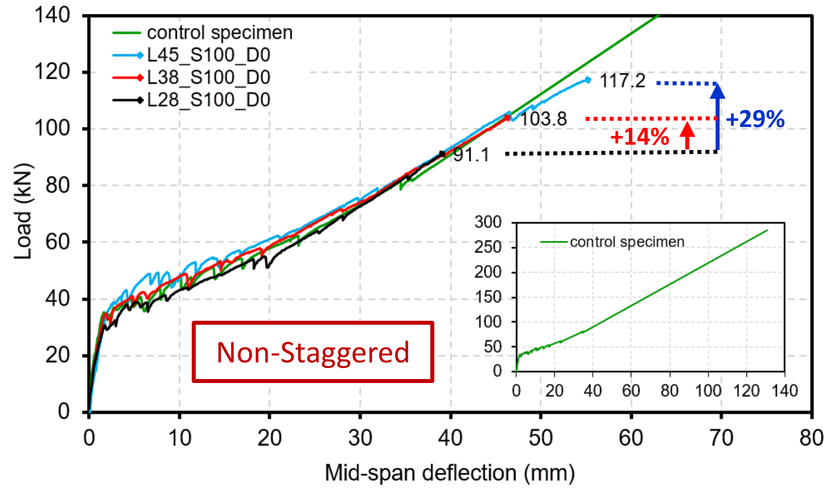

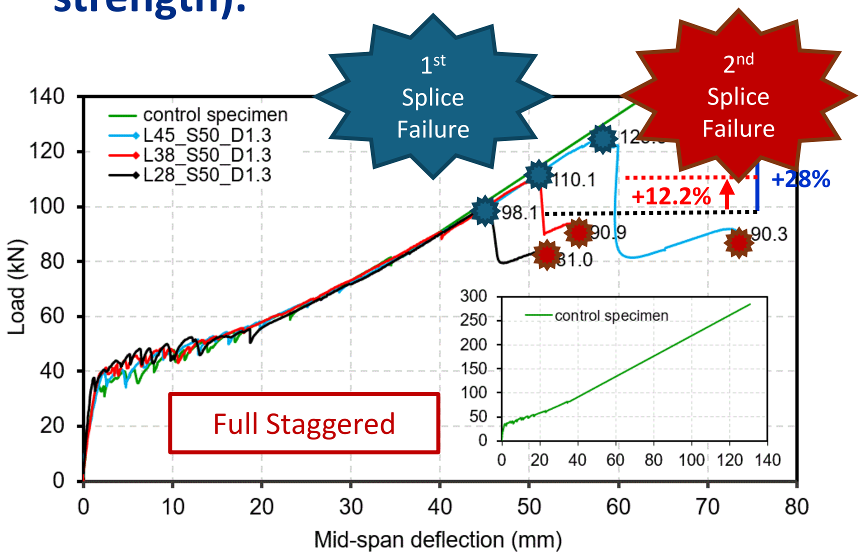

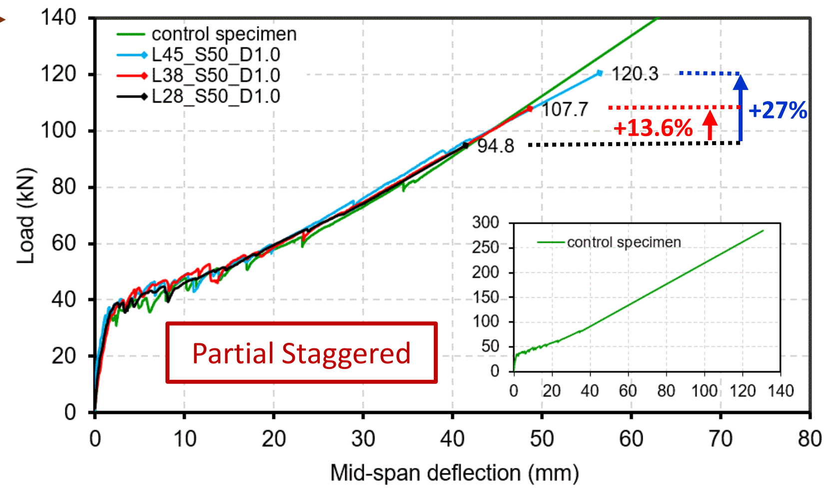

< Failure Modes>

- **Failure modes:**

Non-staggered >
brittle splitting failure + concrete cover spalling.

Partial staggered >
less brittle splice failure + splitting cracks + rebar slippage.

Full staggered >
multi-stage splice failure + splitting cracks + rebar slippage.

- **<u>Staggering</u> resulted in narrower flexural cracks, preventing crack accumulation at splice ends and reducing bar slippage.**

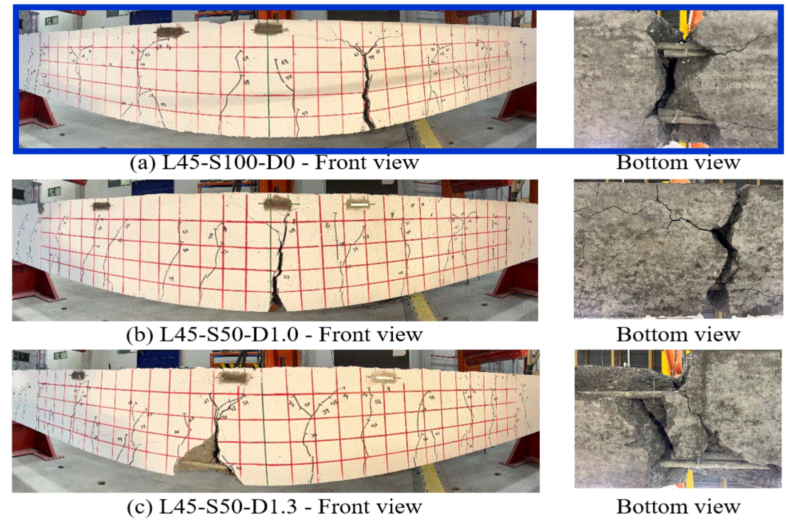

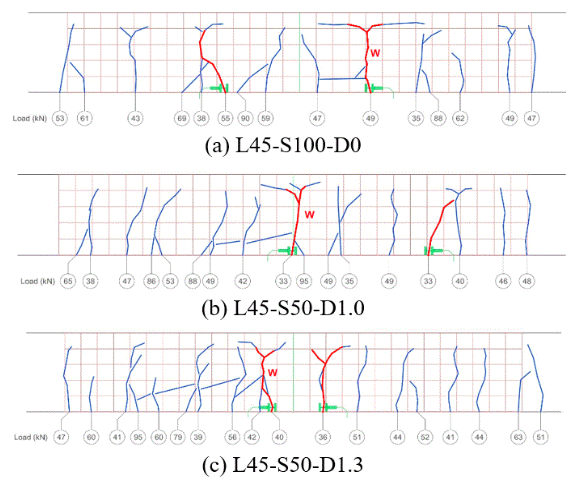

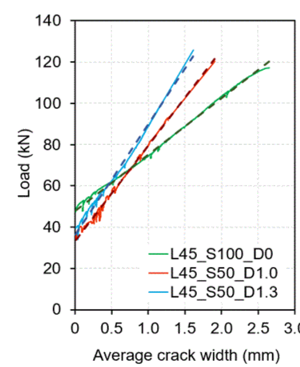

< Average Bond Strength>

- Nonlinear distribution of bond stress: Assuming uniform stress distribution to calculate average bond strength.
- Using strain values extracted from SGs instrumented on bars (at both ends of splice region): The average bond strength values are calculated.
- The experimental values are then compared and verified using moment-curvature analysis: showing less than 8% difference.

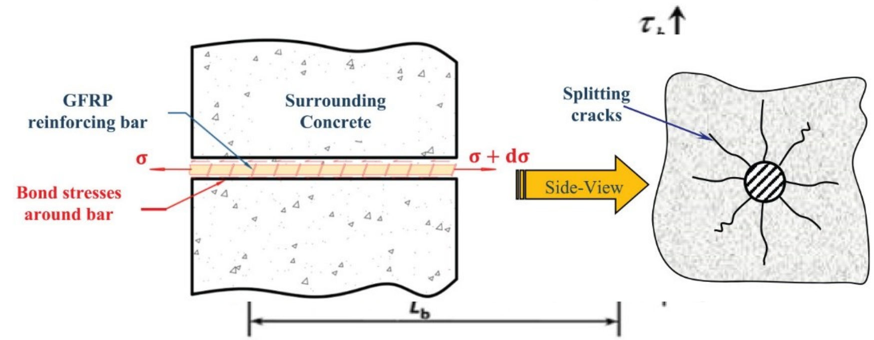

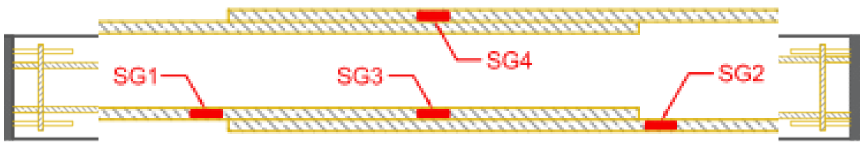

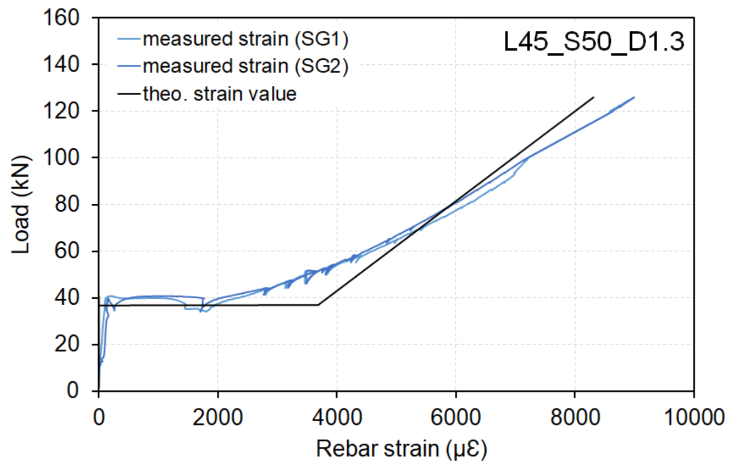

< Bond Strength Assessment >

- Increasing splice length: nonlinear increase in splice strength, decrease in bond strength.
- $28\,d_b$ to $38\,d_b$: 18% increase in splice strength, 15% decrease in bond strength.
- $28\,d_b$ to $45\,d_b$: 32% increase in splice strength, 18% decrease in bond strength.
- Partial and full staggering make the bond and splice strength increased by ONLY 4% and 8%, respectively.

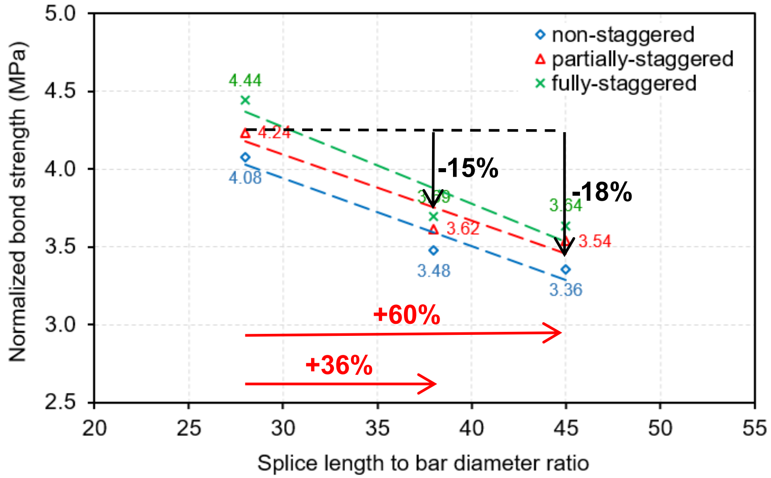

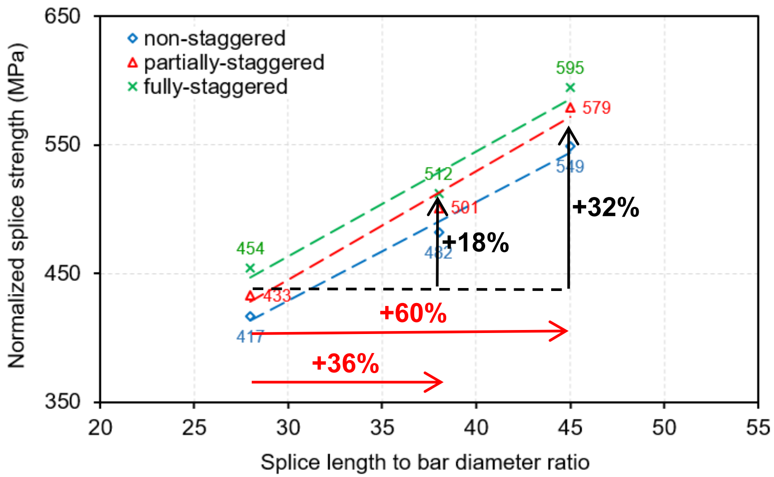

< Design Code Prediction >

- **Experimental bond strength values compared to design codes ($u_{test}/u_{prediction}$).**
- **Equation given by Wambeke and Shield (2006) overestimated the result: test-to-prediction of 0.88, 0.91, and 0.94 for non-, partial, and full staggered splices.**
- **ACI 440.11-22 more accurate code predictions: test-to-prediction of 1.03, 1.08, and 1.11 for non-, partial, and full staggered splices.**

$$l_d = 0.45 \frac{k_1}{k_4\left[d_{cs} + K_{tr}\frac{E_{frp}}{E_s}\right]} \times \frac{f_{fr}}{f_{cr}} \times A_b$$

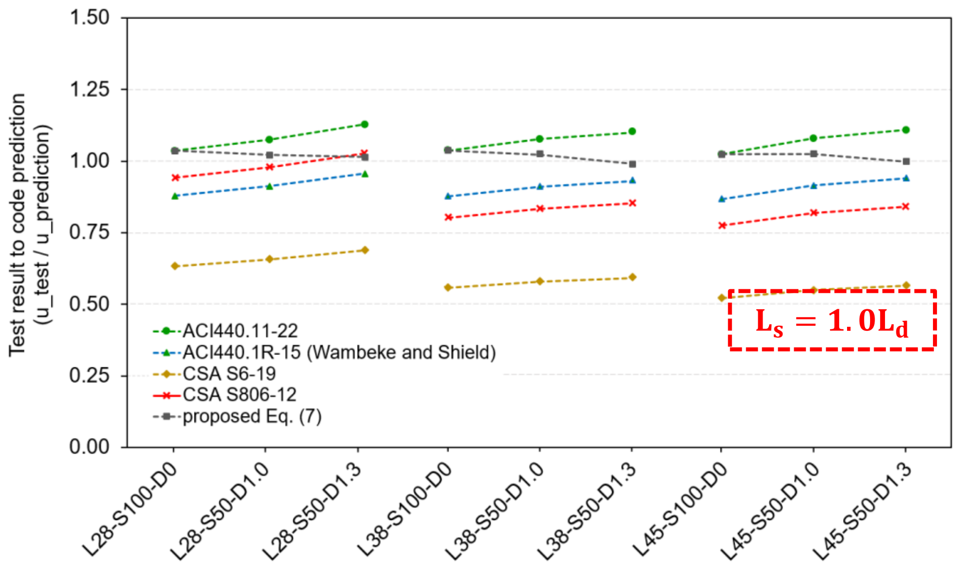

< Proposing New Equation >

- **Development length equation given by ACI440.11-22 give almost accurate prediction of bond strength assuming $L_s = 1.0L_d$ for non-staggered splices.**

- **Considering 1.3 multiplier to convert development to splice length $(L_s = 1.3L_d)$ for non-staggered splices is conservative.**

- **The equation needs to be modified to capture the effect of staggering condition on bond strength and minimum embedment length.**

$$\frac{u}{0.083\sqrt{f'_c}} = \frac{1}{k_1k_2}\left(3.4 + 0.25\frac{c}{d_b} + 85\frac{d_b}{l}\right)$$

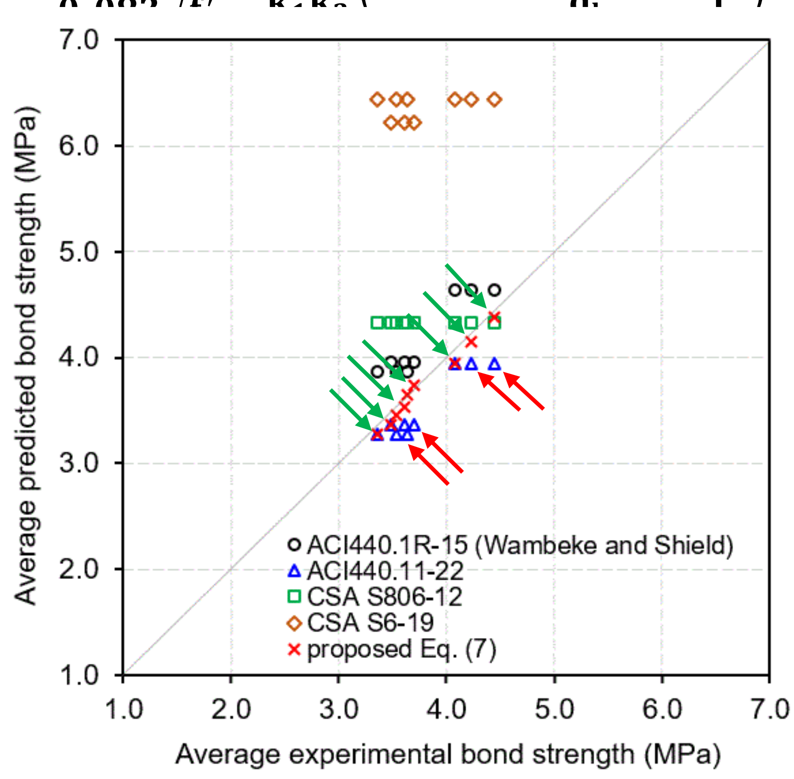

,

staggered splices.

< Conclusion >

- Staggering increases ultimate load carrying capacity (up to 8%) and ductility, with fully staggered setups maintaining post-failure strength (multi-stage failure of splices).
- Staggering reduces crack width and enhances bond and splice strength (up to 8%), especially with increased staggering distances.
- ACI 440.11-22 gives almost accurate predictions of bond strength values with minor underestimation (test-to-predict. of 1.07). While, CSA S806-12 and CSA S6-19 tend to overestimate the bond strength showing test-to-predict. of 0.88 and 0.6, respectively.
- Considering 1.3 multiplier to convert development length to splice length $(\mathbf{L_s = 1.3L_d})$ for non-staggered splices is conservative.
- New equations of bond strength and lap-splice length for new generation GFRP bars: 30% less splice length (non-staggered) + provide modification factor for staggered splices.

< Acknowledgments >

- Tier-1 Canada Research Chair in Advanced FRP Composite Materials for Civil Structures.
- Industrial Research Chair in Innovative FRP Reinforcement for Concrete Structures.
- Natural Sciences and Engineering Research Council of Canada (NSERC).
- Mathematics of Information Technology and Complex Systems (MITACS).
- University of Sherbrooke, Department of Civil Engineering.

Seyed-Arman Hosseini, Ahmed Farghaly, Abolfazl Eslami, Brahim Benmokrane. Effect of staggering distances on the splice strength of new generation GFRP bars. 2024, *ACI Structural Journal* (Accepted: Awaiting Production Checklist).

Bond & Development Length of GFRP Bars: *Addressing Practical Design Gaps*

Amir Fam,

Professor & Vice Dean (Research)

President, International Institute for FRP in Construction (IIFC)

SMITH ENGINEERING
Queen's University

Queen's UNIVERSITY

Among current gaps …….

- The bundling effect

- Bond with UHPC

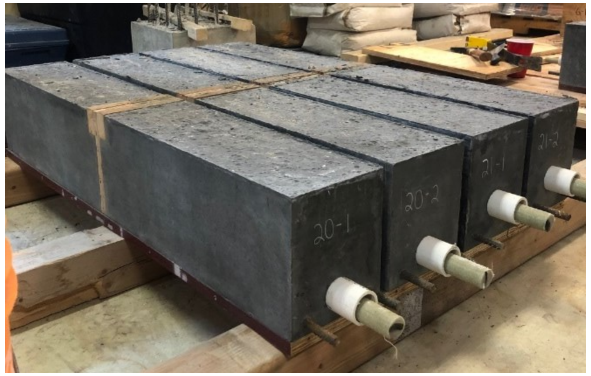

- Bond with Shotcrete

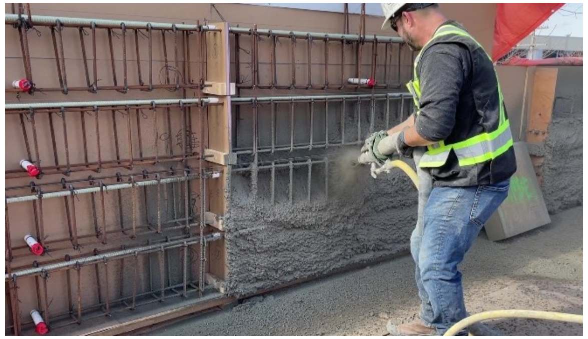

Bundling Effect

The gap

ACI CODE-440.11-22 does NOT have provisions for bundled GFRP bars for development length. Equation is for spaced bars only.

ACI CODE-318-19 uses 20% increase for 3 steel bars & 33% for 4 bars but zero reduction for 2 bars.

25.6.1.5 Development length for individual bars within a bundle, in tension or compression, shall be that of the individual bar, increased 20 percent for a three-bar bundle, and 33 percent for a four-bar bundle.

R25.6.1.5 An increased development length for individual bars is required when three or four bars are bundled together. The extra extension is needed because the grouping makes it more difficult to mobilize bond resistance from the core between the bars.

Background

- Wambeke and Shield (2006) → L_d equation in ACI CODE-440.11-22

Based on data from deformed GFRP bars (spiral wraps or helical lugs).
NO sand-coated bars.

$$L_{d,spaced} = \frac{\frac{f_{fr}}{0.083\sqrt{f'_c}} - 340}{13.6 + \frac{C}{d_b}} d_b$$

- Asadian et al. (2019) → Splices

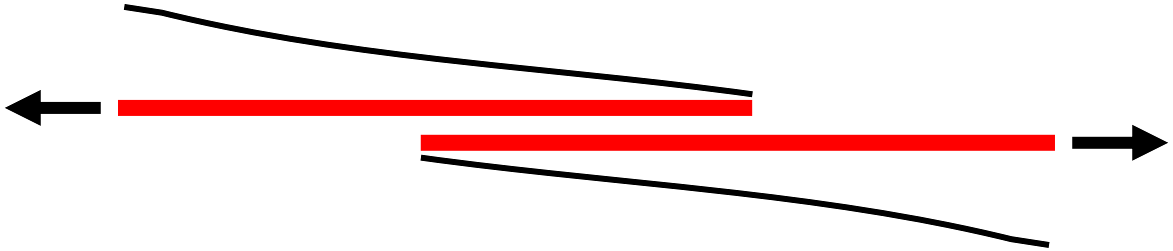

Different from

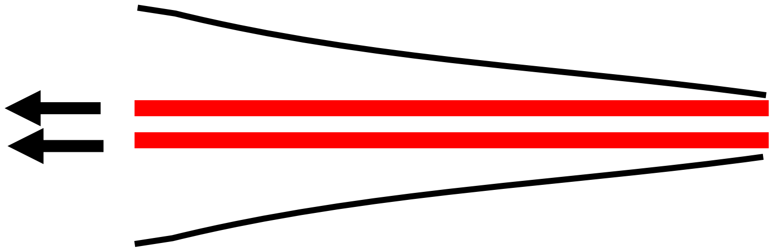

Test Matrix

2 bars → **2 s - 3** ← spaced, 300 mm embedment

bundled → **2 b - 3**

Specimen ID	No. of GFRP bars	Bar arrangement	Cover to center of reinf. (mm)	Embedment length (mm)	Cross-section dimensions (mm x mm)	Cross-section configuration	Span (mm)
3s-3	3	Spaced	49	300	320 x 300	Fig. 2(e)	918
3b-3	3	Bundled	54	300	125 x 300	Fig. 2(d)	918
2s-3	2	Spaced	49	300	215 x 300	Fig. 2(c)	918
2b-3	2	Bundled	49	300	125 x 300	Fig. 2(b)	918
3s-9	3	Spaced	49	900	320 x 300	Fig. 2(e)	1918
3b-9	3	Bundled	54	900	125 x 300	Fig. 2(d)	1918
2s-9	2	Spaced	49	900	215 x 300	Fig. 2(c)	1918
2b-9	2	Bundled	49	900	125 x 300	Fig. 2(b)	1918
3s-15	3	Spaced	49	1500	320 x 300	Fig. 2(e)	3018
3b-15	3	Bundled	54	1500	125 x 300	Fig. 2(d)	3018
2s-15	2	Spaced	49	1500	215 x 300	Fig. 2(c)	3018
2b-15	2	Bundled	49	1500	125 x 300	Fig. 2(b)	3018

17 - 87 d_b

Test Specimens

15M (#5)
17.3 mm d_b
1100 MPa
60 GPa
Sand-coated

f_c' = 30-34 MPa

Criteria:

Same clear cover for spaced & bundled

Used 1.5” cover = 40 mm (ACI440.11-22)

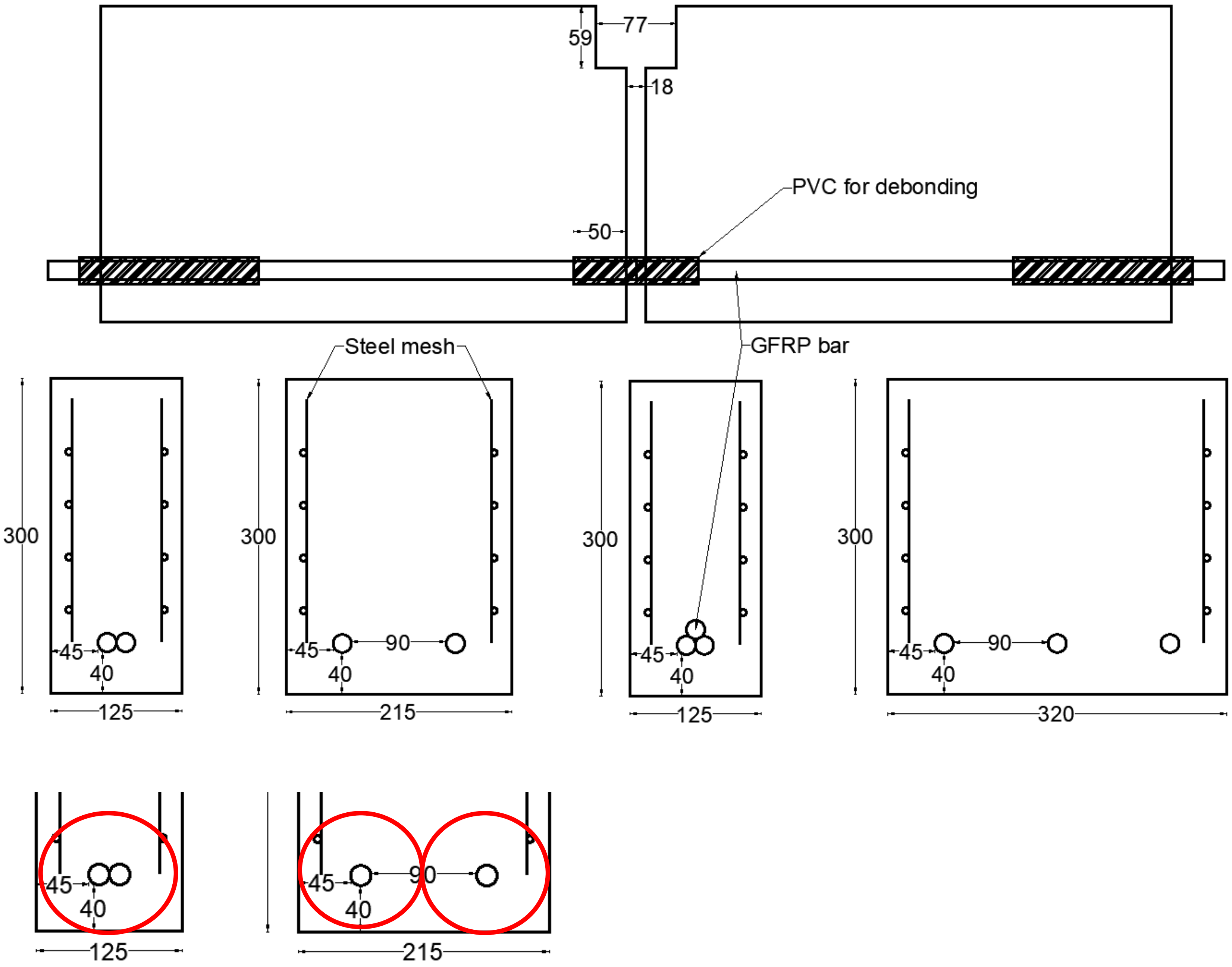

Test Setup

RILEM RC5 (1994)
“notched beam”

$$u = \frac{P\,a}{2\pi\,y\,d_b\,L_e}$$

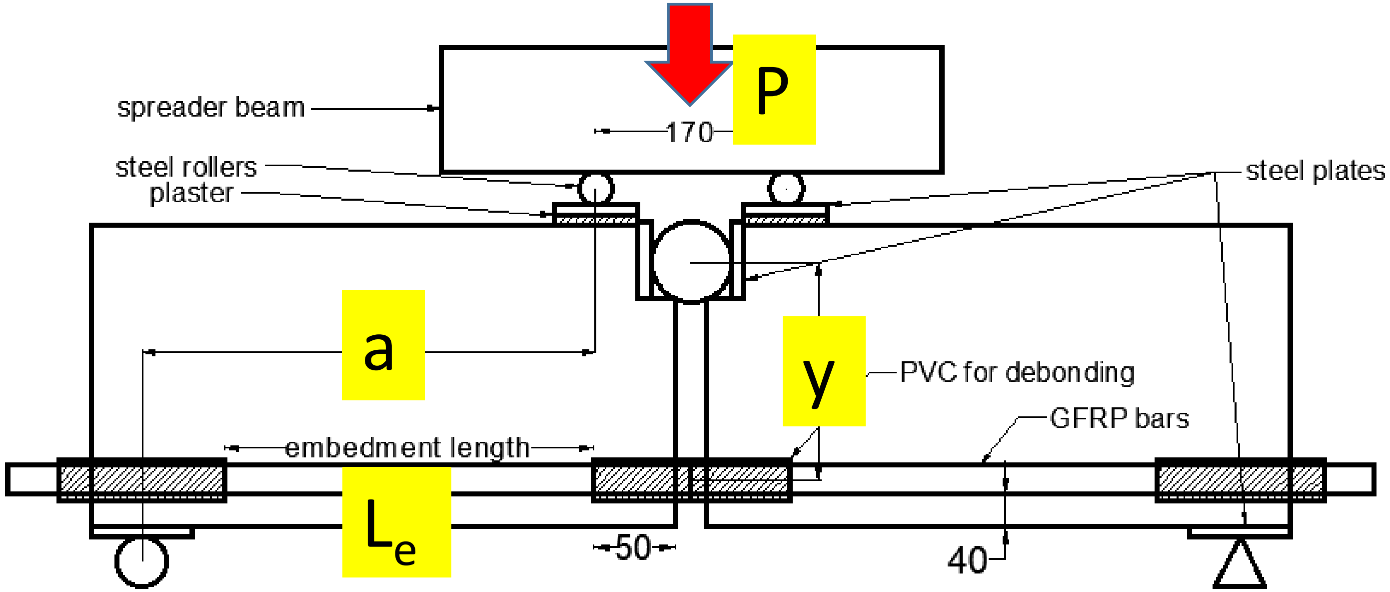

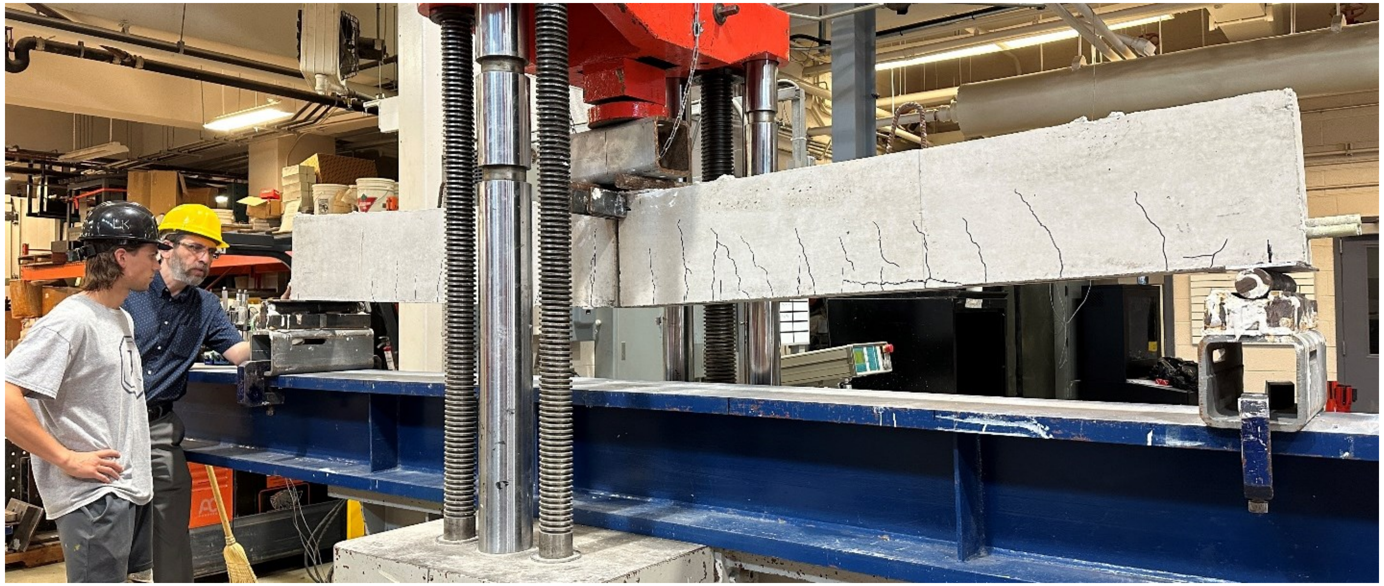

Results:
Failure mode

All beams splitting bond failure

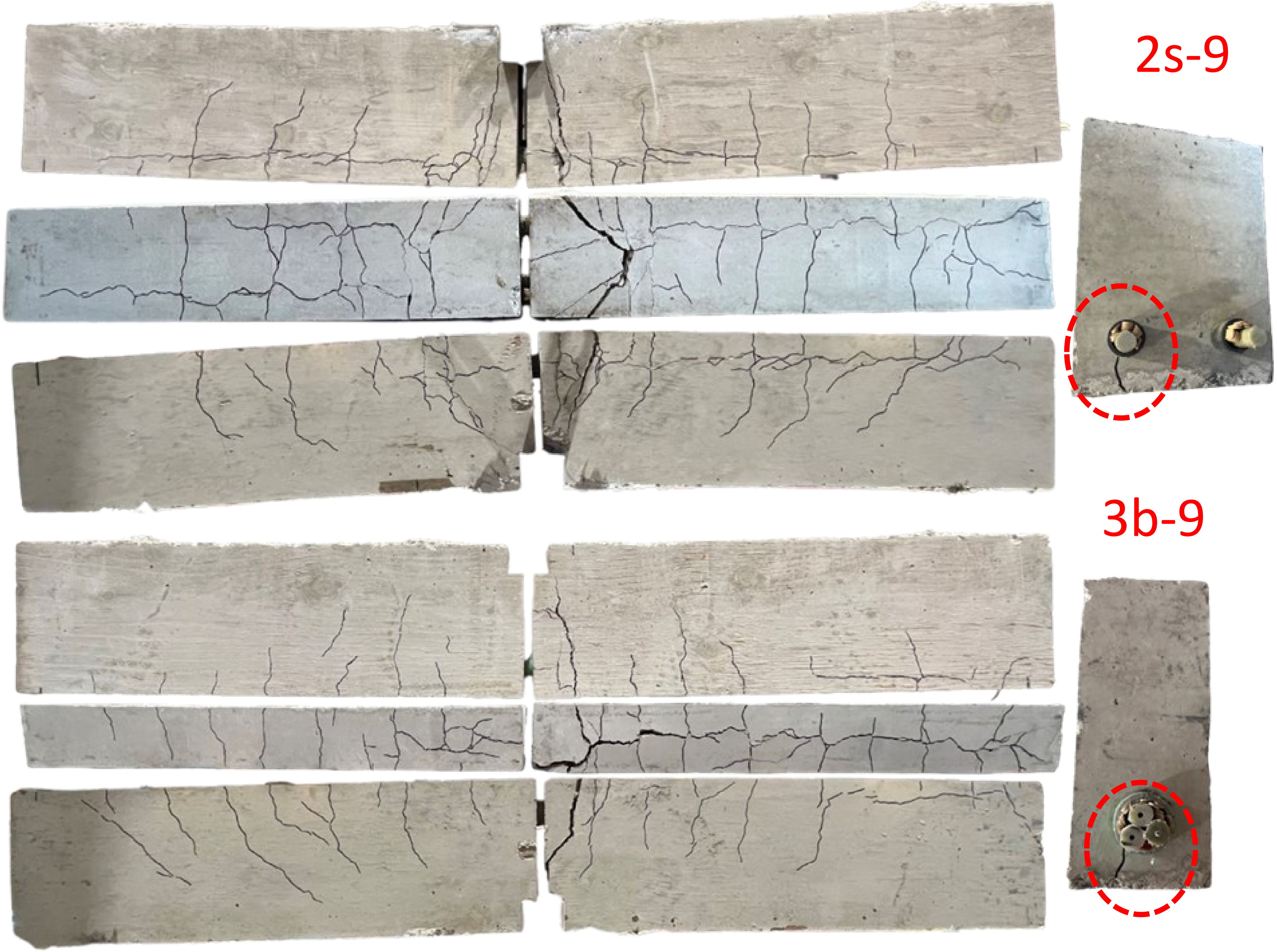

Results: Bar longitudinal stress

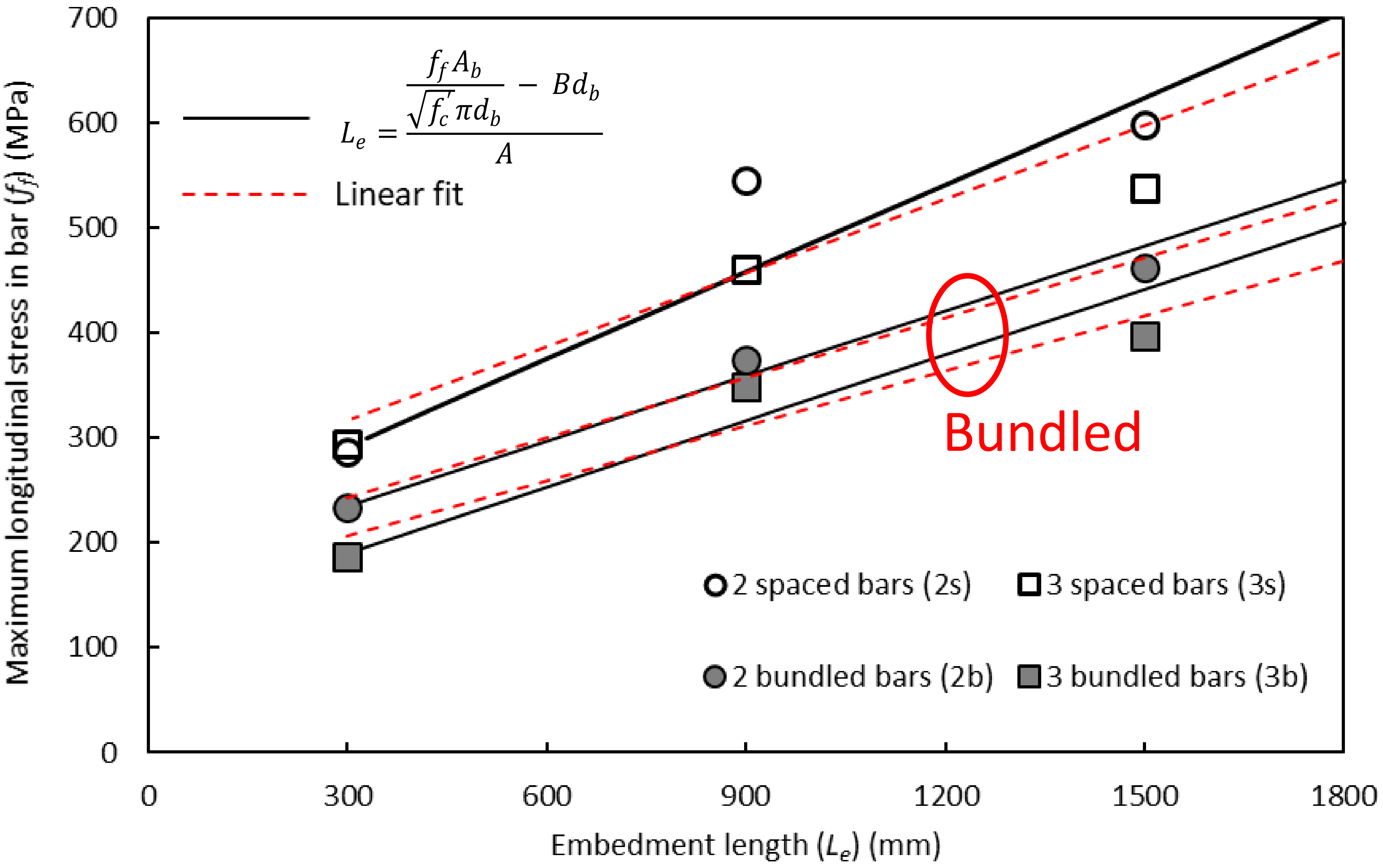

Results: Development length (L_d)

Conclusion 1

Bundled bars

At $f_{fu} = C_E \cdot f_{fu}^* = 880$ MPa

$L_d = 1.4\ L_{d,\ spaced}$ (2 bars)
$L_d = 1.5\ L_{d,\ spaced}$ (3 bars)

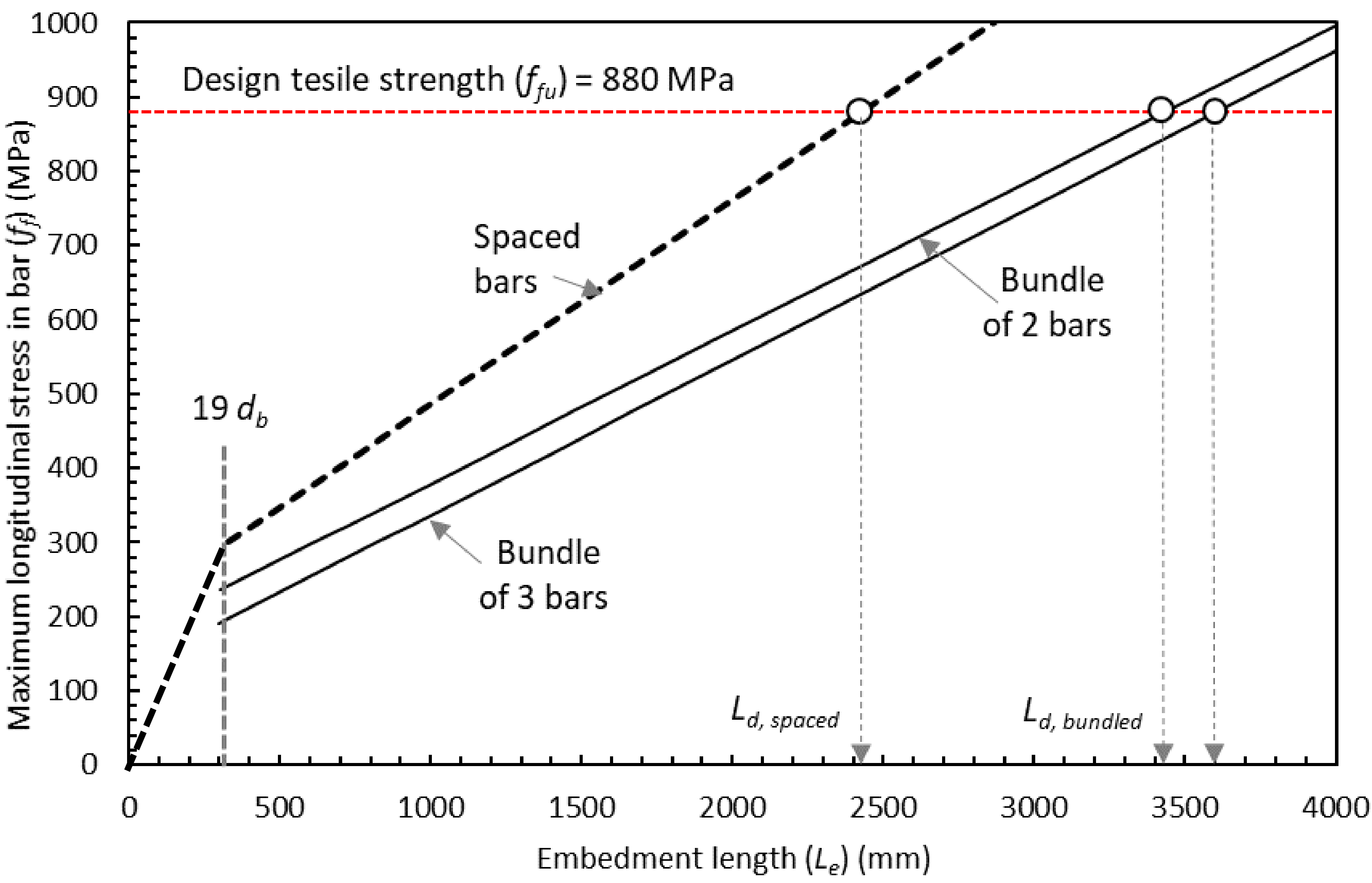

Results: Bundling Factor (K)

Unlike steel, which is always at f_y :
What if $f_f < f_{fu}$ *(compression failure)* ?

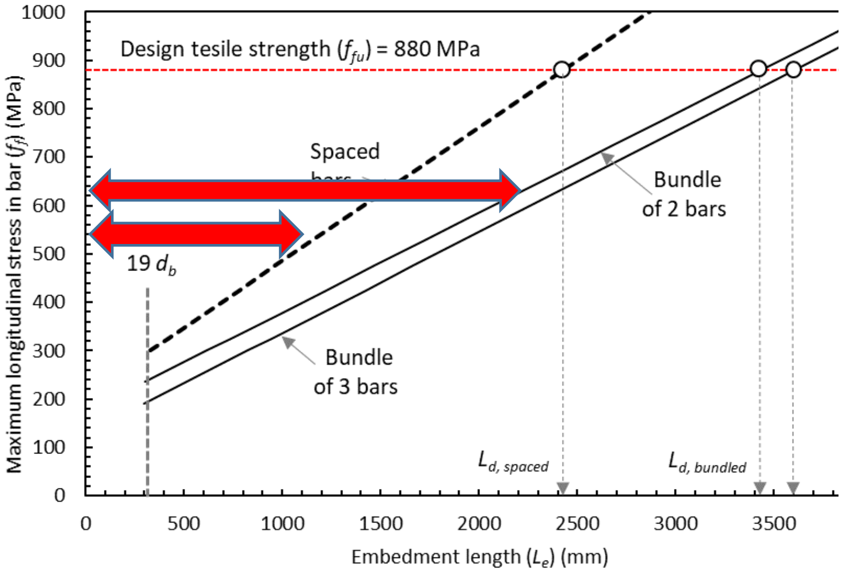

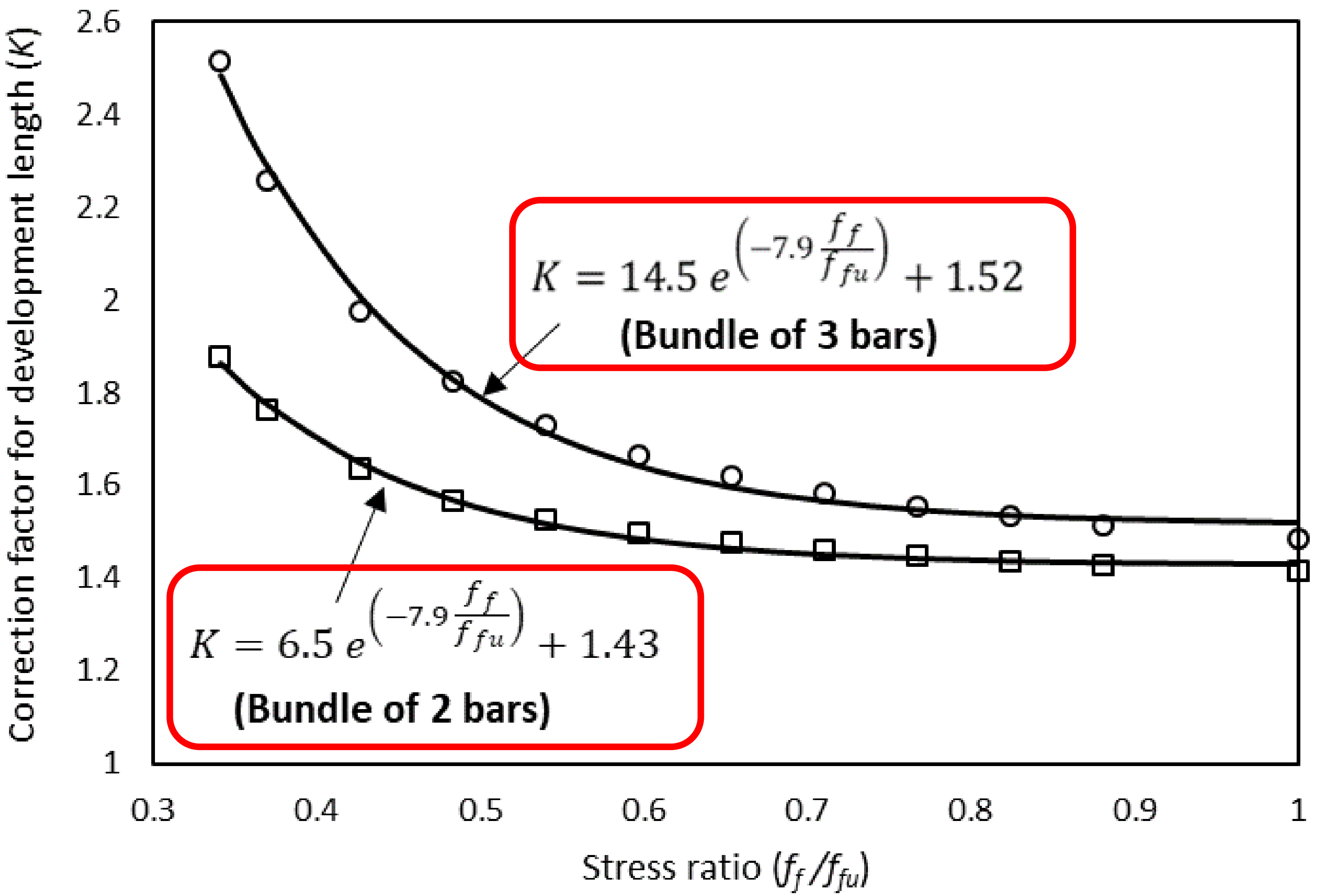

Conclusions

- Development length (L_d) of bundles of 2 & 3 GFRP sand-coated bars at full design tensile strength (f_{fu}) are 1.4 and 1.5 times larger than spaced bars.

- Unlike steel which is always at Fy, bundling factor depends on stress level in GFRP bar at failure. Simple equation now available.

- For more details:

Kaufman, L. and Fam, A. (2024) "Bundling Effect on Bond and Development Length of Sand Coated GFRP Bars", *ASCE Journal of Composites for Construction*, 28 (5), 04024031

Bond in UHPC

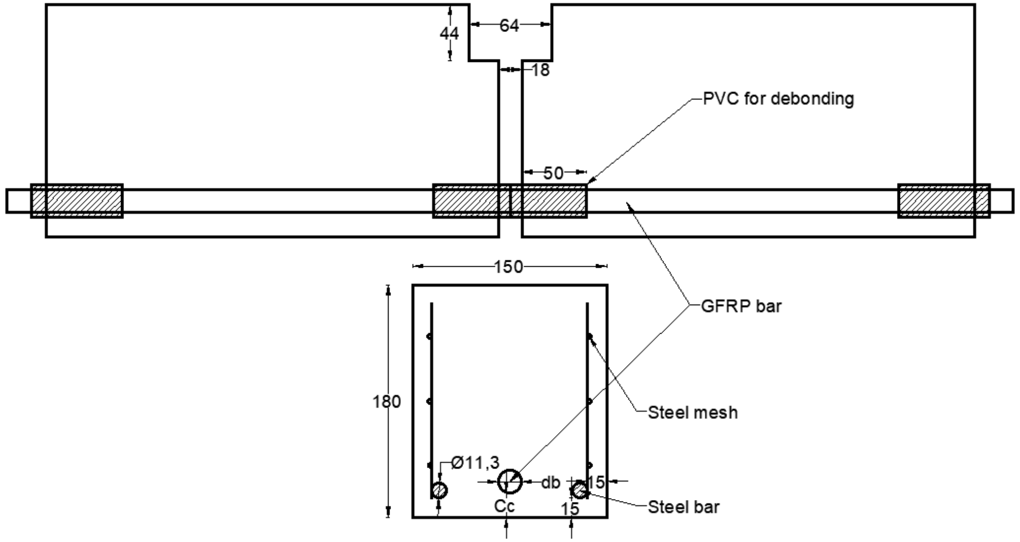

Average concrete strength: 129 M

2% steel fibers

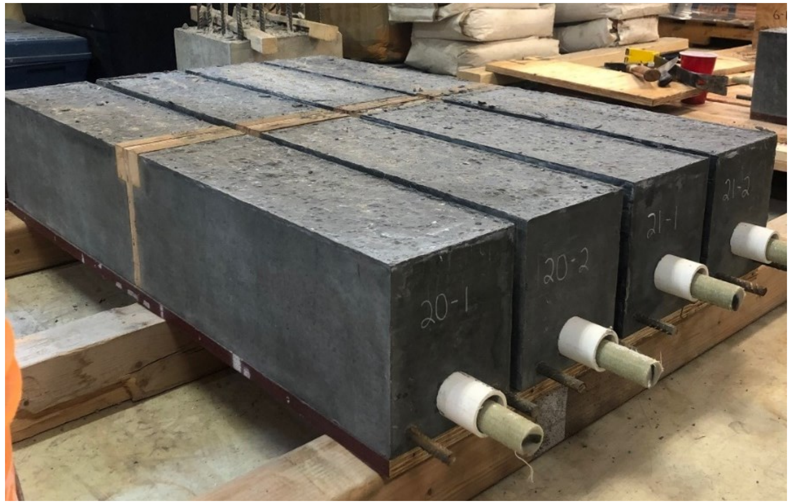

Parameters:

- Bar size (d_b): #4, #5, #8 (~13, 17, 27 mm)
- Clear cover: ~17, 23, 42 mm
- Embedment (L_e/d_b): ~4, 9, 14

Total ~70 beam tests

Failure modes

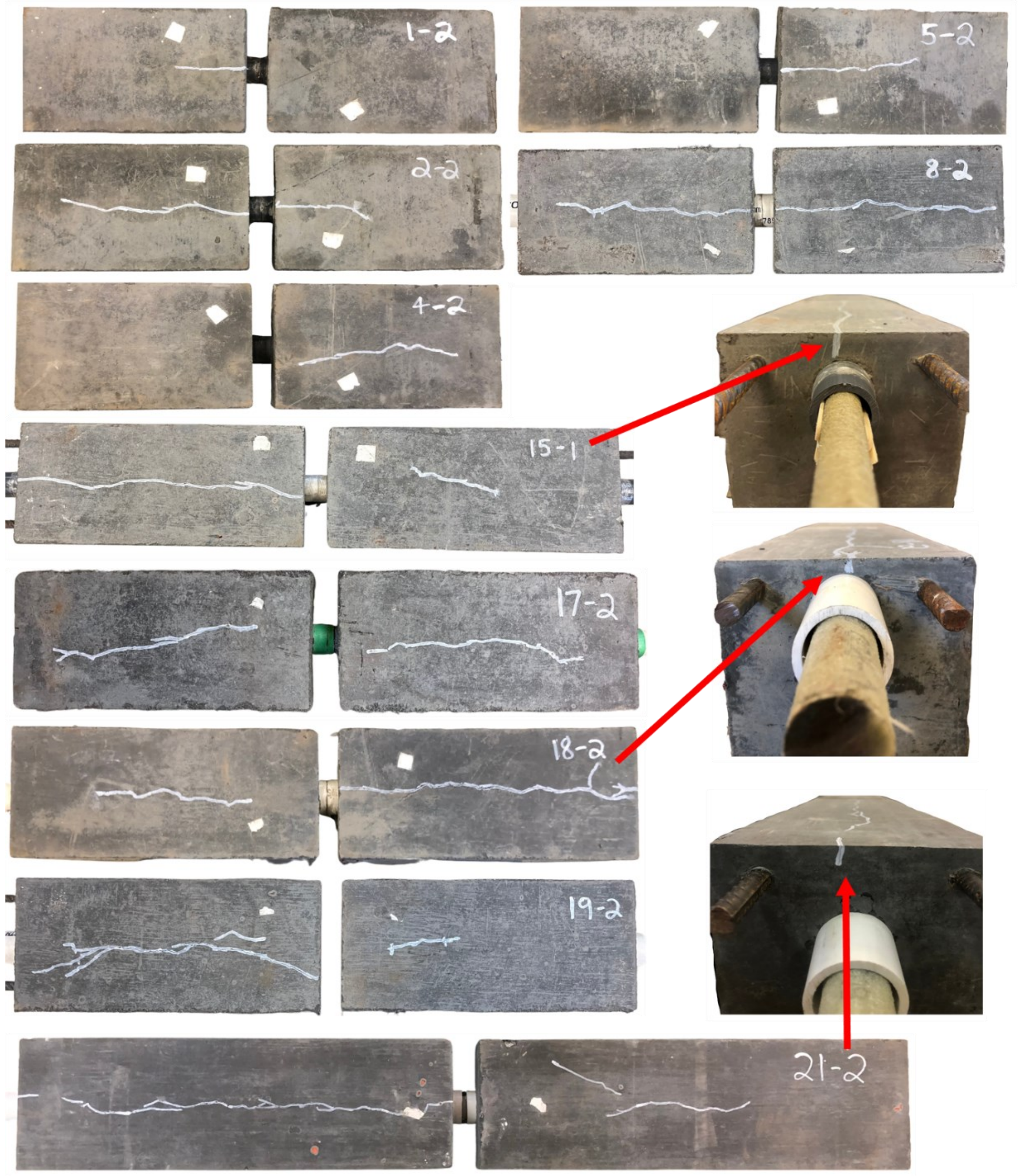

Splitting bond
(most specimens)

Pullout bond
(no surface cracking)
(only 4 specimens)

Results:

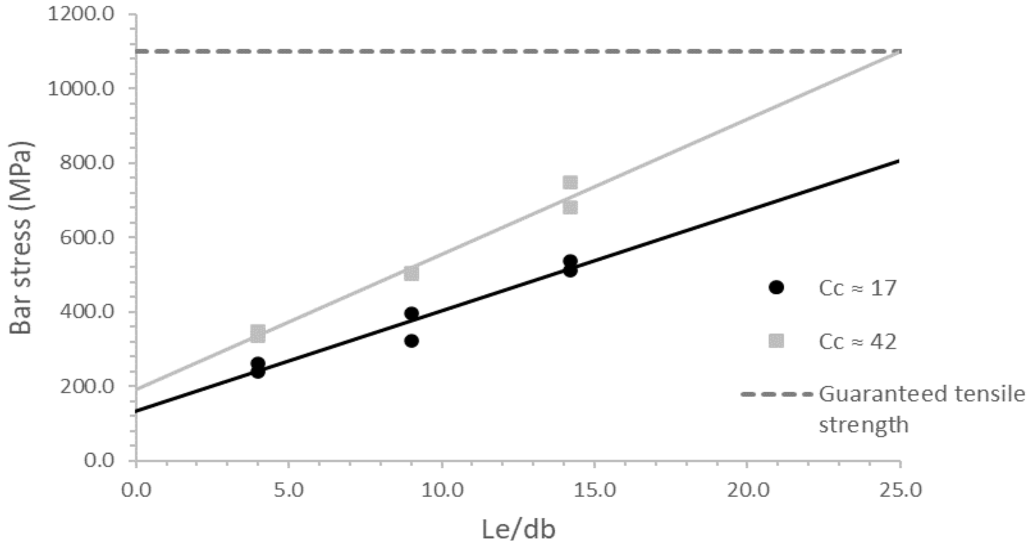

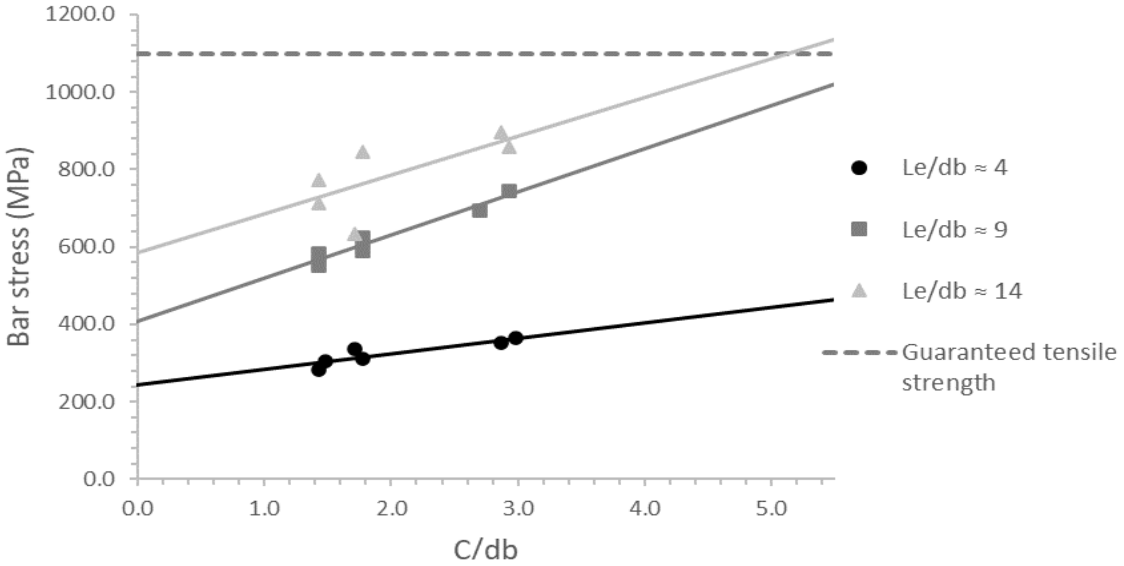

Linear regression

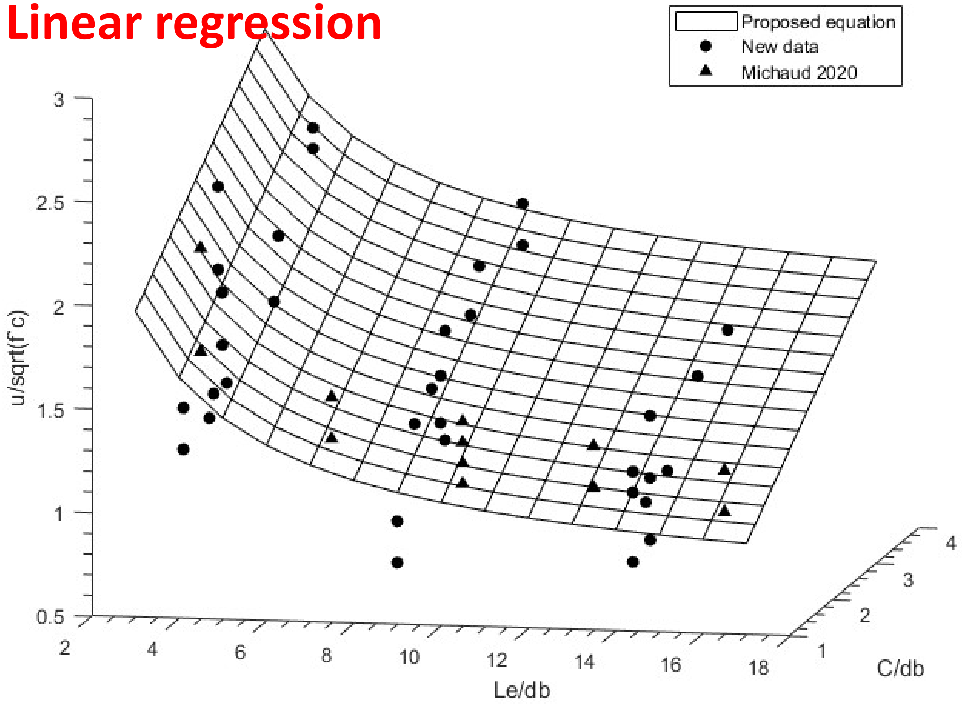

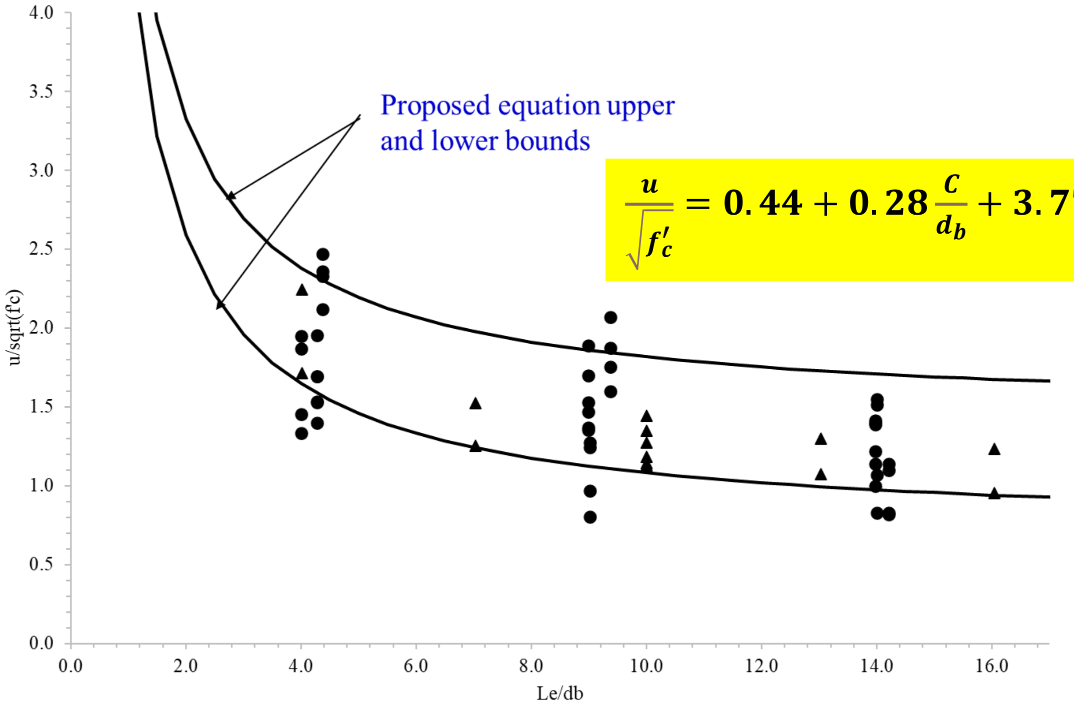

$$\frac{u}{\sqrt{f'_c}} = 0.44 + 0.28\frac{C}{d_b} + 3.77\frac{d_b}{L_e} \quad \textbf{(Proposed)}$$

$$\frac{u}{\sqrt{f'_c}} = 0.44 + 0.28\frac{C}{d_b} + 3.77\frac{d_b}{L_e} \quad \text{(Proposed)}$$

$$u = \frac{f_f\, A_b}{\pi d_b L_e} = \frac{f_f\, d_b}{4L_e}$$

$$L_d = \frac{\dfrac{f_{fr}}{4\sqrt{f'_c}} - 3.77}{0.44 + 0.28\dfrac{C}{d_b}}\, d_b$$

Proposed development length for GFRP bars embedded in UHPC with 2% steel fibers

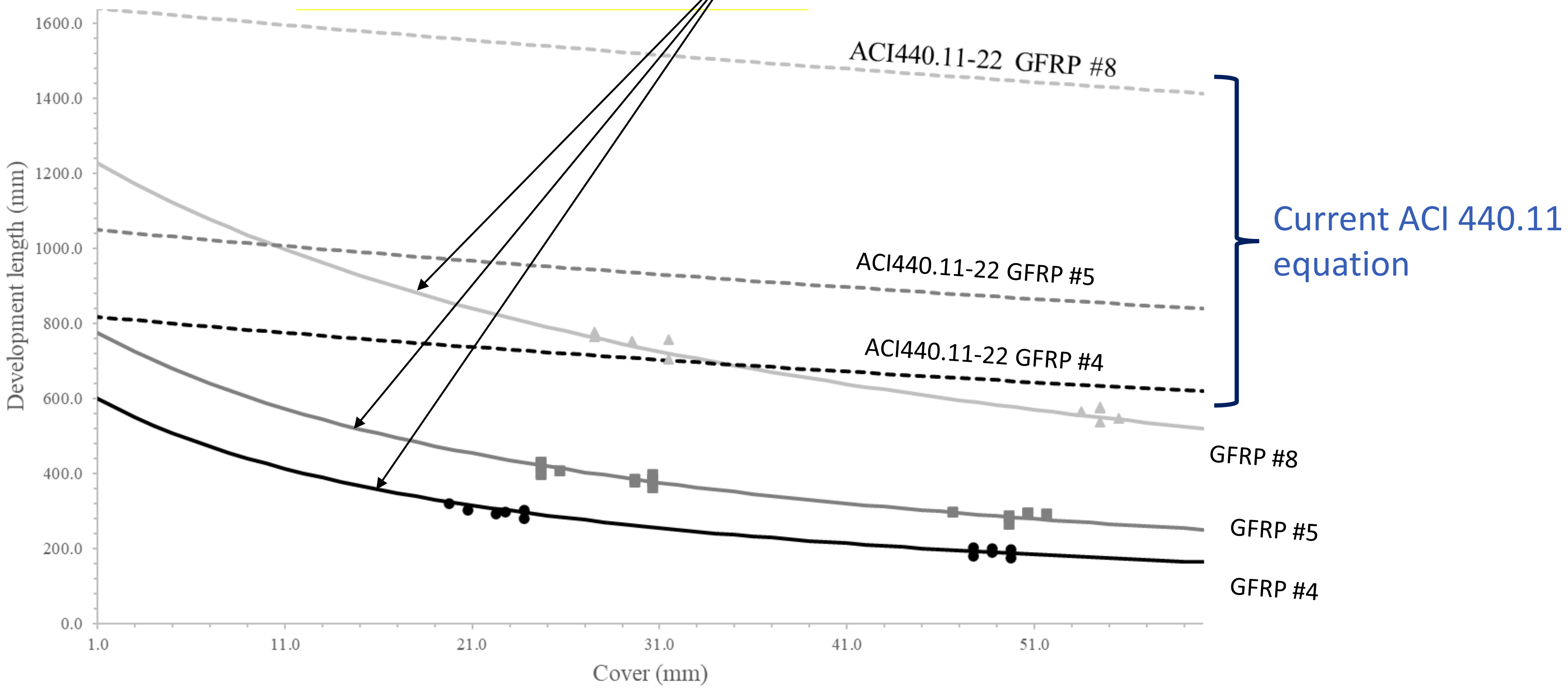

Conclusions

- L_d of GFRP bars **significantly shorter** in UHPC than regular NSC.

- ACI 440.11-22 **overestimates L_d by 2.0 to 3.5 times** for covers of 1.0 to 3.7d_b, respectively.

- **New equation** proposed for UHPC:

$$L_d = \frac{\dfrac{f_{fr}}{4\sqrt{f_c'}} - 3.77}{0.44 + 0.28\dfrac{C}{d_b}} \, d_b$$

- For more details:

Kaufman, L. and Fam, A. (2024) "Effect of GFRP Bar Diameter and Concrete Cover on Bond and Development Length in UHPFRC", *Construction and Building Materials*, 418, 135445.

Bond in Shotcrete

How shotcrete differs from cast concrete ?

- Shotcrete is sprayed at velocities of 97-129 km/hr (60-80 mi/hr) (Hanksat, 2017)
- Consolidation is provided by high-velocity impact rather than vibration
- Shotcrete has a different mix design, with smaller aggregate (10 mm max), higher w/cm ratio, and commonly uses SCMs (e.g., silica fume) (Austin and Robins, 1995)

Modern shotcrete – New construction not just retrofitting

Questions

1. Voids (air or sand pockets from rebound) behind bar ?

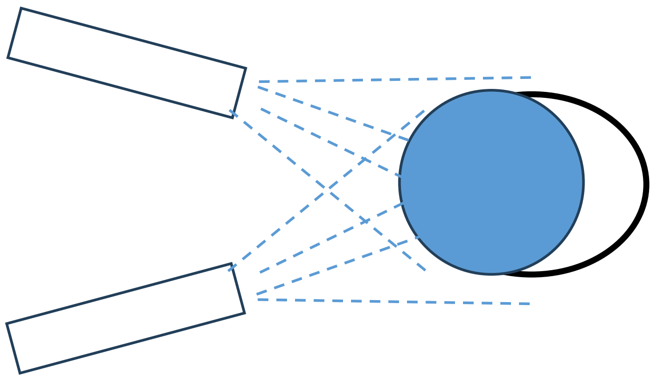

2. Any rebar vibration ?

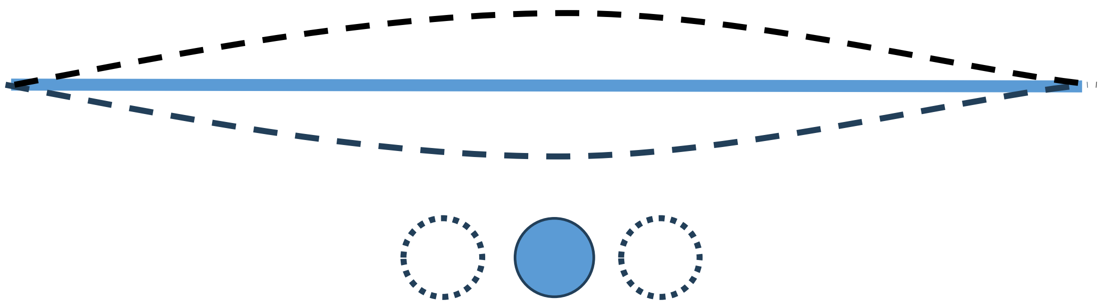

3. Small aggregates & different mix effect ?

4. Any damage to bar surface ?

Bar integrity

Bond

Shotcrete mix design

- Using the wet-mix process for shotcrete placement
  - Wet-mix process: fully mixed concrete (e.g., ready-mix) is projected from the nozzle with compressed air
  - Did not use dry-mix, which involves mixing in water at the nozzle immediately before spraying
- Mix design:

Specification type	Specified quantity
Specified 28-day strength (f'_c)	**40 MPa**
Maximum w/cm	0.40
Nominal maximum aggregate size	**10 mm**
Plastic air content	6-9%
Silica fume	~8% of cementitious materials
Slump	70 ± 10 mm

Beam design

- No confinement in tension
- Clear covers used are the minimum ACI 440.11-22 covers for walls (exposed and unexposed used)

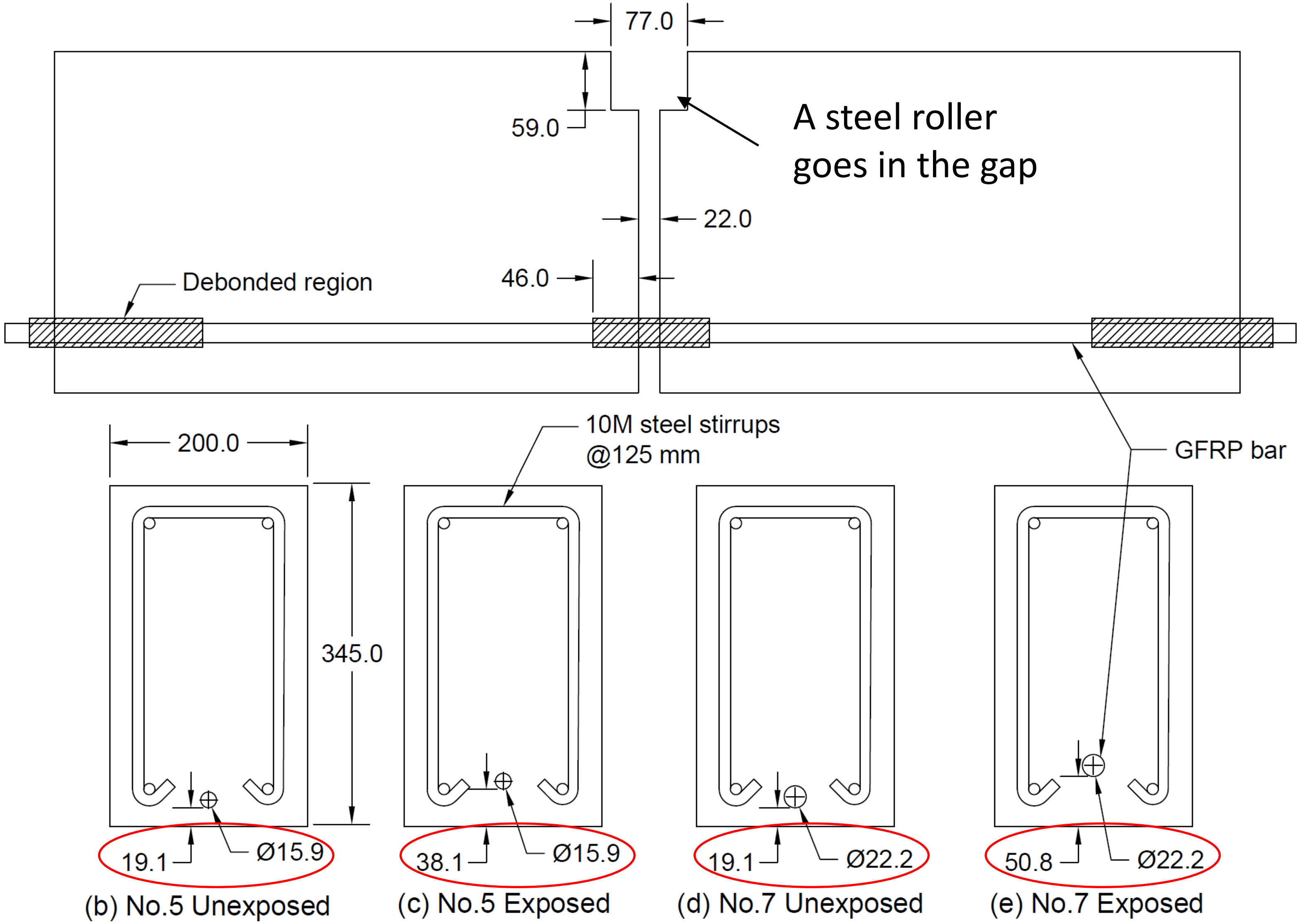

Shotcrete casting configuration

- Beams stacked vertically as single walls then cut longitudinally into beams
  - Allowed air and aggregate to escape during shotcrete spraying

Control samples cast from same mix and vibrated

Beam cutting

- Using rail-mounted wall saws
- Cores & prisms cut from shotcrete test panels for properties

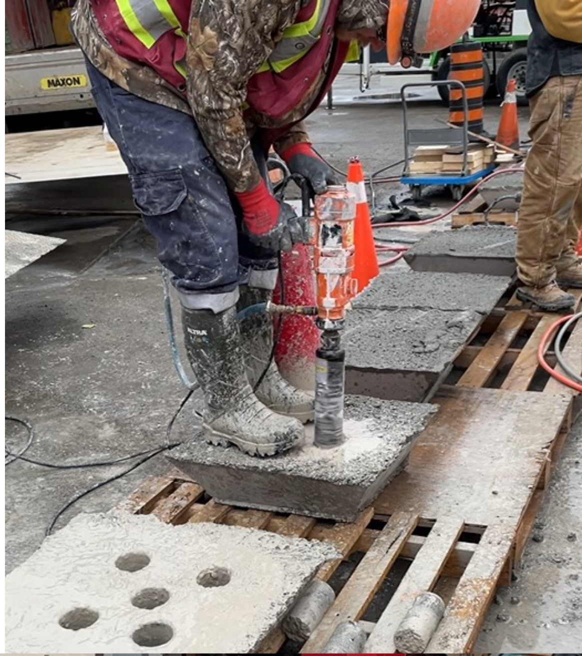

Testing

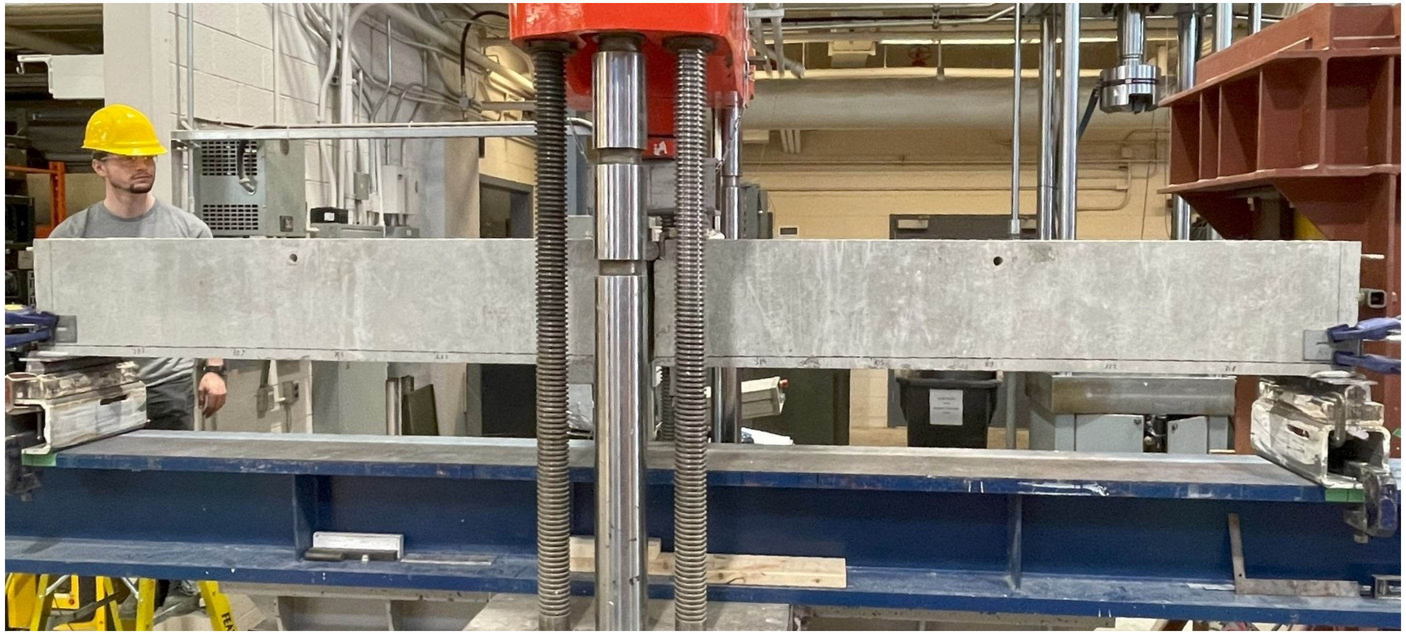

Splitting bond

Inspection (sand-coated)

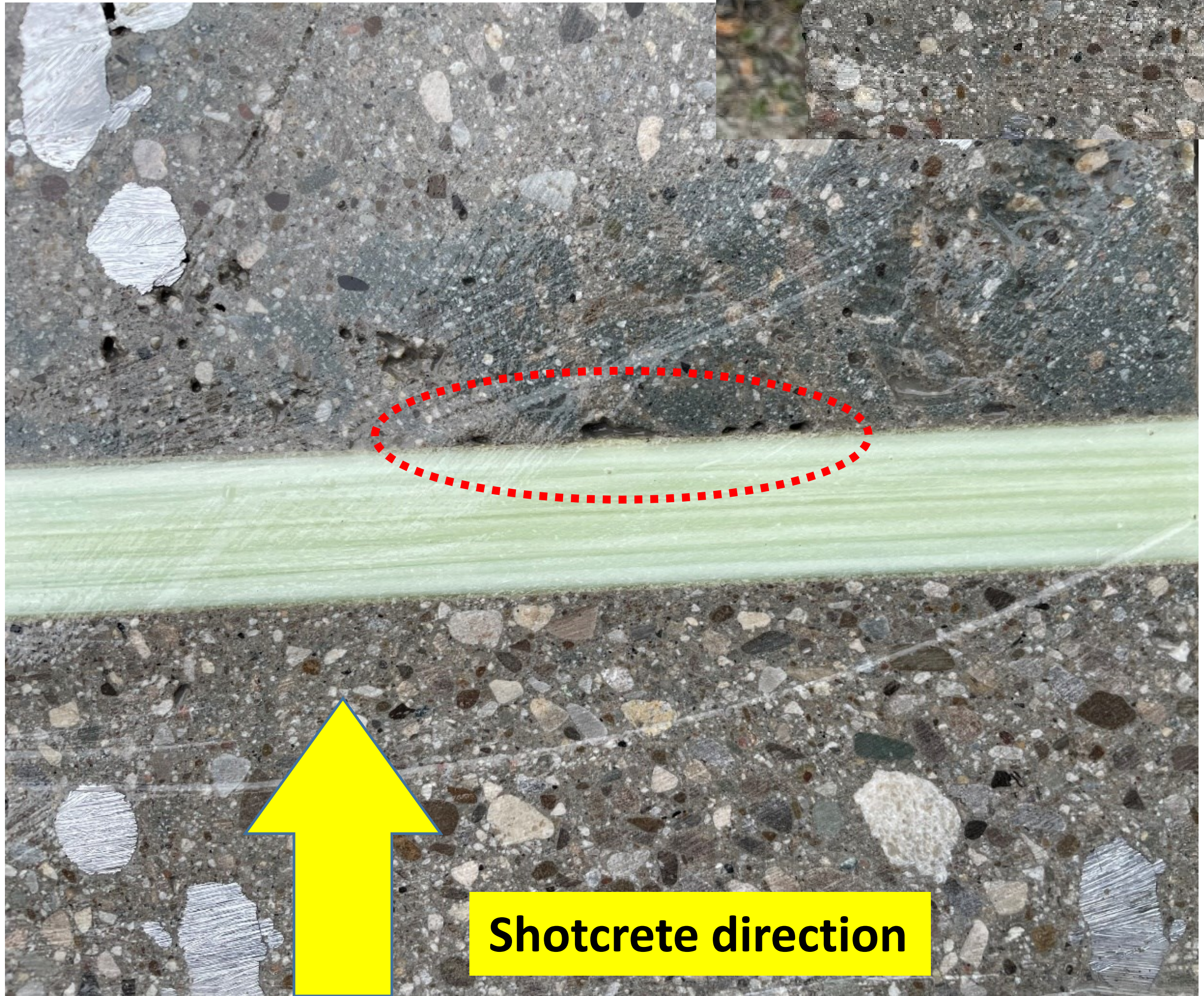

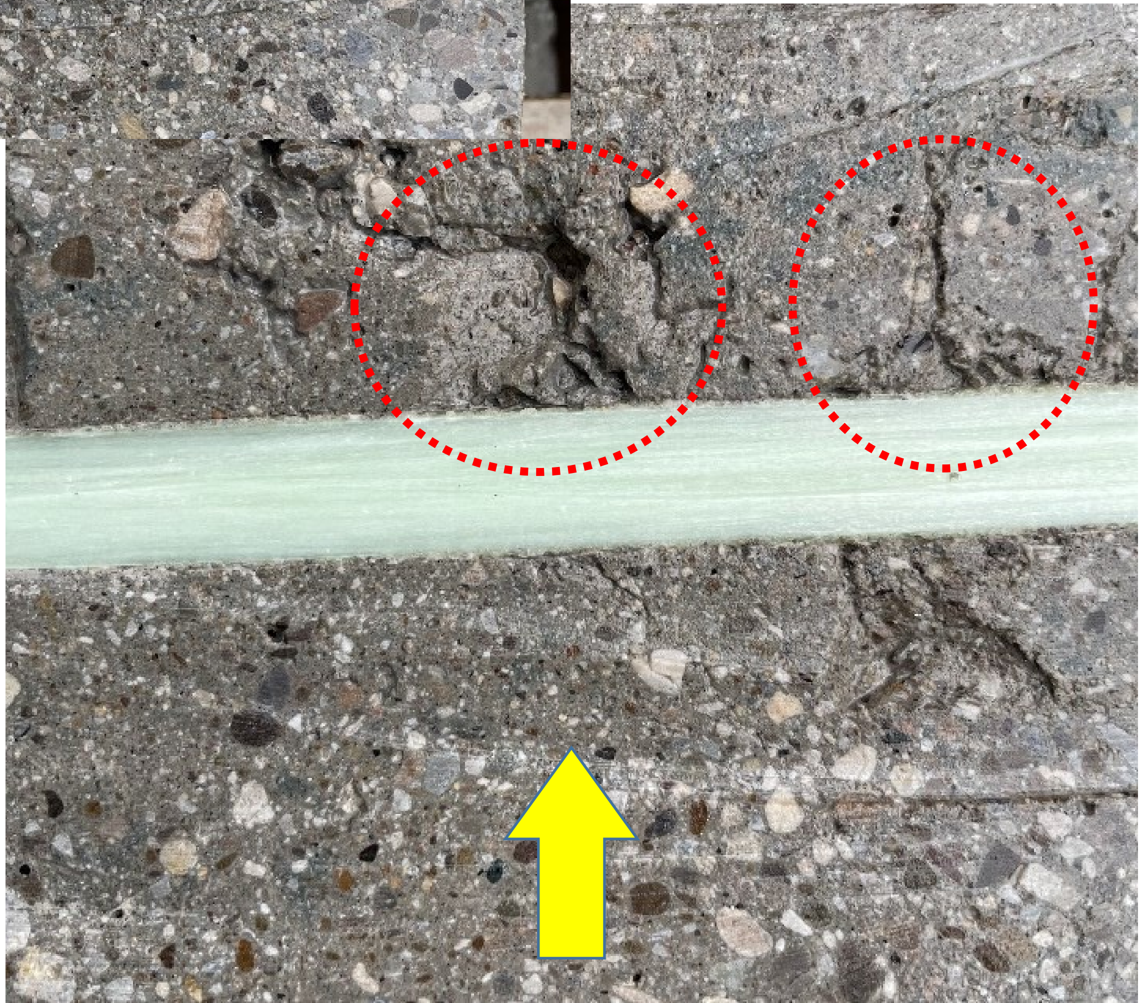

Inspection (Ribbed bars)

Preliminary results

$L_e = 20\ d_b$

Avg:
~ 3% - 13%

All embedment Lengths:

Avg:
~ 17%

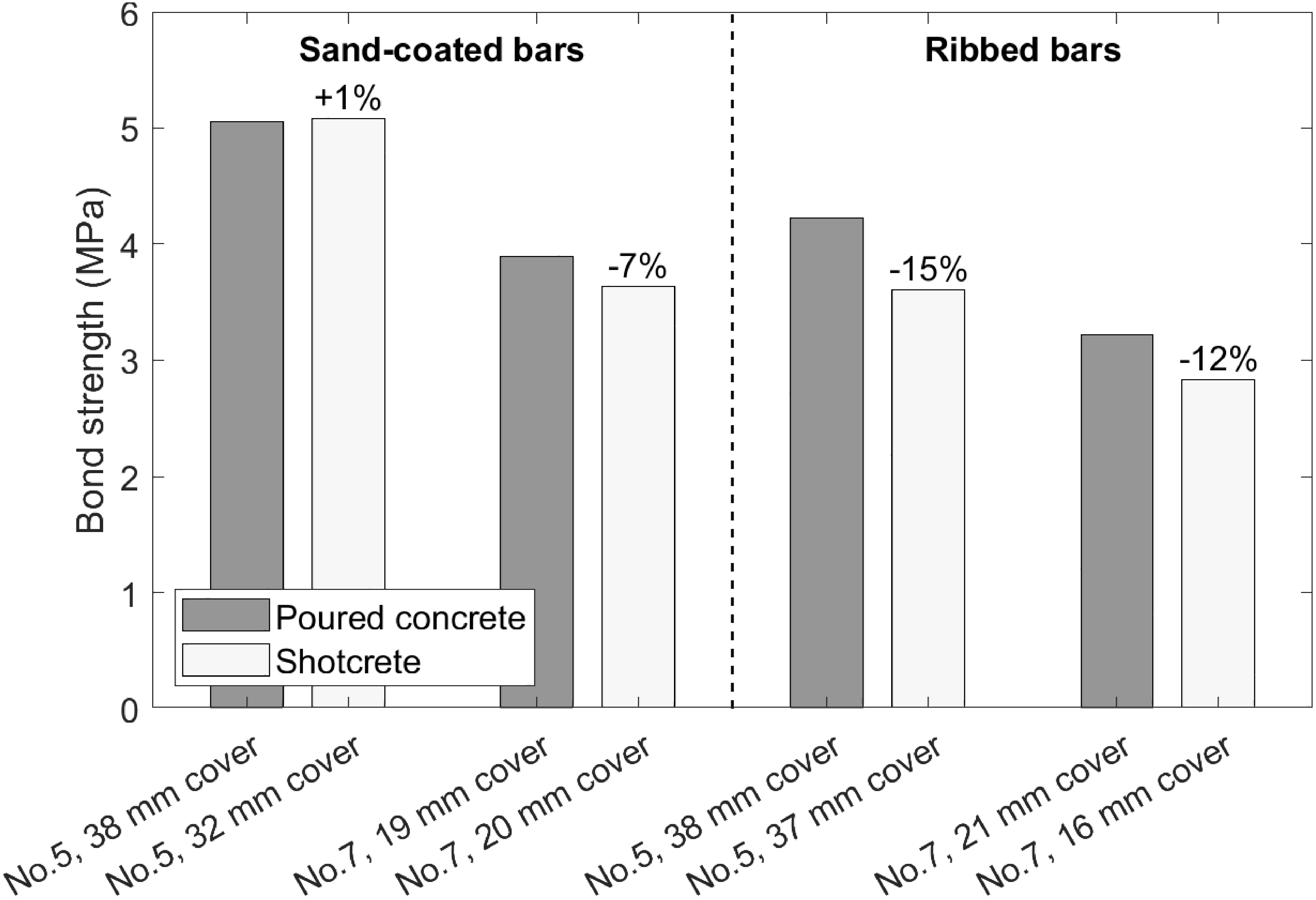

Conclusions

- Shotcrete of GFRP rebar is feasible and practical. There is a potential for a few isolated small pockets behind the bar, but almost certainly the same with steel bars too

- Bond strength in shotcrete may see 3% to 17% average reduction, with deformed bars being more on the higher end compared to sand coated. Again, likely the same in steel rebar.

- Ongoing: Spraying GFRP rebar then cleaning for surface inspection then tension tests

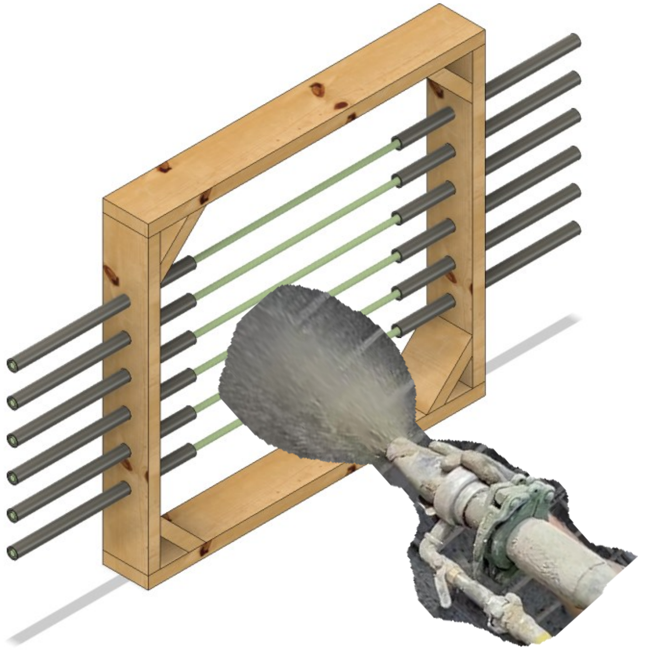

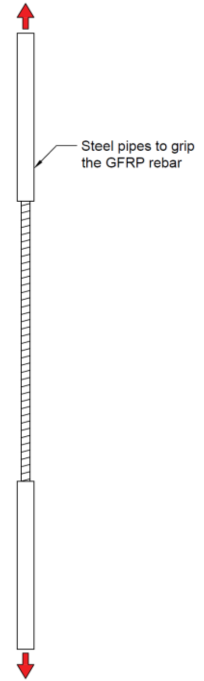

Acknowledgements

Richard Sturm (PhD student)
Hannah Kassenar (MASc student)
Lukas Kauffman (former MASc student)

MST BAR
Pultrall / V-Rod

Thank you !

FOURTH INTERNATIONAL WORKSHOP ON FRP BARS FOR CONCRETE STRUCTURES

"Advances in concrete reinforcement"

August 8-9, 2024 - Toronto, Ontario

R&D on Advancing FRP Rebar Manufacturing & Product Development to Meet Market Needs

OMAR ALAJARMEH

Centre for Future Materials – University of Southern Queensland - Australia

SPONSORED BY:

Centre for Future Materials – University of Southern Queensland

- **Established in 1995**
- **One of the leading research centres in Australia for engineered fibre composites**
- **Delivering R&D to Reality**
  - **Working closely with industry partners**
  - **Development of advanced/sustainable materials & manufacturing**
  - **Application in resilient structures**
  - **From research laboratory to real-life applications**
- **+100 industrial partners**
- **+70 researchers**

Total of more than 850 publications from 2016 to 2023

Industry Partners

Centre for Future Materials – University of Southern Queensland

Advanced Composites Manufacturing

- Filament Winding
- Pultrusion and Braiding
- Repair
- Infusion Processing

Functional Materials

- Flame Retardant
- Morphing Material
- Energy Material
- Environmental Material
- Geopolymer

Civil Composites

- FRP Bar
- Rock Bolt
- Bio-epoxy and recycled thermoplastic resins
- Repair/Rehabilitation
- High Performance Concrete

Sustainable Industry Design

- Circular Economy Modelling
- Materials Recycle & Reuse
- Microprocessing
- System Design

Centre for Future Materials – University of Southern Queensland

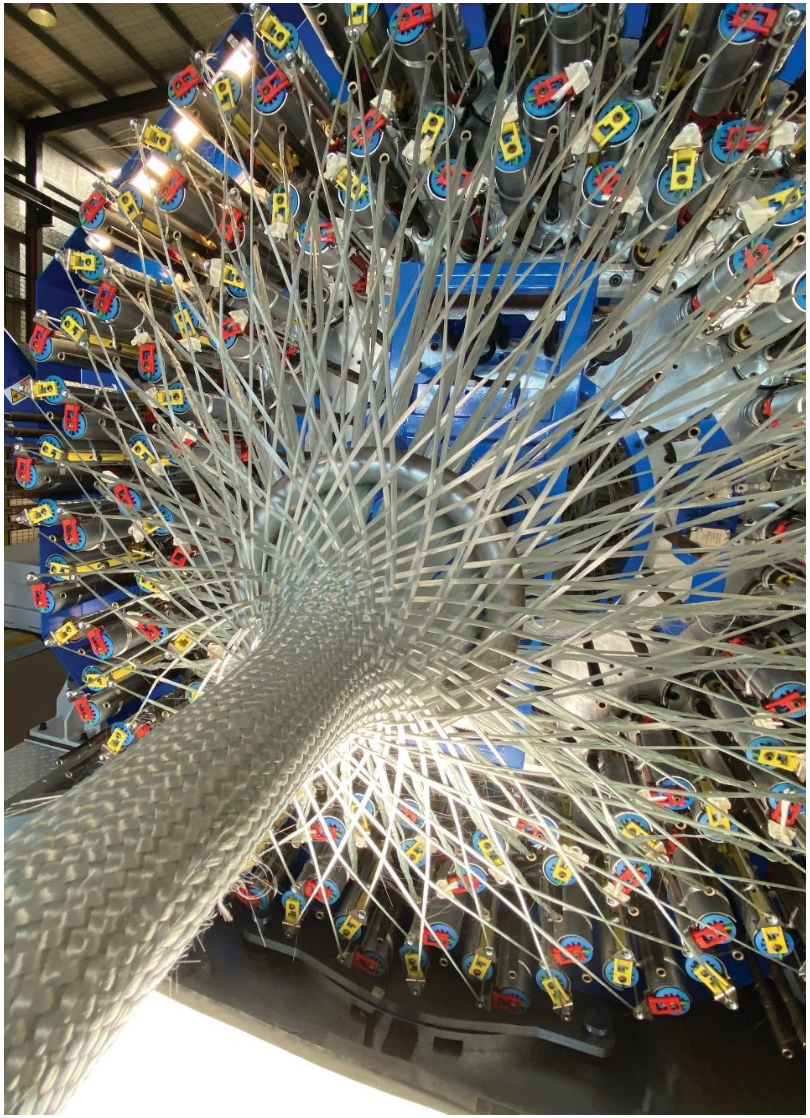

Sustainable resilient reinforcing system

Corrosion → **GFRP bars**

(a) Glass fibre guide (b) Wetting fibres in the resin bath (c) Forming die of the GFRP bar

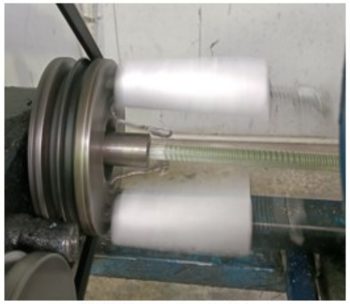

(d) Thread winding (e) Sand coating (f) Cured GFRP bar

- ✓ High strength; Light weight
- ✓ Non-corrosive; Non-conductive
- ✓ 75% Less manufacturing power
- ✓ 43% Less CO_2 emission
- ✓ 100% less transport expenses

Projects conducted at UniSQ

- **Precast GFRP-RC segmental decks for flood resilient**

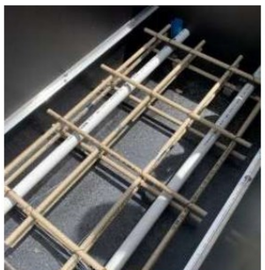


- **Precast GFRP-RC seawall panels under debris impact**



Projects conducted at UniSQ

- **Torsional Behaviour of GFRP-RC pontoon decks**

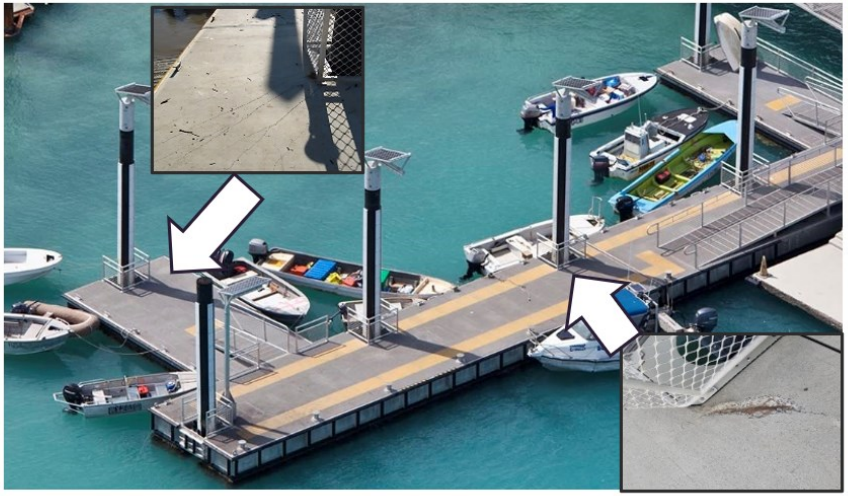

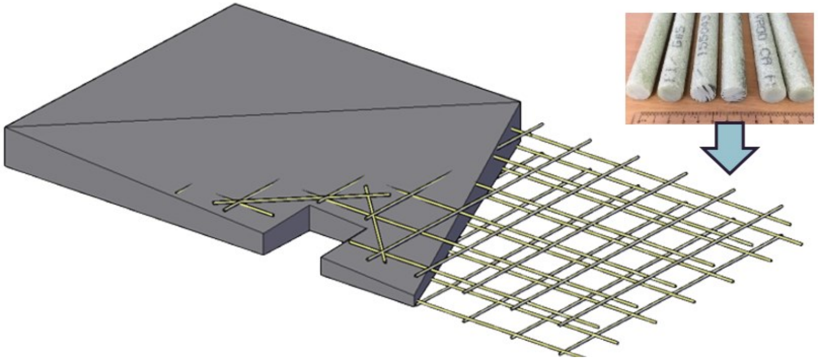

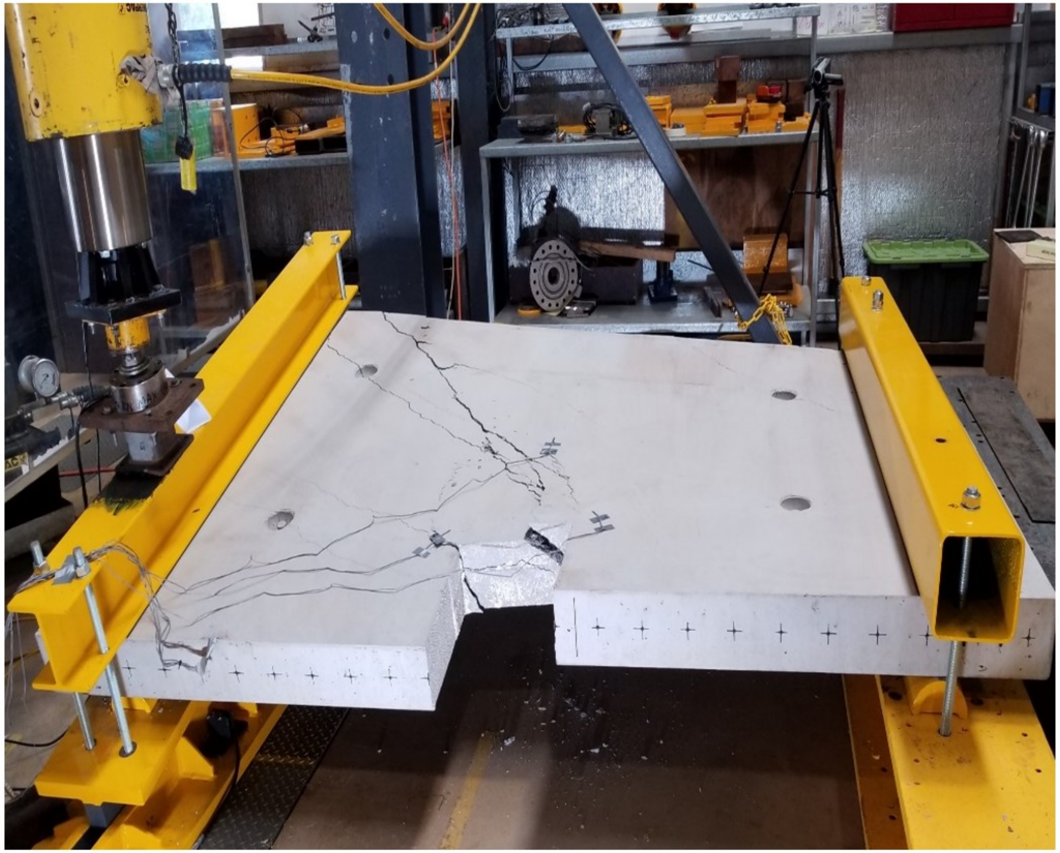

Projects conducted at UniSQ

- **Flexure and shear Behaviour of GFRP-RC culverts**

New opportunities !!

Are GFRP rebars limited to Grade III ?!

Flexibility of Design Codes to absorb new changes ?!

Are GFRP rebars limited to epoxy/vinyl ester ?!

Grade IV GFRP bars (70 Gpa)

- Changing the fibre content of GFRP bars (fibre volume 65%, 68%, 71%) (10mm dia)

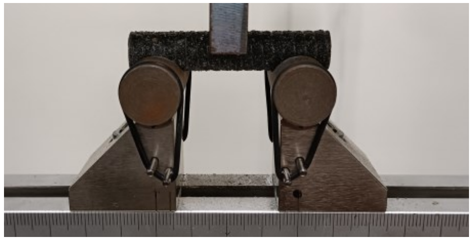

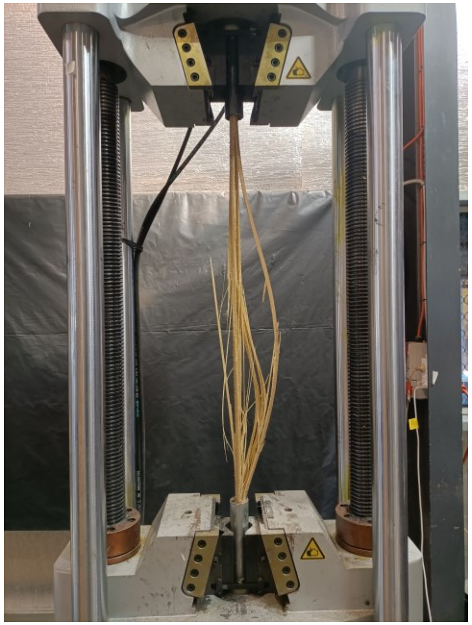

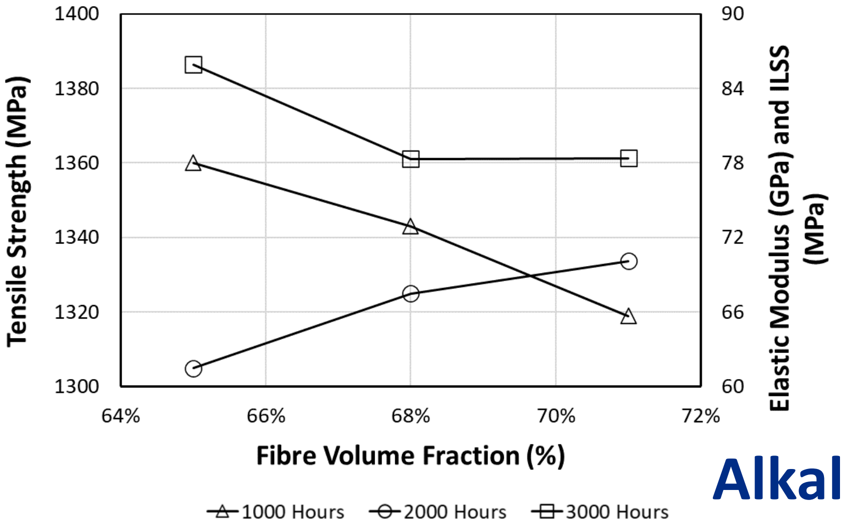

Alkaline Conditioning

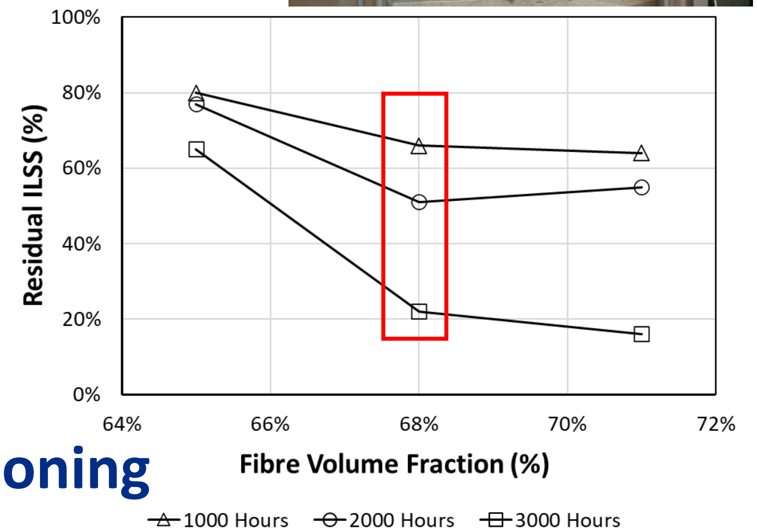

NexGen GFRP rebars Grade V (80 Gpa)

- **Effect of additive manufacturing (GNPs)**

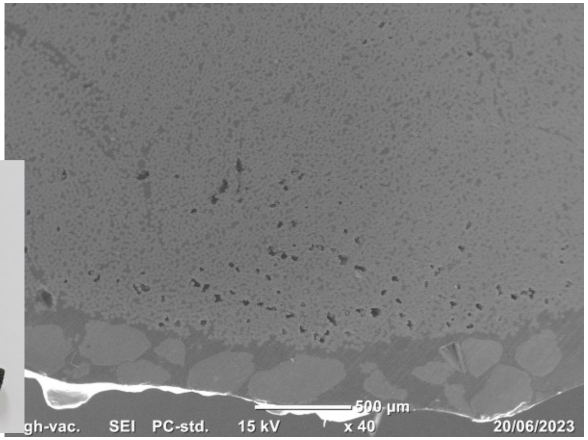

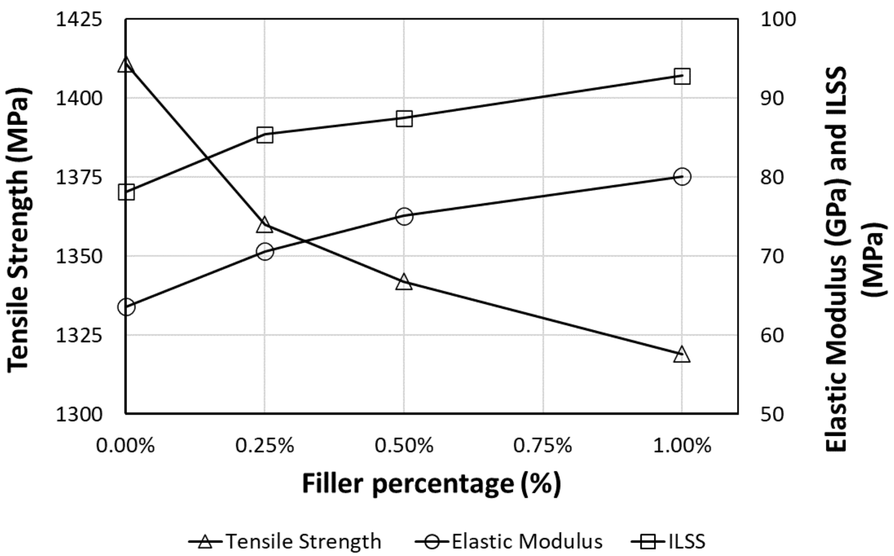

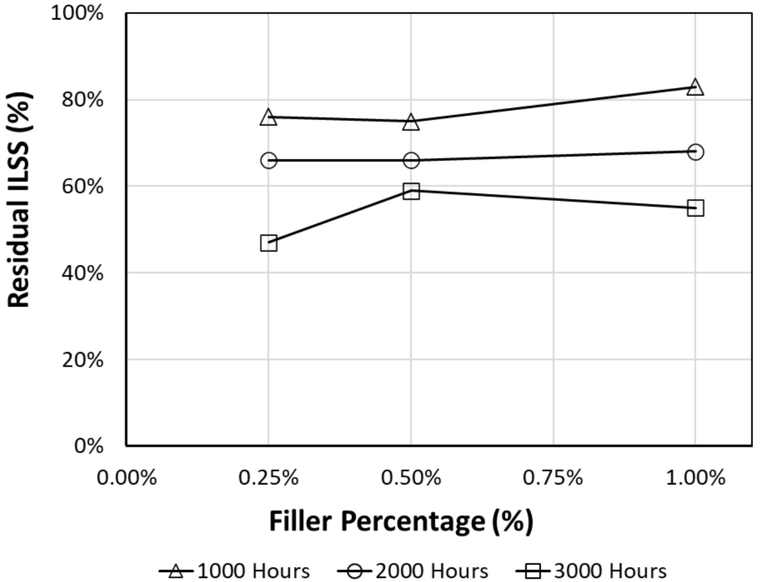

Alkaline Conditioning

Development of new resin systems

- **Sustainable Bio-based resin system**

Project: New development of Bio-epoxy resin system

Partners: Incomat and Climate Change

Diglycidyl ether Bisphenol A (DGEBA)

↓

Bio-based epoxy resin system: glycerol core

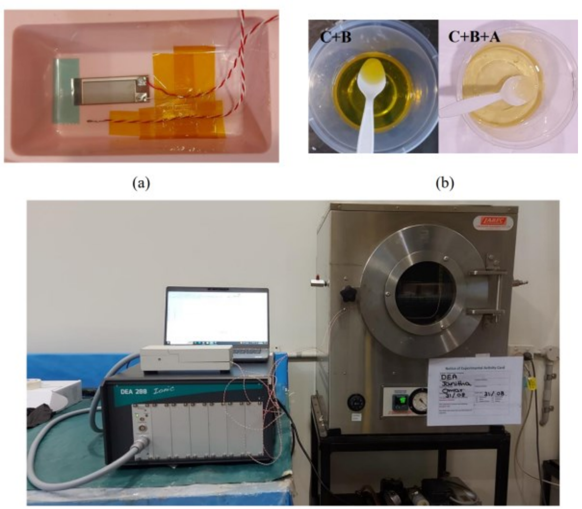

(a) (b) (c)

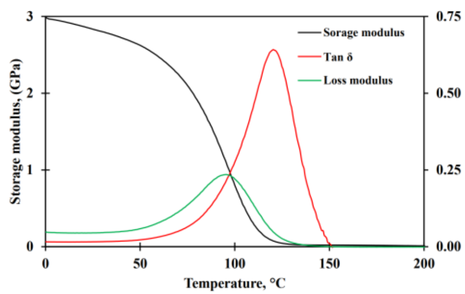

Outcomes:

- ✓ Produce new novel Bio-epoxy resin reliable for pultrusion manufacturing
- ✓ Reducing at least 80% of CO2 emission at production
- ✓ Pultrude new version of environmental-friendly pultruded products

Development of new resin systems

- **Recyclable thermoplastic reinforcing system**

Project: New development of Thermoplastic GFRP rebars (up to 85% fibre content)

Partners: Beyond Materials Group, Zero Waste Matters

Reforming

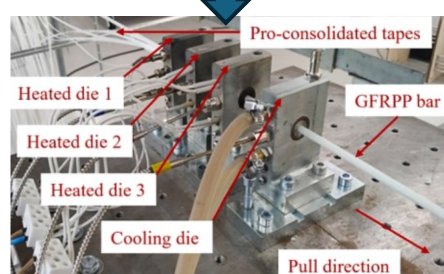

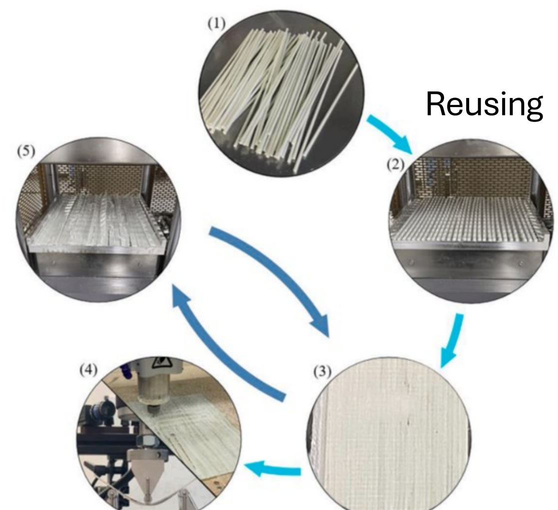

- ➢ Recycled Polypropylene (PP)
- ➢ Recycled Polyethylene terephthalate (PET)
- ➢ Recycled High-density polyethylene (HDPE)

Outcomes:

- ✓ Producing recycled thermoplastic GFRP rebar through pultrusion
- ✓ Pultrude new version of environmental-friendly pultruded products

Contact

Dr Omar Alajarmeh
omar.alajarmeh@unisq.edu.au
Tel: +61 7 4631 5516
Mob:+61497394088

www.youtube.com/c/USQCentreforFutureMaterials

More Information on
https://composites.usq.edu.au/research/facilities/

CRICOS : QLD00244B NSW02225M
TEQSA:PRIV12081

FOURTH INTERNATIONAL WORKSHOP ON FRP BARS FOR CONCRETE STRUCTURES

"Advances in concrete reinforcement"

August 8-9, 2024 - Toronto, Ontario

Horizontal Shear Capacity of Composite T-Beams Reinforced with GFRP Interface Shear Reinforcement

Mohamed Eladawy

Civil Engineering Analyst, PhD., M.Sc. PMP.
Candu Energy [AtkinsRéalis]

SPONSORED BY:

Presentation Outline

1. Background
2. Literature Review
3. Research Hypothesis
4. Experimental Program
5. Results and Discussion
6. Theoretical Investigation
7. Conclusions

Background

- The use of **precast concrete girders** in composite concrete bridge construction.
- Precast **girders** and **panels** are constructed in a controlled environment.

Background

A key part of this type of construction is developing **composite action** between the **girders** and **deck slab**.

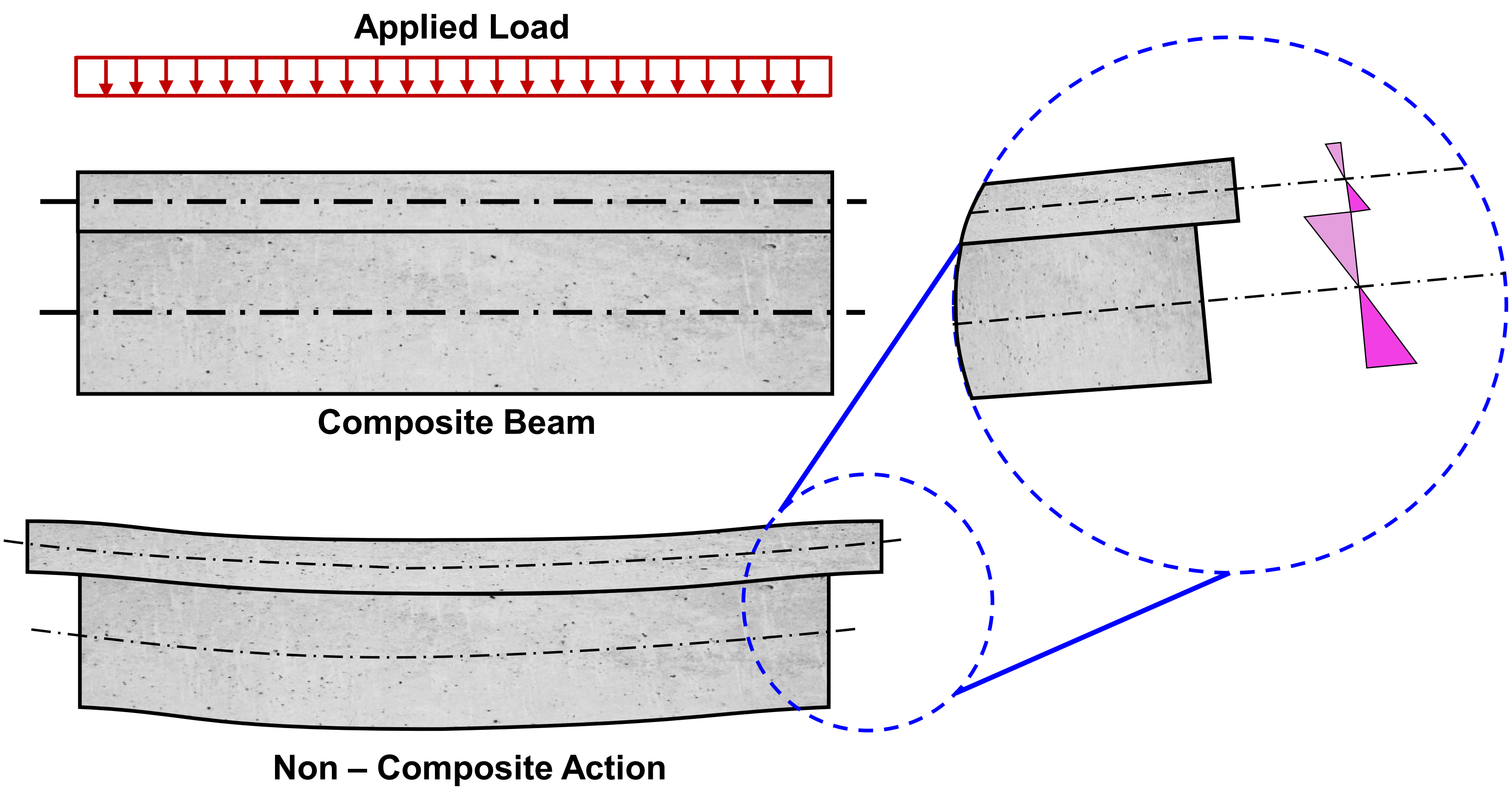

Background

A key part of this type of construction is developing **composite action** between the **girders** and **deck slab**.

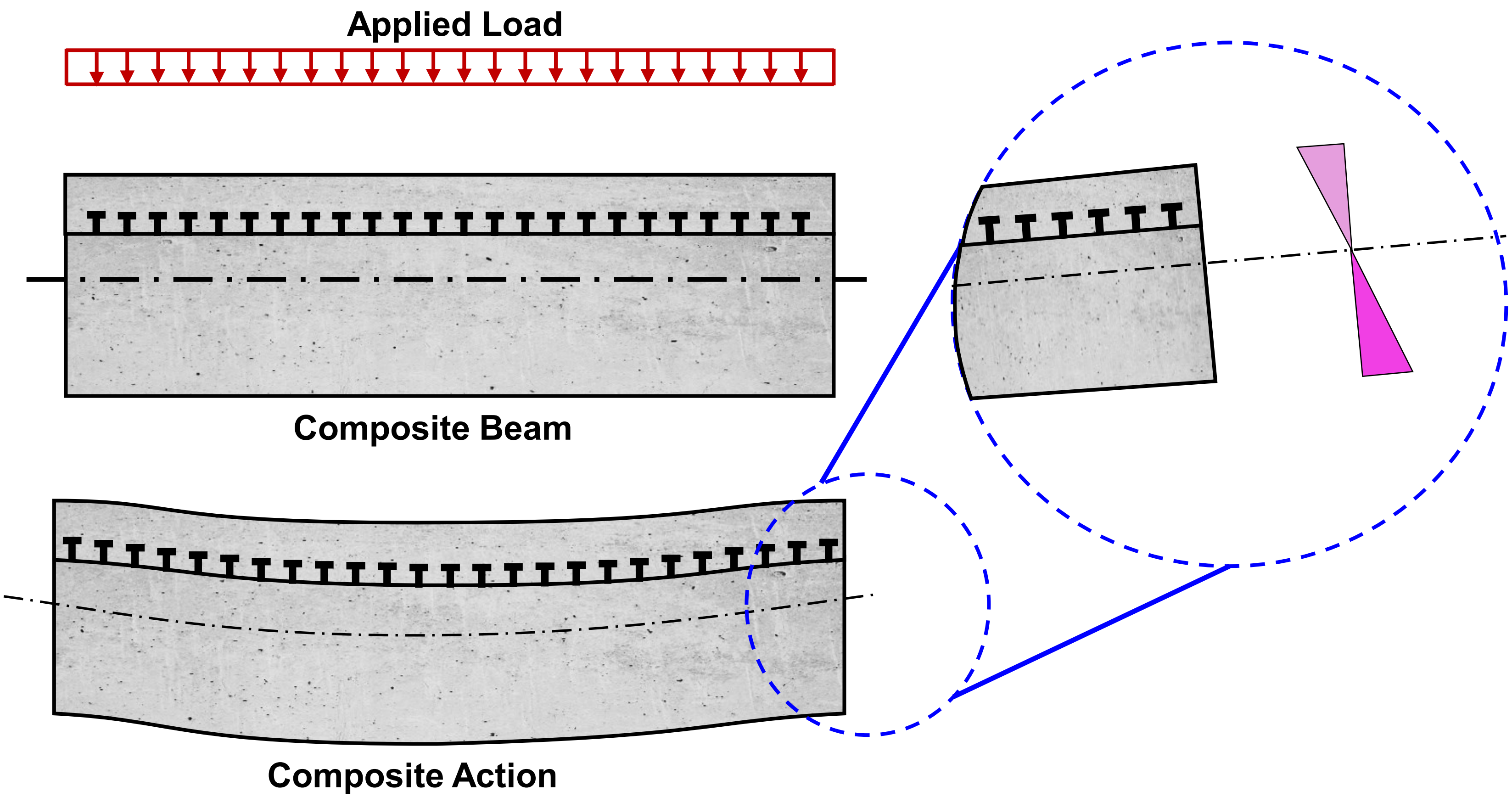

Background

The composite action is achieved by three mechanisms:

1. **Shear-friction.**
2. **Cohesion between surfaces.**
3. **Dowel action of reinforcement.**

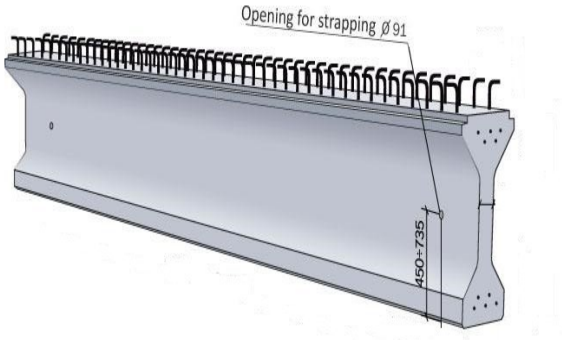

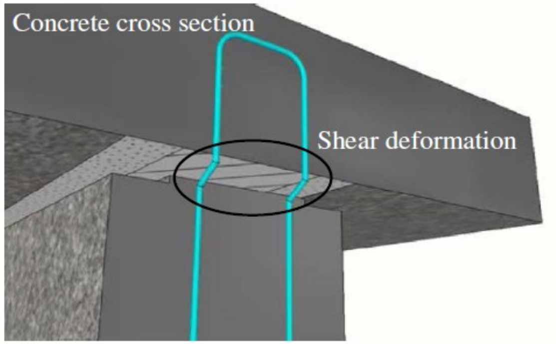

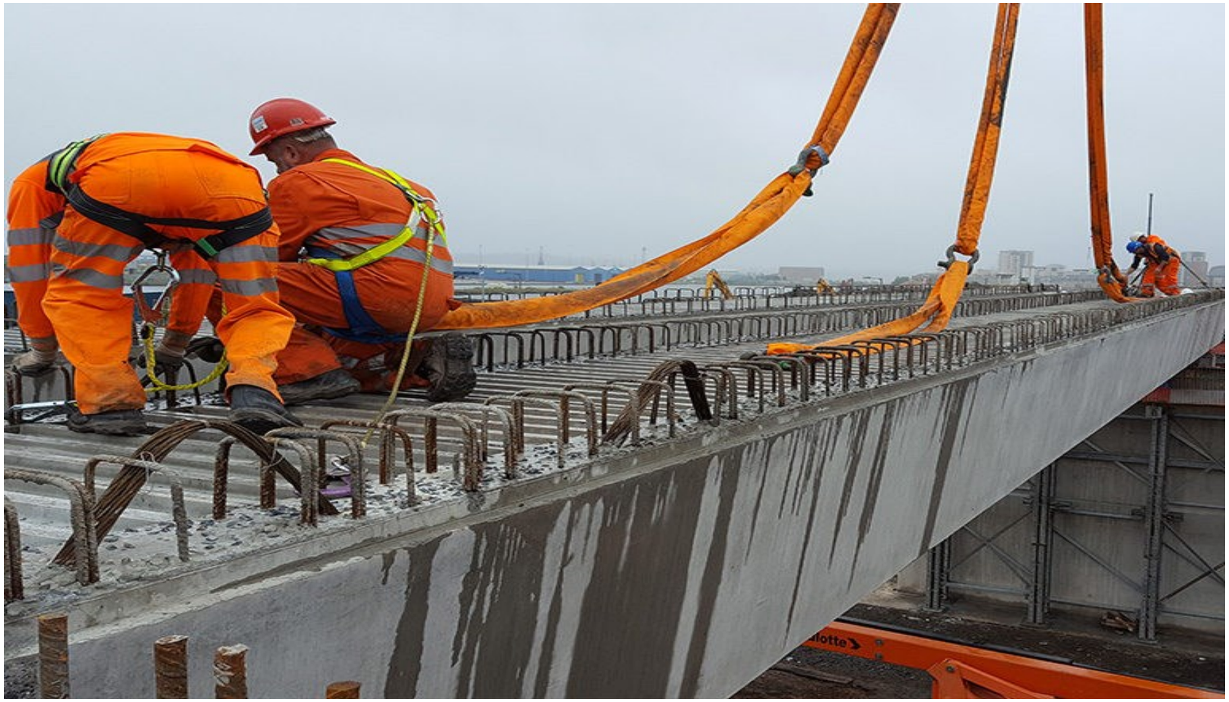

Composite Action

Background

- **Bridges** in Canada are exposed to **harsh environments** characterized by a wide range of temperature variations and the use of salt for de-icing.
- This results in the gradual loss of the **monolithic behavior** and the strength of the **composite concrete beams**.

Deterioration of the Bridges

Literature Review

All studies concerning the **interface shear** with **FRP** as a shear connector were executed by testing **Push-off specimens.**

FRP reinforcing bars

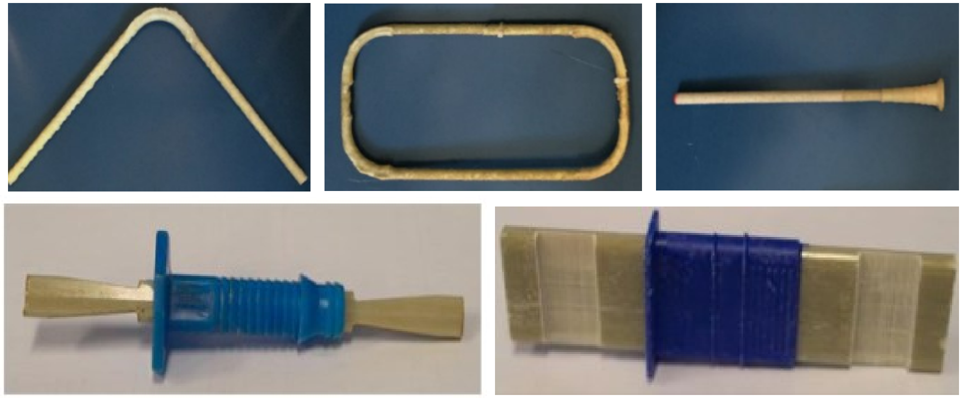

Different Types of Connectors

Specimen Details and Test Setup

Literature Review

Alkatan et al. (2016) Investigate the **shear transfer strength** and the behavior of the **concrete cold-jointed interfaces** when **GFRP** is utilized as a **shear transfer reinforcement**. A total of 20 push-off specimens were cast and tested.

Main Variables

- **Concrete Strength**
- **GFRP Shear Reinforcement Shape**
- **GFRP Shear Reinforcement Stiffness**

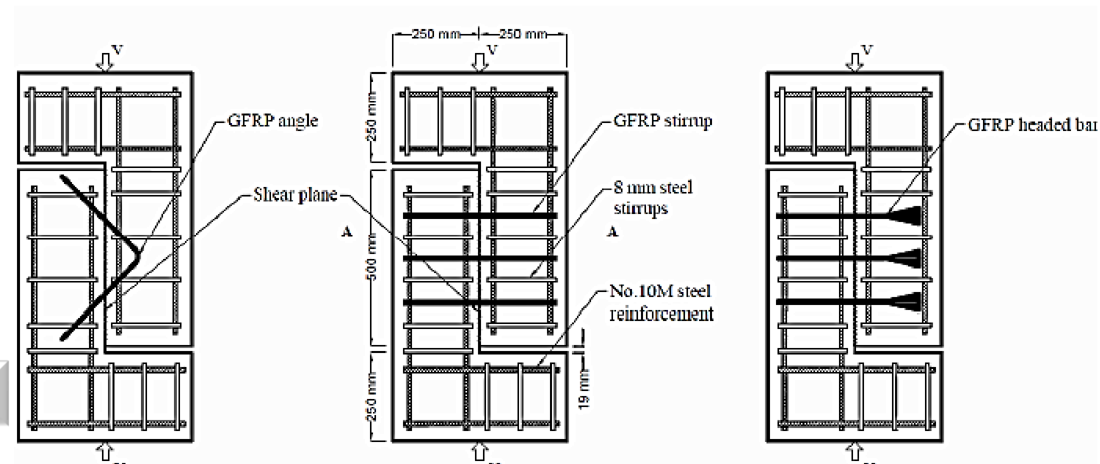

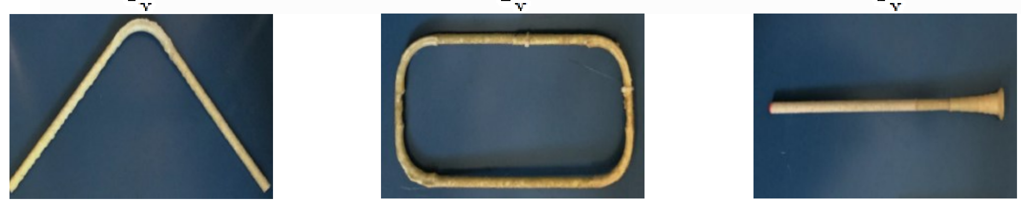

GFRP Shear Reinforcement

Literature Review

Alruwaili et al. (2018) Conducted a research that was an extend for the investigation conducted by Alkatan, (2016) to study the **interface response** for **higher values** of the **GFRP reinforcement stiffness** on the **shear transfer behavior and strength**.

Main Variables

- **Shear Plan Area**
- **GFRP Shear Reinforcement Shape**
- **GFRP Shear Reinforcement Stiffness**

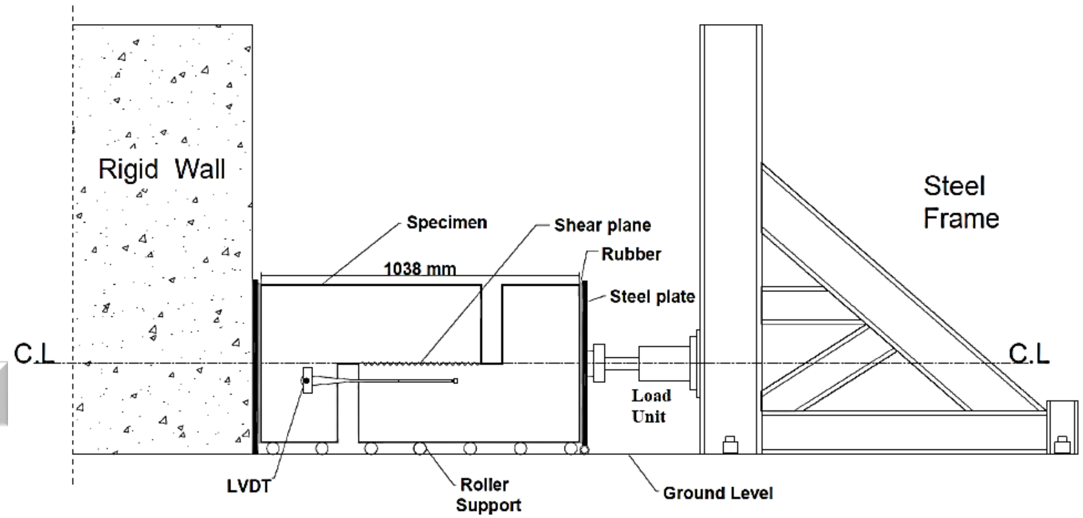

Specimen Details and Test Setup

Literature Review

Connor et al. (2016) Study the **shear-friction** behavior of **sand-coated GFRP** reinforced concrete. A total of **9 push-off specimens** were cast and tested.

Main Variables
- Types of Reinforcement
- Reinforcement Orientation Angles

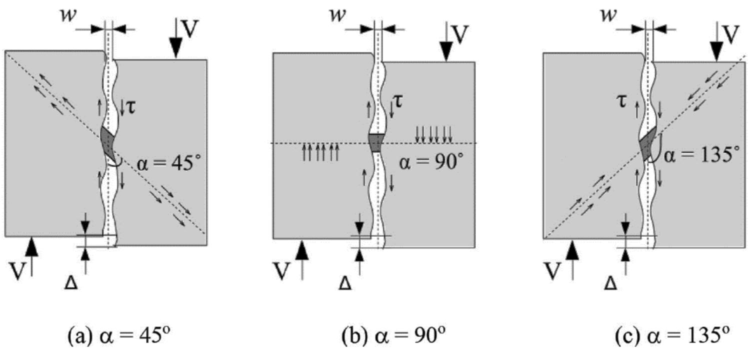

Reinforcement Orientation Angles

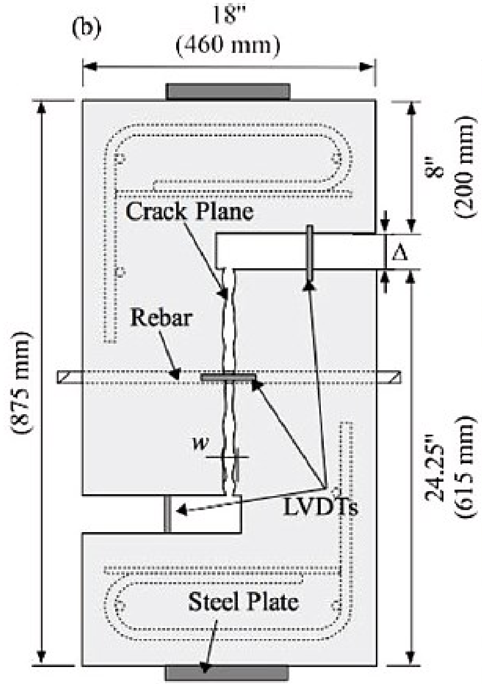

Specimen Details and Test Setup

Research Hypothesis

- Several **ongoing challenges** are related to internal **FRP reinforcement** performance, such as the **bond**, and **dowel-action** (CSA Technical Committee S6-19).
- There are no research results in the literature on the **interface shear** of the **FRP composite T-beams**.
- The performance and behavior of **composite T-beams** reinforced with **GFRP** and **BFRP** as **shear friction** reinforcement needs to be investigated.
- The new edition of **CSA S6-25 (2025)** includes provisions for BFRP bars without any Investigation of the **horizontal shear capacity of BFRB composite T- beams.**

Research Hypothesis

- To assess the structural performance of full-scale **composite concrete T-beams** reinforced with **FRP shear connectors** and **bars** under flexural loading conditions.

- To investigate the influence of different parameters as the **shape of shear reinforcement**, and **shear reinforcement stiffness ratio.**

- To evaluate the **validity** of the current **design guidelines** and equations for the **horizontal shear stress** of **FRP composite T-beams**.

Experimental Program

- A total of **6 specimens** represent **pre-cast girders** and **cast-in-place slabs** are designed according to **CSA S6-19**, and **AASHTO-LRFD-18**.
- **Composite T-Beams** were designed with high resistance in **flexural** and **diagonal shear** to ensure that specimens would fail in **horizontal shear**.

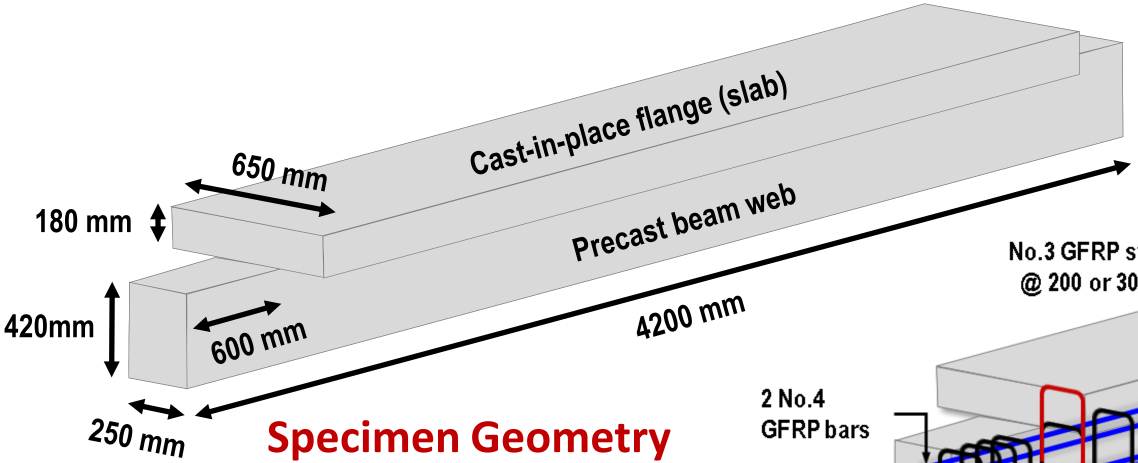

Specimen Geometry

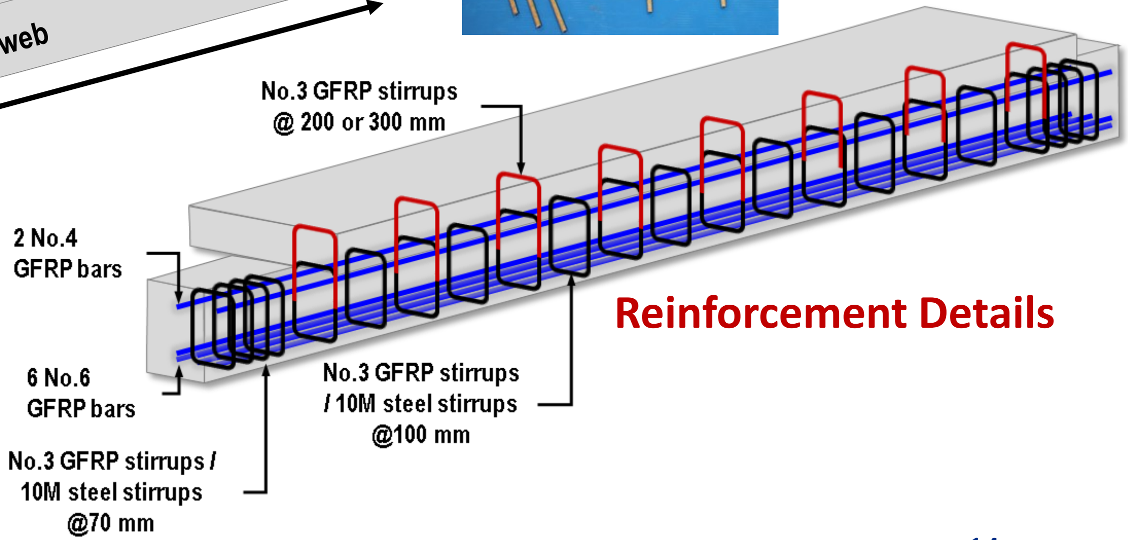

Reinforcement Details

Experimental Program

A total of **six full-scale composite T-beams** reinforced with **GFRP shear reinforcement** were designed and tested under flexural loading.

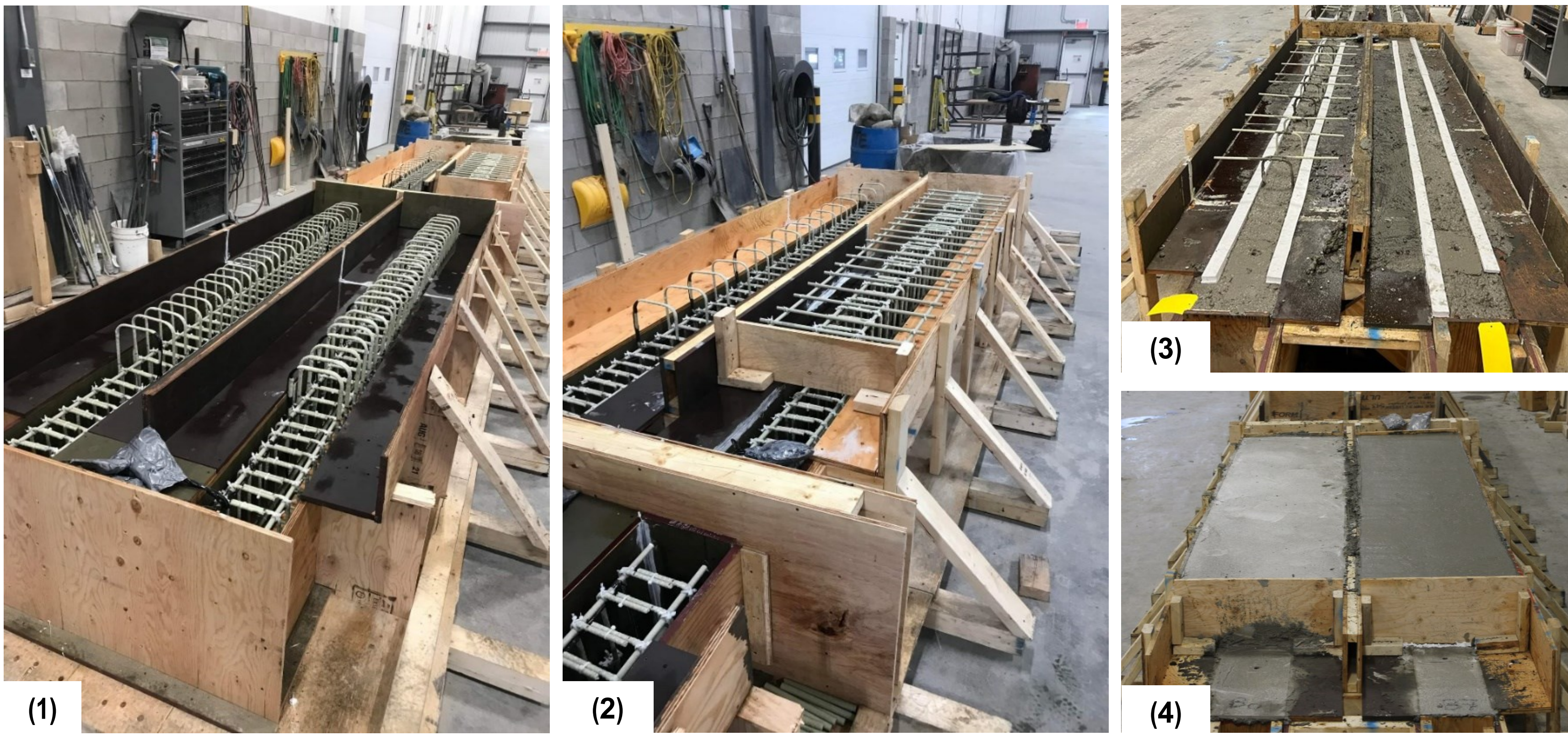

Fabrication Procedures

Experimental Program

All specimens were tested in the structural laboratory at the **University of Sherbrooke** under **concentric load** acting at **one point** until failure.

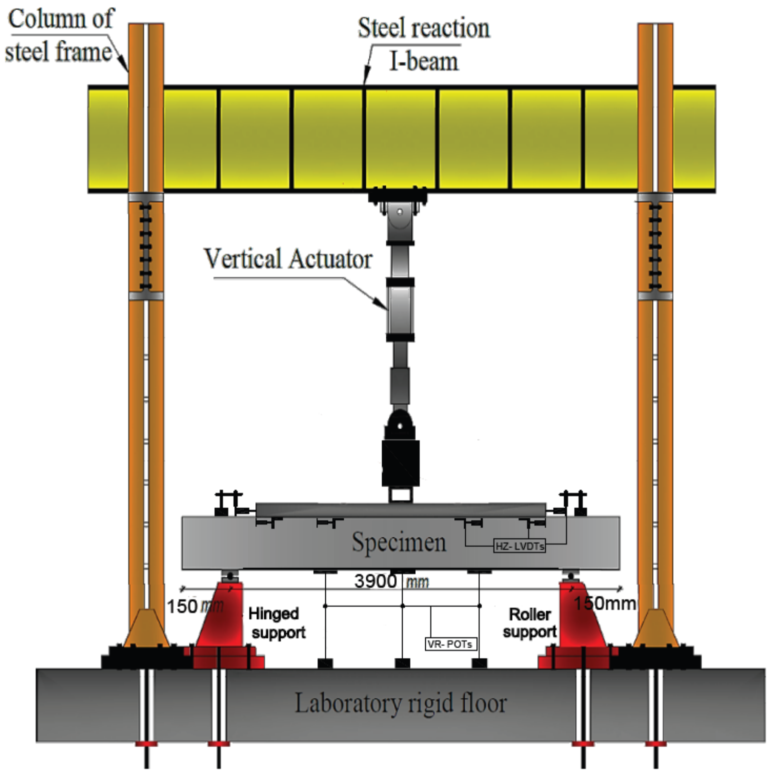

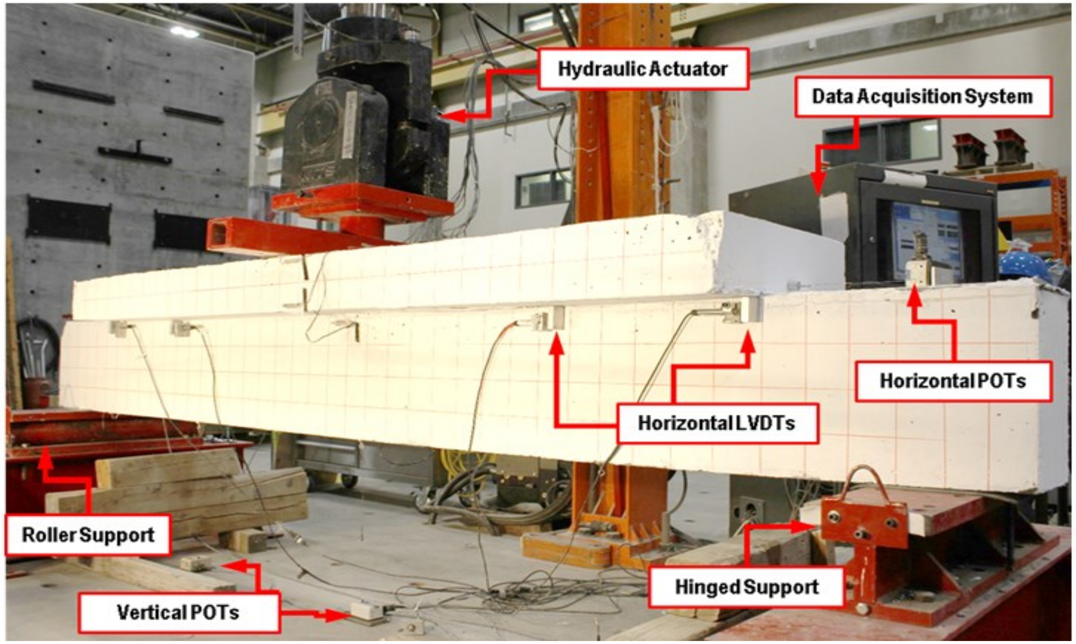

Test Setup and Instrumentation

Results and Discussion

Crack Pattern and Failure Modes

GFRP shear reinforcement

Specimen	Concrete Strength *MPa* After 28 days		Area of Longitudinal Bars mm^2	Interface Width *mm*	Shear Connectors		
	Web	Flange			Type	Shape	ρ_v (%)
BG0	36.2	35.6	1710	150	-	-	-
BG1	36.2	35.6	1710	150	-	-	0.00
BSS_{300}	35.5	35.0	1885	150	Steel	Stirrup	0.35
BGS_{300}	35.5	35.0	1710	150	GFRP	Stirrup	0.32
BGL_{300}	35.5	35.0	1710	150	GFRP	Bent bars	0.32
BGL_{200}	35.5	35.0	1710	150	GFRP	Bent bars	0.48

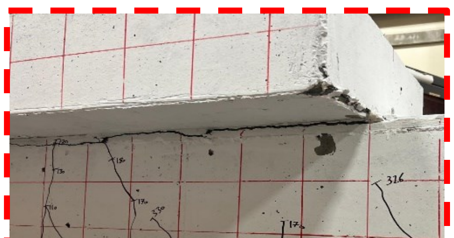


Separation crack

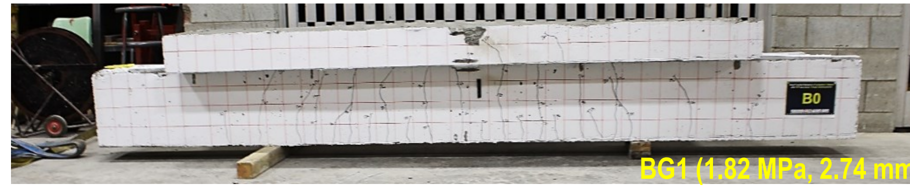

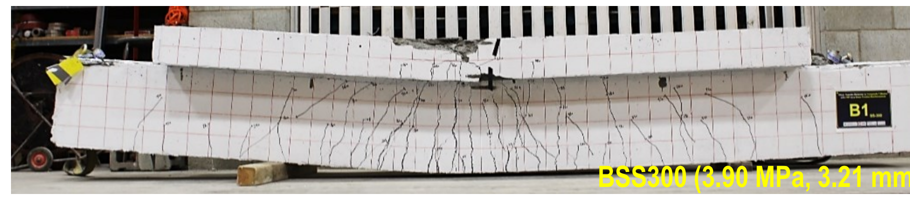

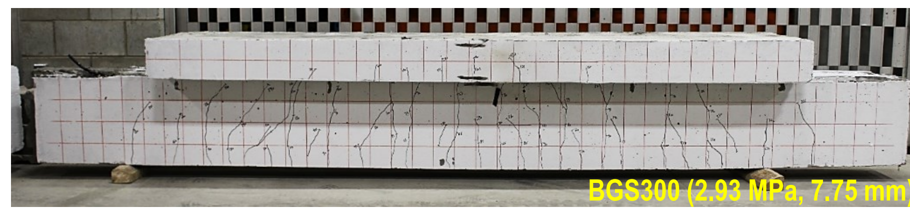

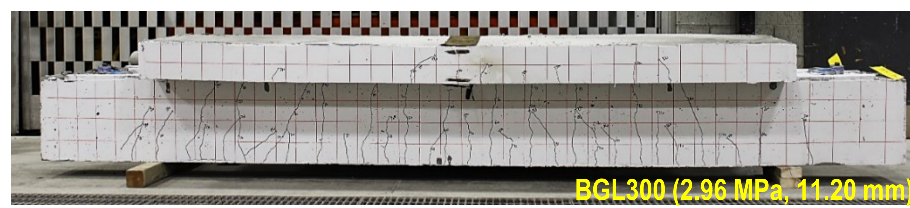

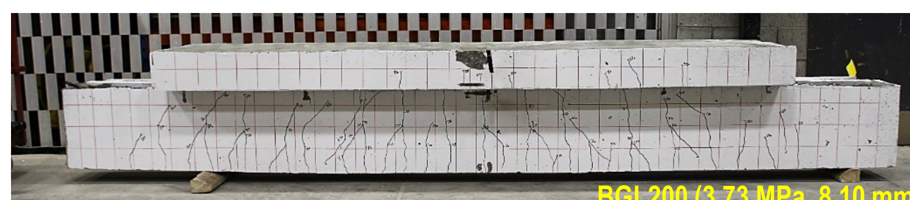

Horizontal shear failure modes

Results and Discussion

Deflection Characteristics

GFRP shear reinforcement (Stirrups / L-Shape)

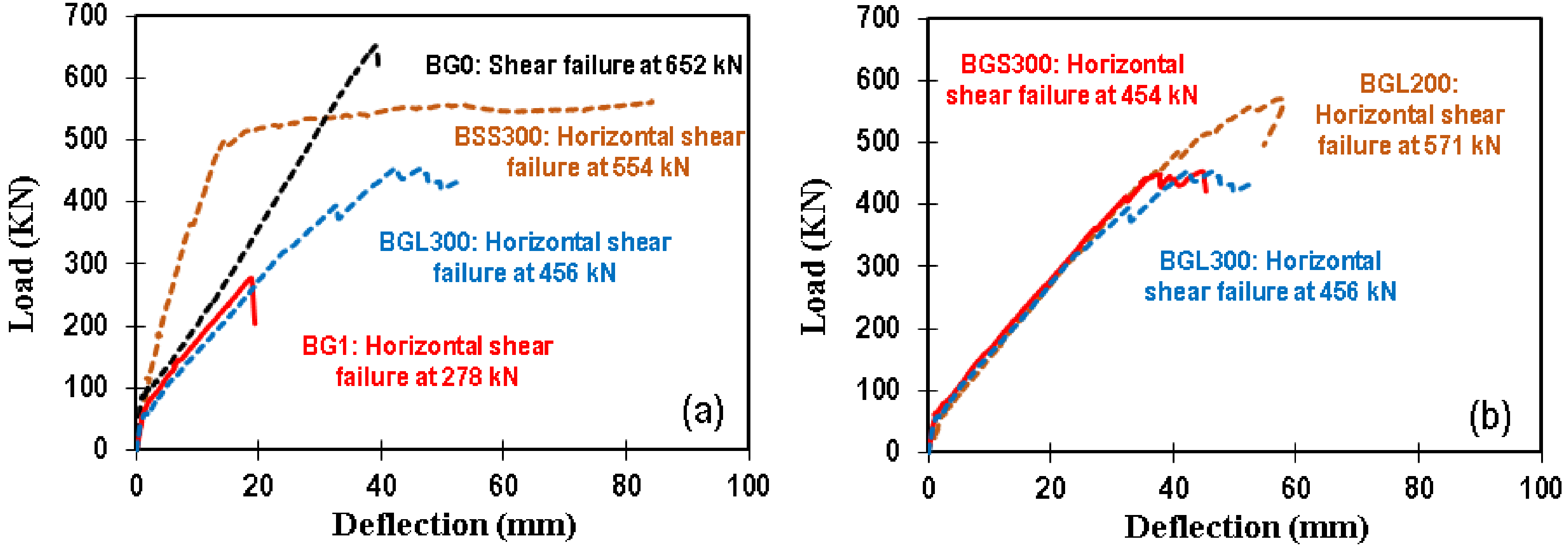

Load-deflection curves at mid-span for all beams

Results and Discussion

Horizontal Shear Stress and Slip

GFRP shear reinforcement (Stirrups / L-Shape)

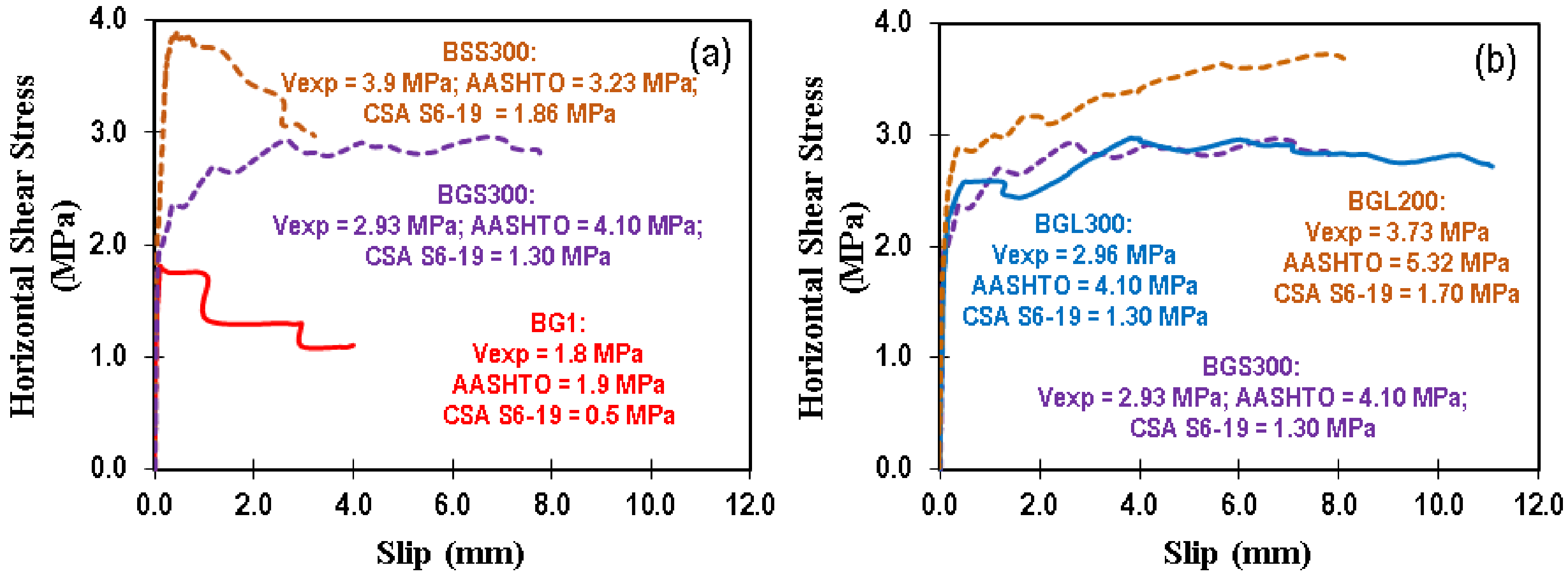

Typical slip curves for the tested beams

Theoretical Investigation

This section summarizes an investigation of the **interface behavior** of **composite T-beams** and a review of the common equations in the codes for calculating the **interface shear stress**.

AASHTO LFRD Bridge Design Guide Specifications for GFRP-Reinforced Concrete **(AASHTO, 2018)**

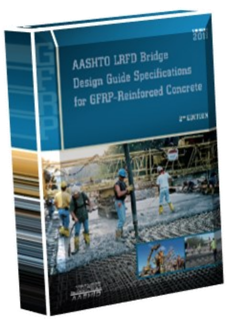

$$v_u = cA_{cv} + \mu(\rho_v f_v + P_c) \leq v_{u\,max}$$

$$v_{u\,max} \leq \ 0.3\, f'_c \text{ or } 9\ MPa$$

$$f_v = \ C_e\, f_{fu}$$

Canadian Highway Bridge Design Code **(CSA S6-19)**

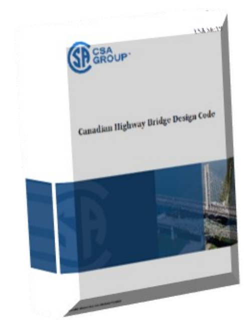

$$v_r = \O_c\,(c + \mu\sigma)$$

$$\sigma = \ \rho_v \varepsilon_f E_f + \frac{N}{A_{cv}}$$

$$\rho_v = \frac{A_{vf}}{A_{cv}} \ \geq \ 0.44\ \%$$

Alkatan's Equation (2016)

$$v_u = 0.04f'_c + 0.005E_f\,\rho_v \sin\alpha + 0.005E_f\,\rho_v \cos\alpha$$

Theoretical Investigation

The **AASHTO LRFD (2018)**, **CAN/CSA S6-19** and **Alkatan's Equation** design provisions were assessed by comparing their predictions to the experimental results.

GFRP shear reinforcement (Stirrups / L-Shape)

Specimen	ρ_v %	Experimental	AASHTO LRFD-18		CSA S6-19		Alkatan (2018)	
		v_{exp}	v_{eq}	v_{exp}/v_{eq}	v_{eq}	v_{exp}/v_{eq}	v_{eq}	v_{exp}/v_{eq}
BG1	0	1.82	1.90	0.95	0.50	3.5	1.40	1.30
BSS_{300}	0.32	3.90	3.23	1.21	1.86	2.10	-	-
BGS_{300}	0.32	2.93	4.10	0.71	1.30	2.25	2.36	1.24
BGL_{300}	0.32	2.96	4.10	0.72	1.30	2.28	2.36	1.25
BGL_{200}	0.48	3.73	5.32	0.70	1.7	2.20	2.84	1.31

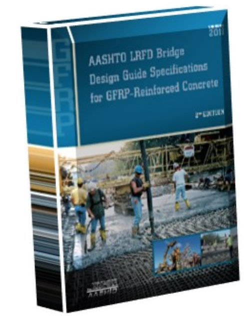

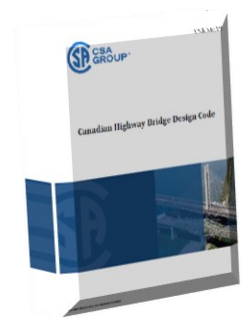

Conclusions

- The composite **GFRP-RC** T-beams exhibited **adequate interface shear resistance** before failure and achieved reasonable values of **slip** when compared to the steel-reinforced concrete specimen.
- All of the **composite FRP-RC T-beams** were able to sustain **high horizontal shear strength** after the interface crack occurred and at **higher values of slip** till failure. The **horizontal shear capacity** and **slippage** were significantly impacted by increasing the **shear interface reinforcement ratio**, even after separation had occurred.
- All the **FRP interface shear reinforcement** experienced a strain higher than **5000 με** at the ultimate state. This emphasizes the role of **FRP shear connectors** before and after slippage and is consistent with **CAN/CSA S6-19** provisions.
- The **AASHTO LRFD** and **CAN/CSA S6-19** equations could not accurately predict the **horizontal shear stress** of the interfaces with **GFRP** shear reinforcement. A new equation should be presented for the horizontal shear transfer of FRP shear connectors.

Conclusions

https://www.concrete.org/publications/internationalconcreteabstractsportal

ACI Structural Journal 121(4) – DOI: 10.14359/51740718

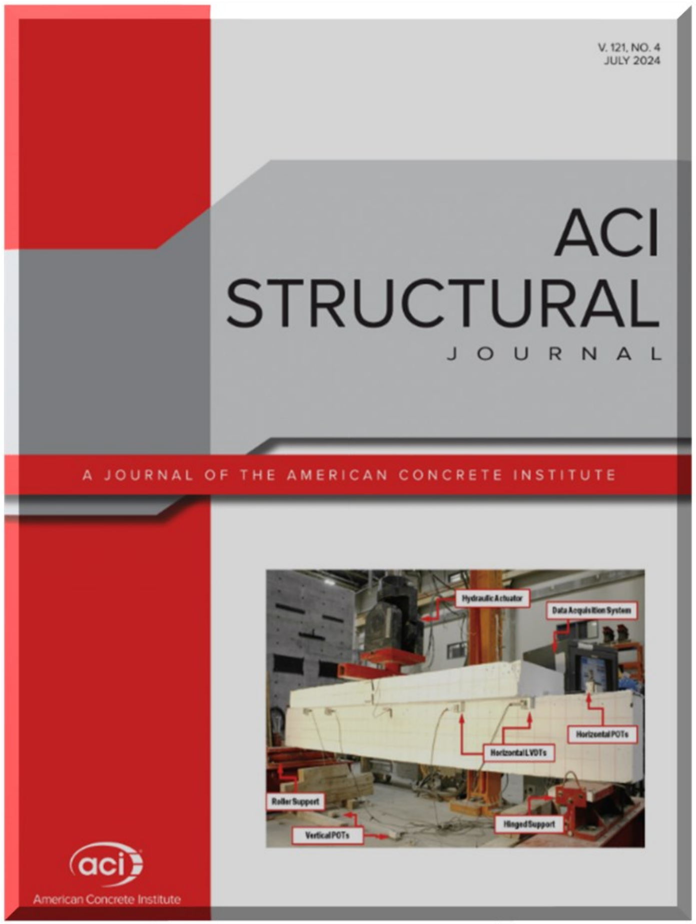

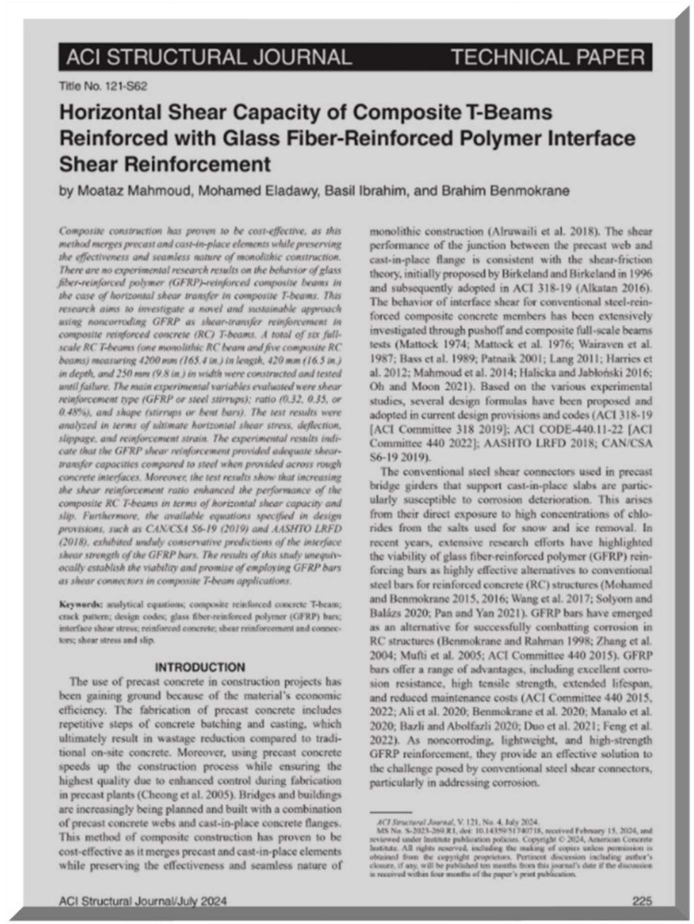

ACI STRUCTURAL JOURNAL TECHNICAL PAPER

Title No. 121-S62

Horizontal Shear Capacity of Composite T-Beams Reinforced with Glass Fiber-Reinforced Polymer Interface Shear Reinforcement

by Moataz Mahmoud, Mohamed Eladawy, Basil Ibrahim, and Brahim Benmokrane

Composite construction has proven to be cost-effective, as this method merges precast and cast-in-place elements while preserving the effectiveness and seamless nature of monolithic construction. There are no experimental research results on the behavior of glass fiber-reinforced polymer (GFRP)-reinforced composite beams in the case of horizontal shear transfer in composite T-beams. This research aims to investigate a novel and sustainable approach using noncorroding GFRP as shear-transfer reinforcement in composite reinforced concrete (RC) T-beams. A total of six full-scale RC T-beams (one monolithic RC beam and five composite RC beams) measuring 4200 mm (165.4 in.) in length, 420 mm (16.5 in.) in depth, and 250 mm (9.8 in.) in width were constructed and tested until failure. The main experimental variables evaluated were shear reinforcement type (GFRP or steel stirrups); ratio (0.32, 0.35, or 0.48%), and shape (stirrups or bent bars). The test results were analyzed in terms of ultimate horizontal shear stress, deflection, slippage, and reinforcement strain. The experimental results indicate that the GFRP shear reinforcement provided adequate shear-transfer capacities compared to steel when provided across rough concrete interfaces. Moreover, the test results show that increasing the shear reinforcement ratio enhanced the performance of the composite RC T-beams in terms of horizontal shear capacity and slip. Furthermore, the available equations specified in design provisions, such as CAN/CSA S6-19 (2019) and AASHTO LRFD (2018), exhibited unduly conservative predictions of the interface shear strength of the GFRP bars. The results of this study unequivocally establish the viability and promise of employing GFRP bars as shear connectors in composite T-beam applications.

Keywords: analytical equations; composite reinforced concrete T-beam; crack pattern; design codes; glass fiber-reinforced polymer (GFRP) bars; interface shear stress; reinforced concrete; shear reinforcement and connectors; shear stress and slip.

INTRODUCTION

The use of precast concrete in construction projects has been gaining ground because of the material's economic efficiency. The fabrication of precast concrete includes repetitive steps of concrete batching and casting, which ultimately result in wastage reduction compared to traditional on-site concrete. Moreover, using precast concrete speeds up the construction process while ensuring the highest quality due to enhanced control during fabrication in precast plants (Cheong et al. 2005). Bridges and buildings are increasingly being planned and built with a combination of precast concrete webs and cast-in-place concrete flanges. This method of composite construction has proven to be cost-effective as it merges precast and cast-in-place elements while preserving the effectiveness and seamless nature of monolithic construction (Alruwaili et al. 2018). The shear performance of the junction between the precast web and cast-in-place flange is consistent with the shear-friction theory, initially proposed by Birkeland and Birkeland in 1996 and subsequently adopted in ACI 318-19 (Alkatan 2016). The behavior of interface shear for conventional steel-reinforced composite concrete members has been extensively investigated through pushoff and composite full-scale beams tests (Mattock 1974; Mattock et al. 1976; Wairaven et al. 1987; Bass et al. 1989; Patnaik 2001; Lang 2011; Harries et al. 2012; Mahmoud et al. 2014; Halicka and Jabłoński 2016; Oh and Moon 2021). Based on the various experimental studies, several design formulas have been proposed and adopted in current design provisions and codes (ACI 318-19 [ACI Committee 318 2019]; ACI CODE-440.11-22 [ACI Committee 440 2022]; AASHTO LRFD 2018; CAN/CSA S6-19 2019).

The conventional steel shear connectors used in precast bridge girders that support cast-in-place slabs are particularly susceptible to corrosion deterioration. This arises from their direct exposure to high concentrations of chlorides from the salts used for snow and ice removal. In recent years, extensive research efforts have highlighted the viability of glass fiber-reinforced polymer (GFRP) reinforcing bars as highly effective alternatives to conventional steel bars for reinforced concrete (RC) structures (Mohamed and Benmokrane 2015, 2016; Wang et al. 2017; Solyom and Balázs 2020; Pan and Yan 2021). GFRP bars have emerged as an alternative for successfully combatting corrosion in RC structures (Benmokrane and Rahman 1998; Zhang et al. 2004; Mufti et al. 2005; ACI Committee 440 2015). GFRP bars offer a range of advantages, including excellent corrosion resistance, high tensile strength, extended lifespan, and reduced maintenance costs (ACI Committee 440 2015, 2022; Ali et al. 2020; Benmokrane et al. 2020; Manalo et al. 2020; Bazli and Abolfazli 2020; Duo et al. 2021; Feng et al. 2022). As noncorroding, lightweight, and high-strength GFRP reinforcement, they provide an effective solution to the challenge posed by conventional steel shear connectors, particularly in addressing corrosion.

ACI Structural Journal, V. 121, No. 4, July 2024.
MS No. S-2023-269.R1, doi: 10.14359/51740718, received February 15, 2024, and reviewed under Institute publication policies. Copyright © 2024, American Concrete Institute. All rights reserved, including the making of copies unless permission is obtained from the copyright proprietors. Pertinent discussion including author's closure, if any, will be published ten months from this journal's date if the discussion is received within four months of the paper's print publication.

ACI Structural Journal/July 2024 225

NSERC CRSNG
MIAMI
FDOT

ACKNOWLEDGMENT

- **Tier-1 Canada Research Chair** in Advanced FRP Composite Materials for Civil Structures.
- **NSERC/Industrial Research Chair** in Innovative FRP Reinforcement for Concrete Structures.
- **Natural Sciences and Engineering Research Council** of Canada (NSERC).
- **Mathematics of Information Technology and Complex System** (MITACS).
- **Université de Sherbrooke**, Department of Civil Engineering.

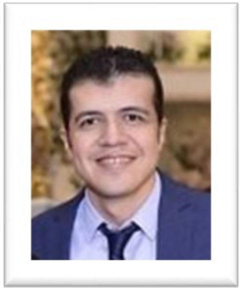

Moataz Mahmoud

Ph.D., M.Sc., Department of Civil Engineering, Université de Sherbrooke,

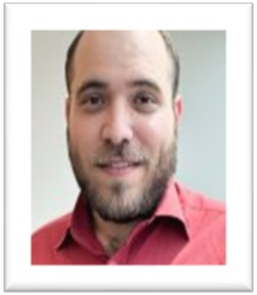

Basil Ibrahim

Ph.D., M.Sc., Postdoctoral fellow, Department of Civil Engineering, Université de Sherbrooke,

FOURTH INTERNATIONAL WORKSHOP ON FRP BARS FOR CONCRETE STRUCTURES

"Advances in concrete reinforcement"

August 8-9, 2024 - Toronto, Ontario

BEHAVIOR OF LIGHTWEIGHT CONCRETE ELEMENTS REINFORCED WITH FRP BARS UNDER FLEXURE, SHEAR AND AXIAL LOAD & DESIGN CODES

Shehab Mehany

Presenter

Ahmed ELbady

SPONSORED BY:

PULTRALL V-ROD FIBERGLASS Innovations ALTAIR MST BAR MAXIMUM STRENGTH GFRP SFTec ACMA American Composites Manufacturers Association FRP Rebar Manufacturers Council

Université de Sherbrooke NSERC CRSNG University of Miami Center for Integration of Composites into Infrastructure FDOT

Reinforced concrete structures

Lightweight Concrete (LWC)

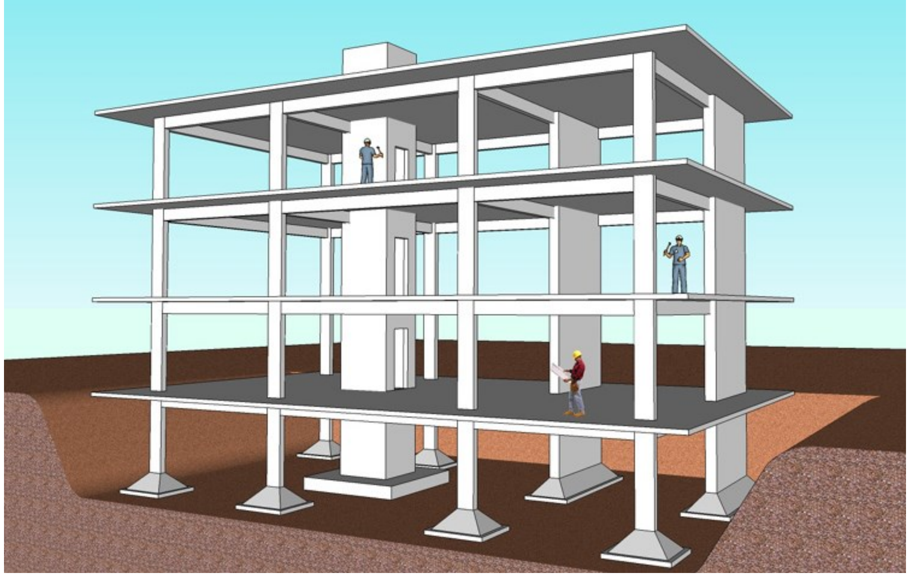

Current FRP design codes and guidelines

The current FRP design codes and guidelines provide limited recommendations for using FRP bars in lightweight concrete elements.

LWC Beams (Shear and Flexure)

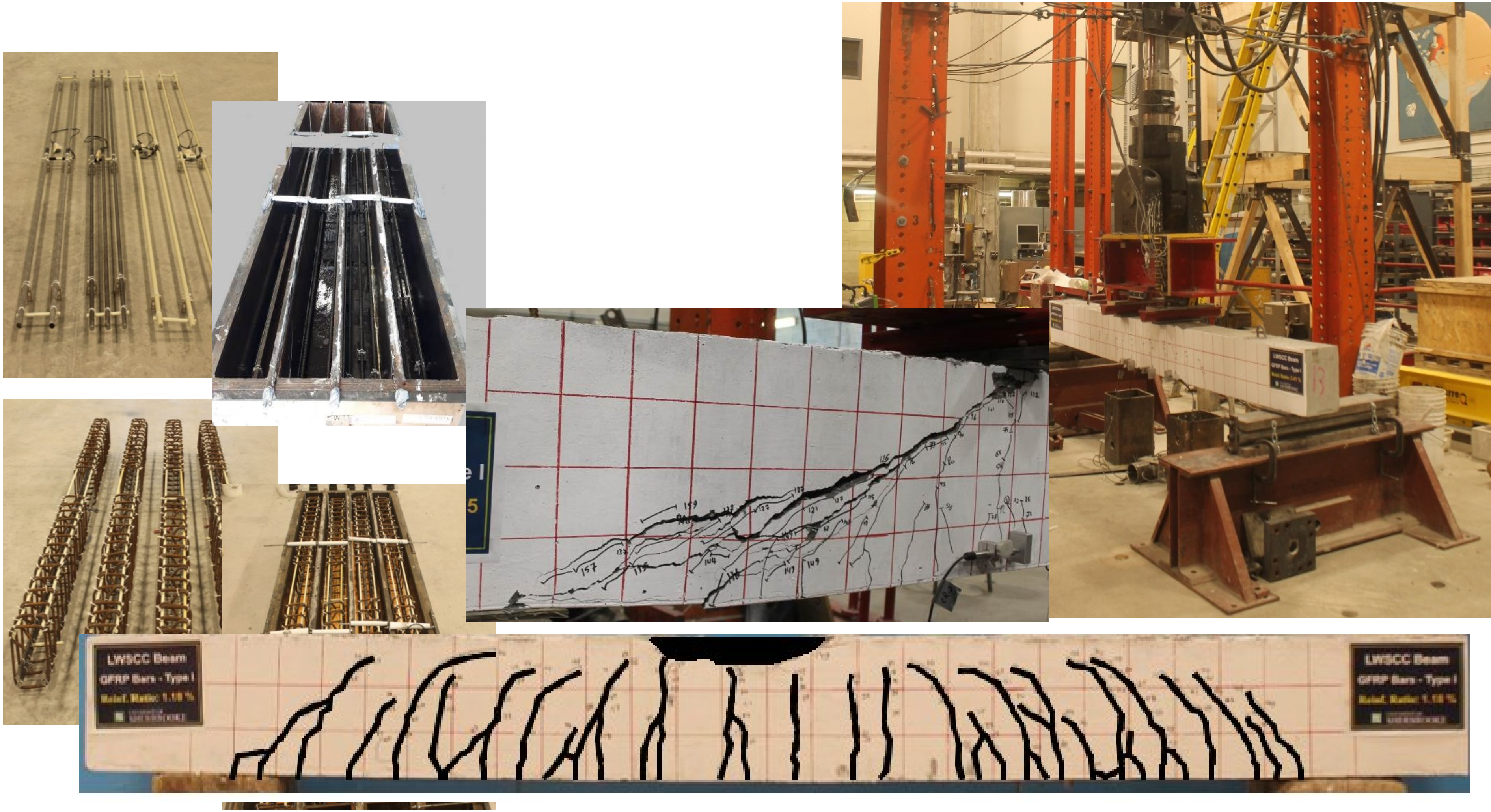

LWC Slabs

LWC Columns

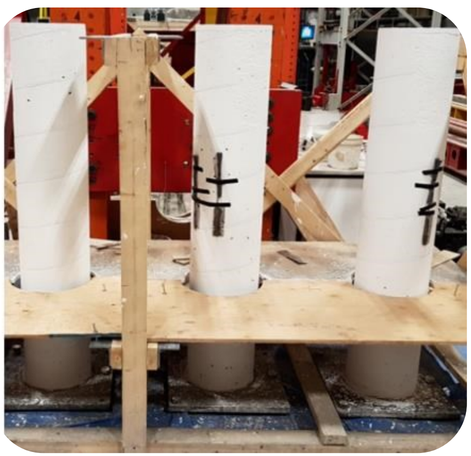

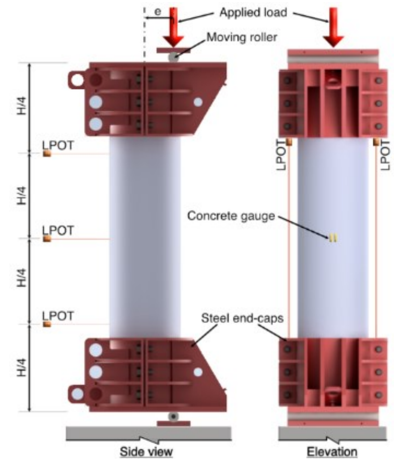
e
Applied load
Moving roller
H/4
H/4
H/4
H/4
LPOT
LPOT
LPOT
LPOT
LPOT
Concrete gauge
Steel end-caps
Side view
Elevation

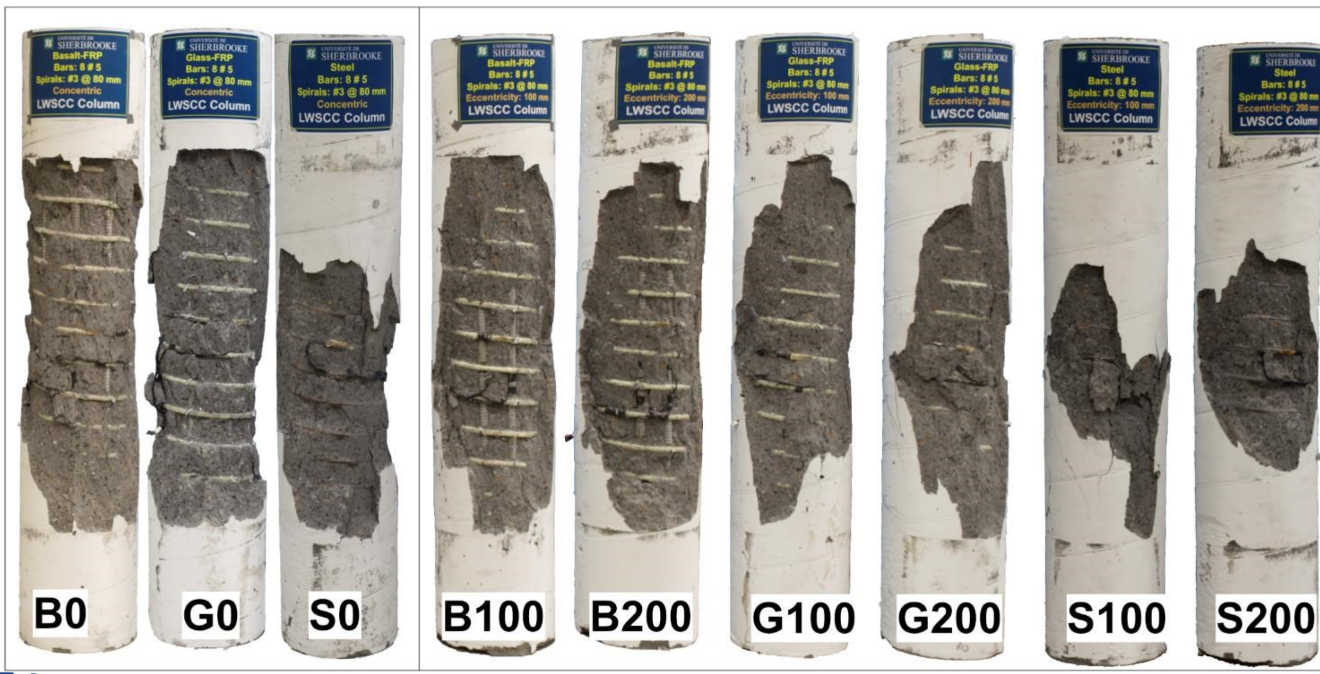
B0
G0
S0
B100
B200
G100
G200
S100
S200

Concrete Shear Strength (Vc)

Evaluation of the Concrete Shear Strength Equations of FRP-reinforced LWC Specimens

CSA S806-12

$\lambda = 0.85$ For semi-low-density concrete

$\lambda = 0.75$ For low-density concrete

ACI 440.1R-15

$\lambda = 0.80$ For Sand-LWC

CSA S6-19

$f_{cr} = 0.30\sqrt{f'_c}$ Density less than 1850 kg/m³

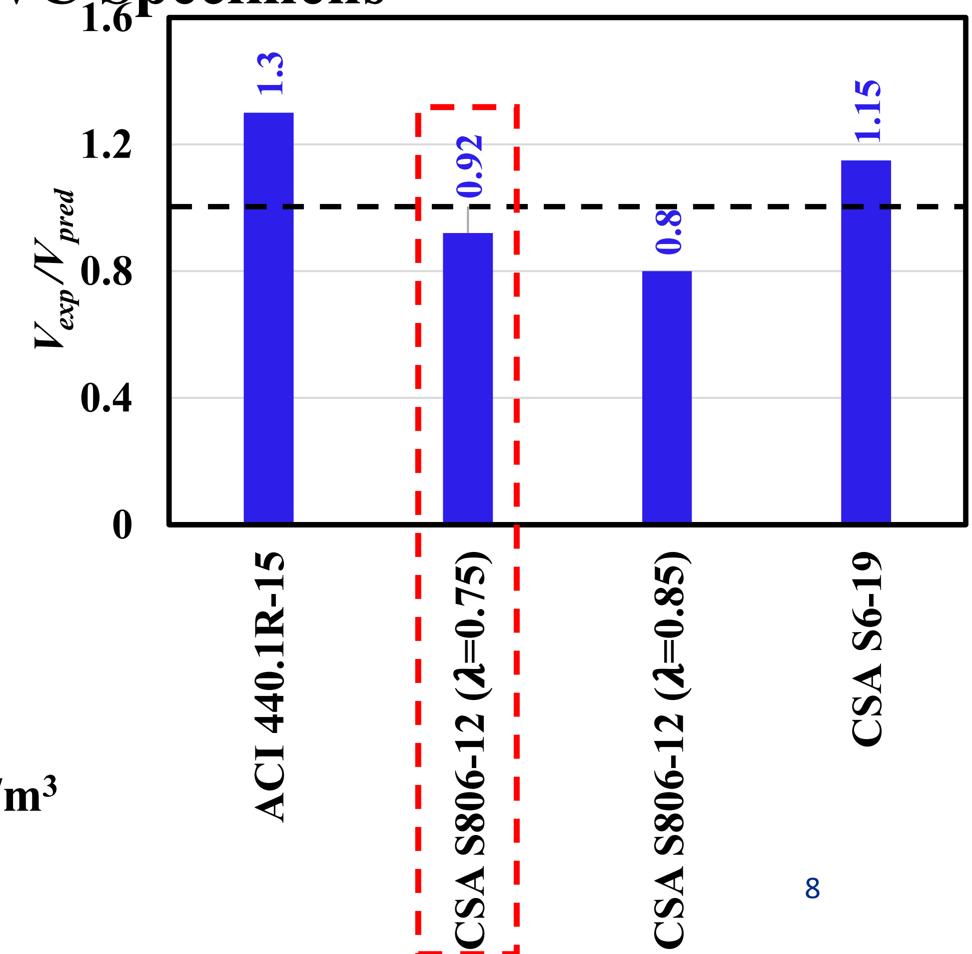

Cracking and Ultimate Moment

The cracking moment can be calculated with the following equation

ACI 440.1R-15

$$M_{cr} = \frac{f_r \times I_g}{y_t} \qquad f_r = 0.62\lambda\sqrt{f'_c}$$

$\lambda = 0.80$ **As recommended by ACI 318-19**

The average normalized tensile strength of the LWC was 81% of that of the NWC

$$M_{cr\text{-}exp}/M_{cr\text{-}pred} = 0.84$$

The cracking moment was controlled by the λ value for LWC

Beam ID	ACI 440.1R-15	
	$M_{cr\text{-}exp}/M_{cr\text{-}pred}$	$M_{n\text{-}exp}/M_{n\text{-}pred}$
LS-BI-2.52	0.80	1.07
LS-BI-1.78	0.83	1.04
LS-BI-1.18	0.80	1.03
LS-BII-1.65	0.83	1.02
LS-BII-1.18	0.78	1.02
LS-BII-0.78	0.75	1.05
LS-BIII-1.15	0.81	1.12
LS-BIII-0.72	0.85	1.22
LS-GI-3#8	0.99	1.02
LS-GI-4#6	0.92	0.99
LS-GI-3#6	0.77	1.02
LS-GI-3#5	0.87	0.96
LS-GI-2#5	0.83	0.94
LS-GII-3#5	0.78	0.96
LS-GII-2#5	0.69	0.95

Cracking and Ultimate Moment

By considering the force equilibrium and strain compatibility

$$\alpha_1 f'_c ba + A'_f f'_f = A_f f_f$$

$$M_n = A_f f_f \left(d - \frac{a}{2}\right) + A'_f f'_f \left(\frac{a}{2} - d'\right)$$

The predictions were in good agreement with the experimental results as the value of $M_{n\text{-}exp}/M_{n\text{-}pred}$ ranged from 0.94 to 1.07

Beam ID	ACI 440.1R-15	
	$M_{cr\text{-}exp}/M_{cr\text{-}pred}$	$M_{n\text{-}exp}/M_{n\text{-}pred}$
LS-BI-2.52	0.80	1.07
LS-BI-1.78	0.83	1.04
LS-BI-1.18	0.80	1.03
LS-BII-1.65	0.83	1.02
LS-BII-1.18	0.78	1.02
LS-BII-0.78	0.75	1.05
LS-BIII-1.15	0.81	1.12
LS-BIII-0.72	0.85	1.22
LS-GI-3#8	0.99	1.02
LS-GI-4#6	0.92	0.99
LS-GI-3#6	0.77	1.02
LS-GI-3#5	0.87	0.96
LS-GI-2#5	0.83	0.94
LS-GII-3#5	0.78	0.96
LS-GII-2#5	0.69	0.95

Crack Control

Evaluation of the Bond-Dependent Coefficient (k_b)

Sand-coated FRP bars

Beam ID	ACI 440.1R-15	ACI 440X-XX	AASHTO-18	CSA S6-19
LS-GS-4#6	0.92	0.94	0.92	0.84
LS-GS-3#6	0.92	0.89	0.92	0.81
LS-GS-3#5	1.00	1.02	1.00	0.99
LS-GS-2#5	0.92	0.96	0.92	0.93
LS-BS-4#6	0.80	0.79	0.80	0.75
LS-BS-3#6	0.86	0.81	0.86	0.77
LS-BS-2#6	0.79	0.81	0.79	0.75

Helically grooved FRP bars

Beam ID	ACI 440.1R-15	ACI 440X-XX	AASHTO-18	CSA S6-19
LS-GH-3#5	1.11	1.03	1.11	1.10
LS-GH-2#5	0.95	0.94	0.95	0.95
LS-BH-4#5	0.95	0.94	0.95	0.95
LS-BH-3#5	1.11	1.10	1.11	1.10
LS-BH-2#5	0.93	0.87	0.93	0.93

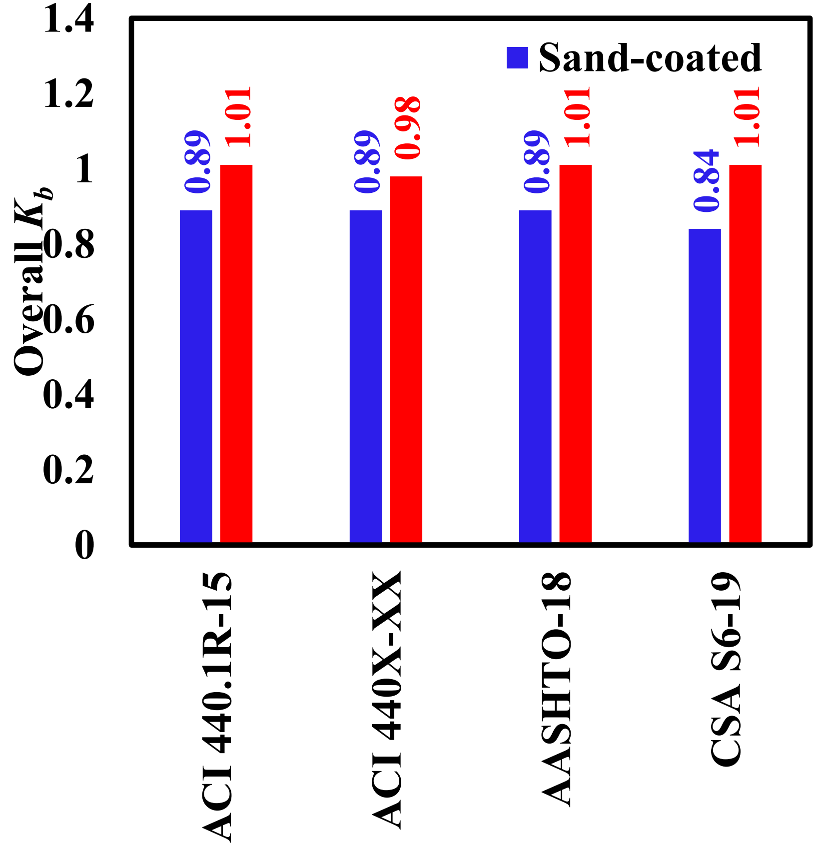

k_b=0.90 Sand-coated FRP bars

k_b=1.10 Helically grooved FRP bars

Deflection

The immediate mid-span deflection for a simply supported RC element

$$\delta = \frac{(P/2)a}{24E_c I_e}\left[3L^2 - 4a^2\right]$$

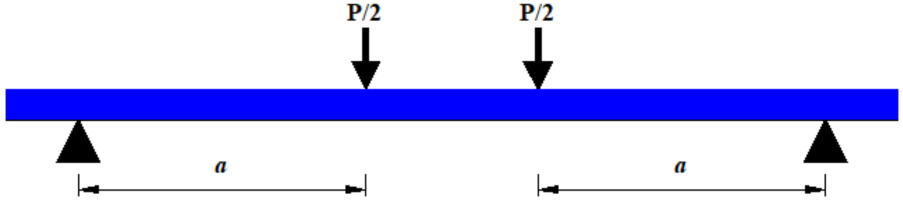

Benmokrane et al. (1996)

$$I_e = \left(\frac{M_{cr}}{M_a}\right)^3 \frac{I_g}{\beta} + \left[1 - \left(\frac{M_{cr}}{M_a}\right)^3\right] \alpha I_{cr} \le I_g$$

Bischoff (2005)

$$I_e = \frac{I_{cr}}{1 - \left(\frac{M_{cr}}{M_a}\right)^2 \left(1 - \frac{I_{cr}}{I_g}\right)}$$

Thériault and Benmokrane (1998)

$$I_e = \left(\frac{M_{cr}}{M_a}\right)^3 \beta_d I_g + \left[1 - \left(\frac{M_{cr}}{M_a}\right)^3\right] I_{cr} \le I_g$$

ISIS-07

$$I_e = \frac{I_t I_{cr}}{I_{cr} + \left(1 - 0.5\left(\frac{M_{cr}}{M_a}\right)^2\right)(I_t - I_{cr})}$$

ACI 440.1R-15

$$I_e = \frac{I_{cr}}{1 - \gamma\left(\frac{M_{cr}}{M_a}\right)^2 \left(1 - \frac{I_{cr}}{I_g}\right)} \le I_g$$

Deflection

Evaluation of the Effective Moment of Inertia of FRP-reinforced LWC Specimens

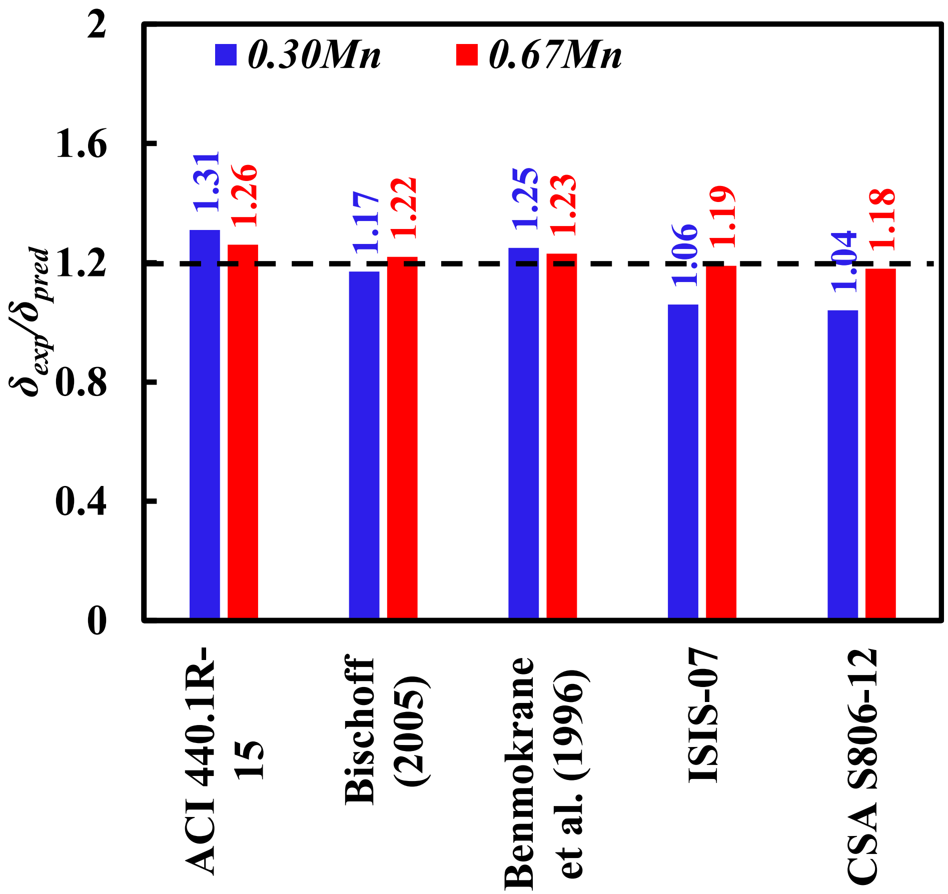

Proposed Modification to the ACI 440.1R-15 Equation for LWC Specimens

The magnitude of M_{cr} has a direct effect on I_e.

The experimental and deflection values predicted according to the ACI 440.1R-15 model were compared

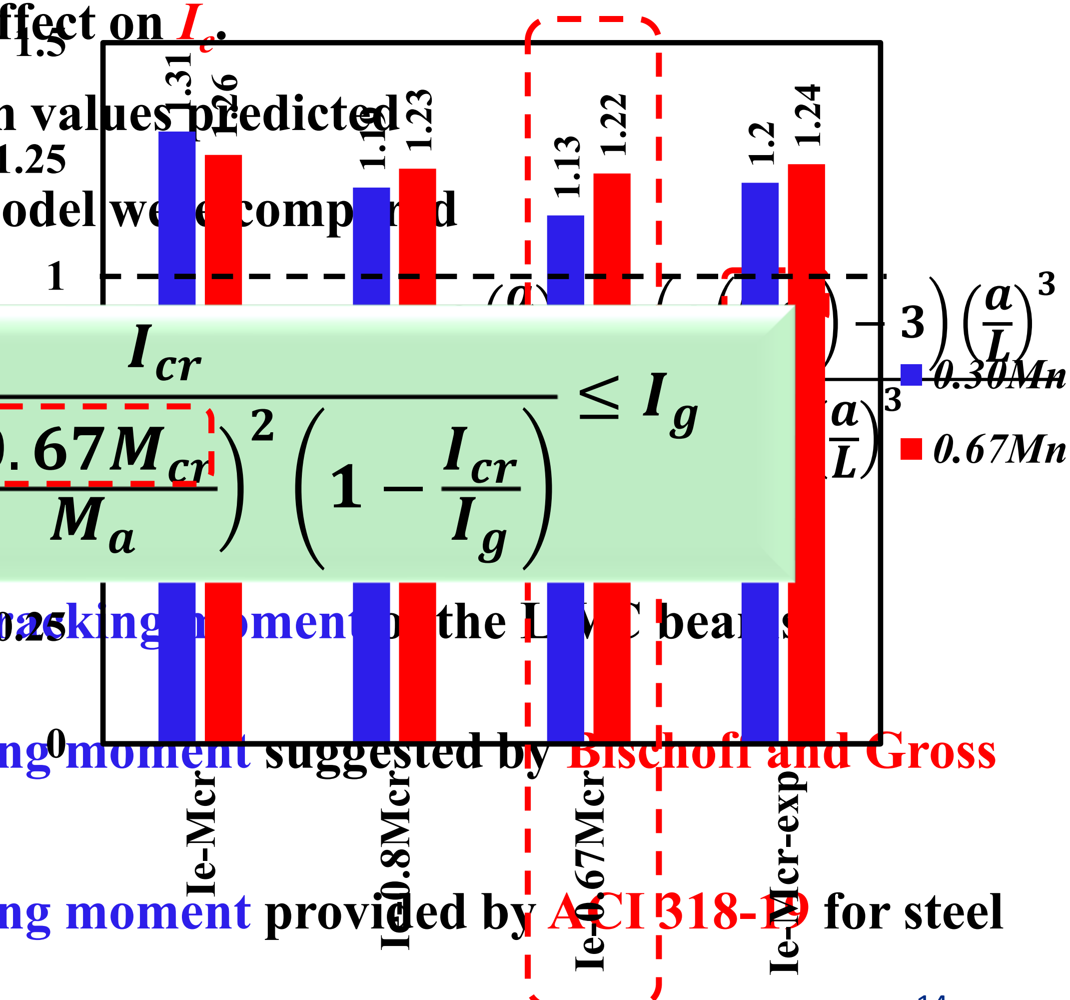

$$I_e = \frac{I_{cr}}{1-\gamma\left(\frac{0.67M_{cr}}{M_a}\right)^2\left(1-\frac{I_{cr}}{I_g}\right)} \le I_g$$

$M_{cr} = M_{cr\text{-}exp}$ The experimental cracking moment of the LWC beams

$M_{cr} = 0.80M_{cr}$ The reduced cracking moment suggested by Bischoff and Gross (2011) for FRP-RC

$M_{cr} = 0.67M_{cr}$ The reduced cracking moment provided by ACI 318-19 for steel

NSERC CRSNG MIAMI FDOT

Significance of the Research Program

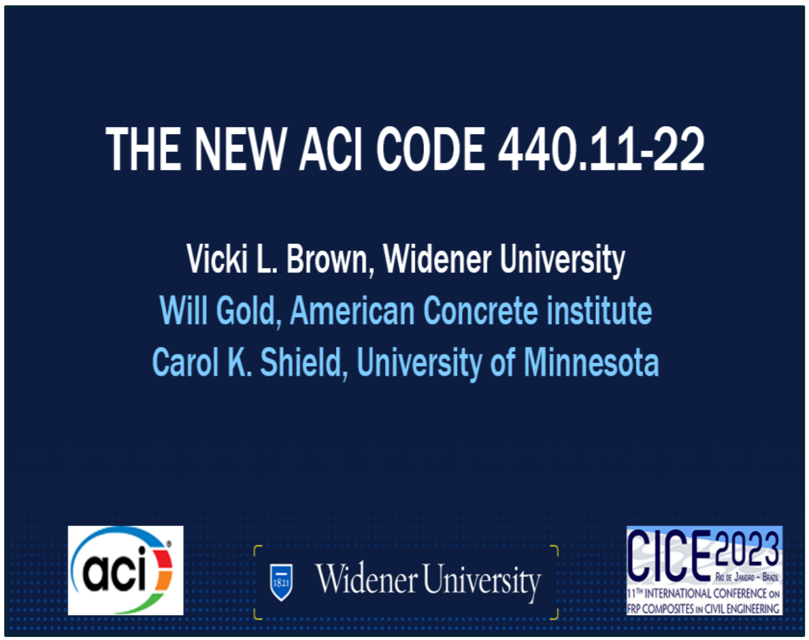

Vicki L. Brown, CICE 2023

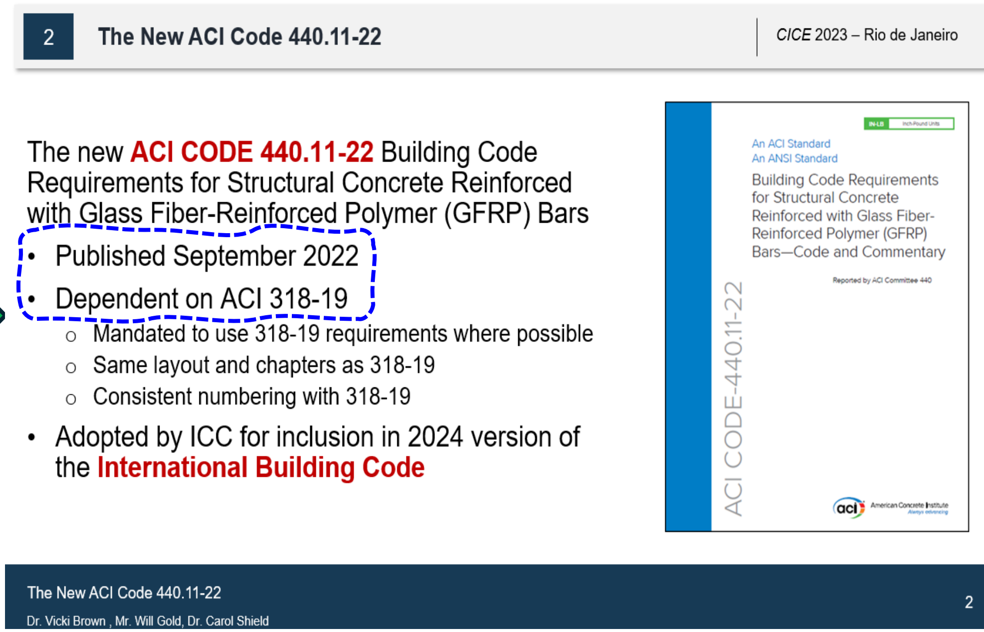

BEFORE…

Significance of the Research Program

8 The New ACI Code 440.11-22 | *CICE* 2023 – Rio de Janeiro

- Chapter 1 – General
- Chapter 2 - Notation and Terminology
- Chapter 3 - Referenced Standards
- Chapter 4 – Structural System Requirements
- Chapter 5 – Loads
- Chapter 6 - Structural Analysis
- Chapter 7 – One-Way Slabs
- Chapter 8 – Two-Way Slabs
- Chapter 9 – Beams
- Chapter 10 – Columns
- Chapter 11 – Walls
- ~~Chapter 12 – Diaphragms~~
- Chapter 13 – Foundations
- ~~Chapter 14 – Plain Concrete~~
- Chapter 15 – Beam-Column and Slab-Column Joints
- Chapter 16 – Connections between Members
- ~~Chapter 17 – Anchoring to Concrete~~
- ~~Chapter 18 – Earthquake-Resistant Structures~~
- Chapter 19 – Concrete: Design and Durability Requirements
- Chapter 20 – GFRP Reinforcement Properties, Durability, and Embedments
- Chapter 21 – Strength Reduction Factors
- Chapter 22 – Sectional Strength
- ~~Chapter 23 – Strut &Tie Models~~
- Chapter 24 – Serviceability Requirement
- Chapter 25 – Reinforcement Details
- Chapter 26 – Construction Documents a
- Chapter 27 – Strength Evaluation of Exi Structures

The New ACI Code 440.11-22
Dr. Vicki Brown , Mr. Will Gold, Dr. Carol Shield

9 The New ACI Code 440.11-22 | *CICE* 2023 – Rio de Janeiro

Code DOES cover:

- Beams
- One-way and two-way slabs
- Columns
- Walls
- Foundations
- Joints/Connections between members
- Strength evaluation of existing structures
- Torsion

Code does not currently cover:

- Lightweight concrete
- Prestressed concrete
- Deep beams
- Shotcrete
- SDC D-F totally excluded
- SDC B-C excluded if part of the lateral load resisting system

The New ACI Code 440.11-22
Dr. Vicki Brown , Mr. Will Gold, Dr. Carol Shield
9

The current ACI 440.11-22 design code does not include using FRP bars in lightweight concrete elements due to limited data and experimental evidences

BEFORE…

Significance of the Research Program

✓ Publications

- Mehany, S., Mohamed, H.M. and Benmokrane, B., 2023. Performance of Lightweight Self-Consolidating Concrete Beams Reinforced with Glass Fiber-Reinforced Polymer Bars without Stirrups under Shear. ***ACI Structural Journal*, *120*(1).**
- Mehany, S., Mohamed, H.M. and Benmokrane, B., 2023. Flexural Behavior and Serviceability Performance of Lightweight Self-Consolidating Concrete Beams Reinforced with Basalt Fiber-Reinforced Polymer Bars. ***ACI Structural Journal*, *120*(3).**
- Mehany, S., Mohamed, H.M. and Benmokrane, B., 2022. Flexural strength and serviceability of GFRP-reinforced lightweight self-consolidating concrete beams. ***Journal of Composites for Construction*, *26*(3), p.04022020.**
- Mehany, S., Mohamed, H.M., El-Safty, A. and Benmokrane, B., 2022. Bond-dependent coefficient and cracking behavior of lightweight self-consolidating concrete (LWSCC) beams reinforced with glass-and basalt-FRP bars. ***Construction and Building Materials*, *329*, p.127130.**

Significance of the Research Program

✓ Publications

- Mehany, S., Mohamed, H.M. and Benmokrane, B., 2021. Contribution of lightweight self-consolidated concrete (LWSCC) to shear strength of beams reinforced with basalt FRP bars. ***Engineering Structures*, *231*, p.111758.**

- Aflakisamani, M., Mousa, S., Mohamed, H.M., Ahmed, E.A. and Benmokrane, B., 2023. Design and Testing of Lightweight Self-Consolidating Concrete Bridge-Deck Slabs Reinforced with Glass Fiber-Reinforced Polymer Bars. ***ACI Structural Journal*, *120*(4).**

- Aflakisamani, M., Mousa, S., Mohamed, H.M., Ahmed, E.A. and Benmokrane, B., 2023. Structural behavior of bridge deck slabs made with GFRP-reinforced lightweight self-consolidating concrete. ***Journal of Bridge Engineering*, *28*(3), p.04023001**.

Significance of the Research Program

✓ Publications

- Bakouregui, A.S., Mohamed, H.M., Yahia, A. and Benmokrane, B., 2021. Axial load–moment interaction diagram of full-scale circular LWSCC columns reinforced with BFRP and GFRP bars and spirals: Experimental and theoretical investigations. ***Engineering Structures*, *242*, p.112538.**

- Bakouregui, A.S., Mohamed, H.M., Yahia, A. and Benmokrane, B., 2021. Explainable extreme gradient boosting tree-based prediction of load-carrying capacity of FRP-RC columns. ***Engineering Structures, 245, p.112836.***

- Sanni, B.A., Mohamed, H.M., Yahia, A. and Benmokrane, B., 2021. Behavior of Lightweight Self-Consolidating Concrete Columns Reinforced with Glass Fiber-Reinforced Polymer Bars and Spirals under Axial and Eccentric Loads. ***ACI Structural Journal, 118(3), pp.241-254.***

Continued…….

Significance of the Research Program

The new edition of the ACI 440.11-22 design code will be published in 2026, including guidelines for using FRP bars in lightweight concrete elements such as deck slabs, columns, and beams.

will also cover design equations for shear, flexure, punching, axial load, and serviceability based on the findings of this research program.

The new edition ACI code 440.11-22 (R2026)

AFTER…

Concluding Remarks

1. Using LWC made it possible to fabricate beams with lower self-weight (density of 1800 kg/m3) than with NWC. The FRP-reinforced LWC beams with lightweight aggregate and natural sand behaved similarly to the FRP-reinforced NWC beams.
2. This study demonstrated that FRP-RC beams can be designed with LWC provided that an appropriate concrete density reduction factor (λ) is applied.
3. Based on the experimental results, a modified ACI 440.1R-15 model was suggested using 0.67Mcr instead of Mcr to predict the actual deflection of the LWC specimens.
4. The λ, K_b , and I_e can contribute significantly to the development of design standards for using FRP bars in LWC structures in the new edition of ACI 440.11-22 (R2026) design code and CSA S806.

Acknowledgments

- **Tier-1 Canada Research Chair in Advanced FRP Composite Materials for Civil Structures.**
- **Industrial Research Chair in Innovative FRP Reinforcement for Concrete Structures.**
- **Natural Sciences and Engineering Research Council of Canada (NSERC).**
- **Mathematics of Information Technology and Complex Systems (MITACS).**
- **University of Sherbrooke, Department of Civil Engineering.**

Can GPR Detect GFRP Bars?

4th International Workshop on FRP Bars for Concrete Structures (IW-FRPCS4)

Hamed Layssi, PEng, PhD

FPrimeC SOLUTIONS

About FPrimeC SOLUTIONS

"We Protect the Built World by Innovative Testing Solutions and Advanced Repair Engineering"

Agenda

- What is Ground Penetrating Radar (GPR)?
- How Does GPR Detect Sub-surface Targets?
- Can GPR Detect Non-Metallic Targets?
- Case Study

What is GPR ?

- Uses Electromagnetic Waves to Detect Sub-Surface Targets

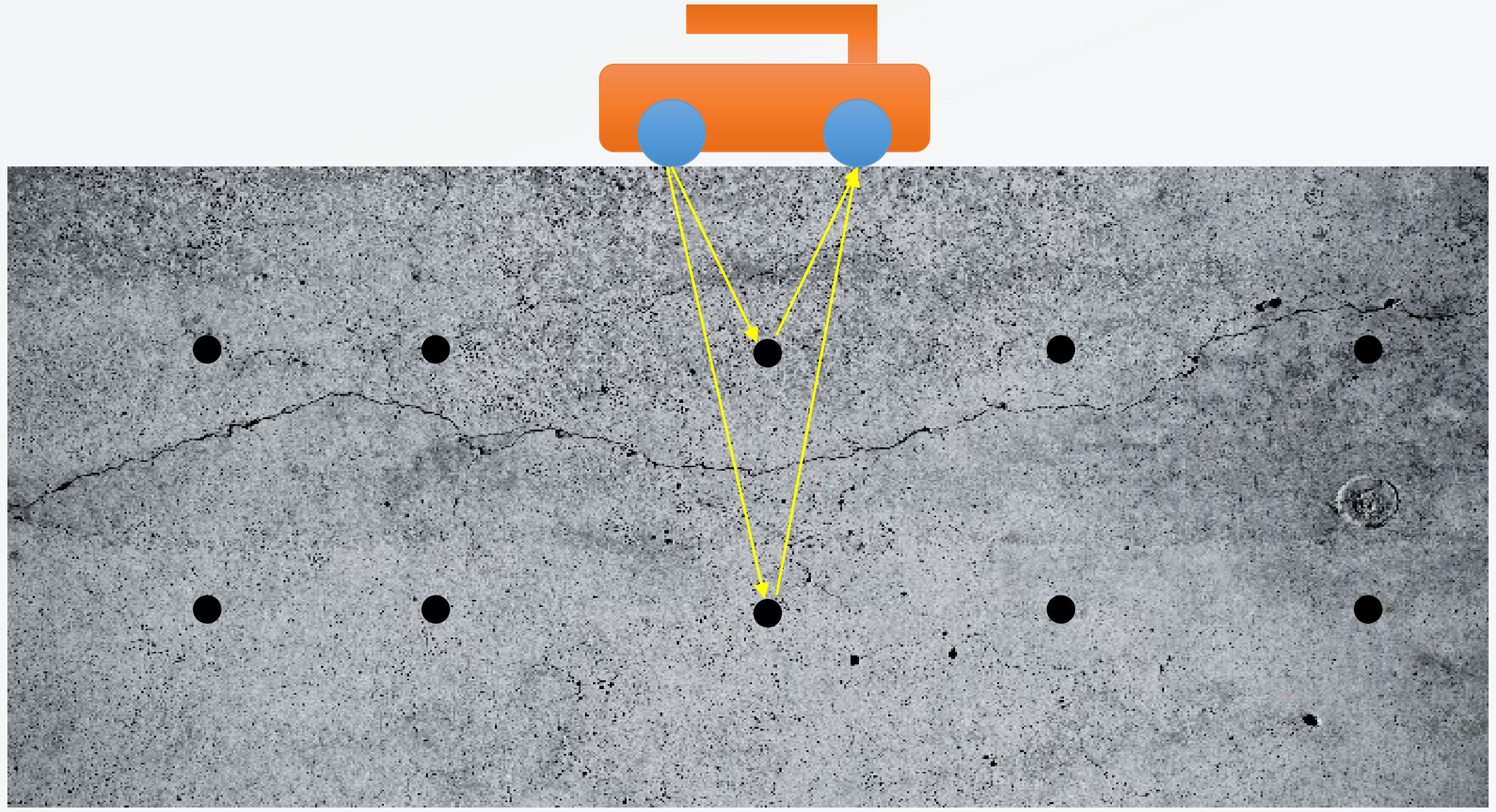

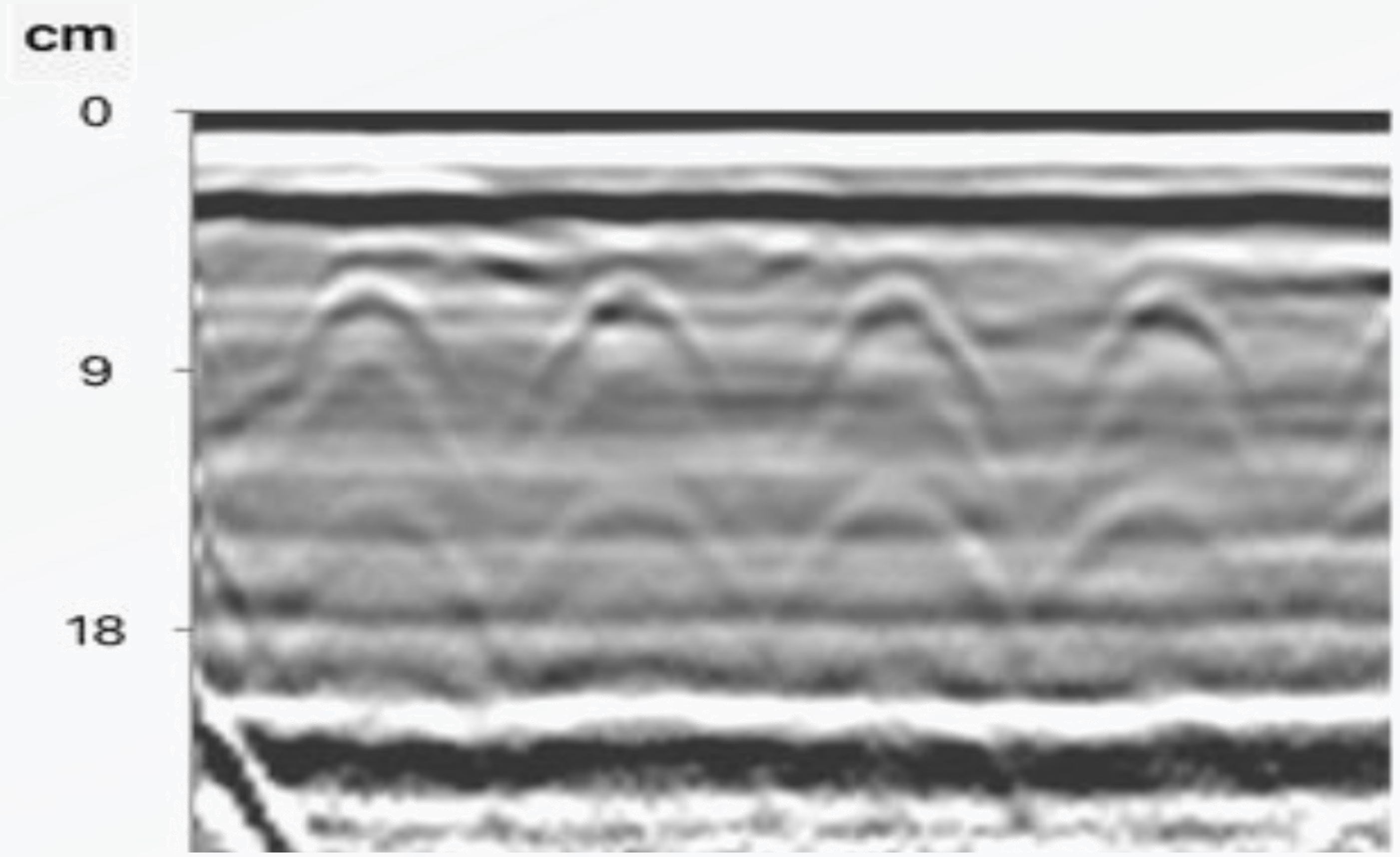

GPR – Key Parameters

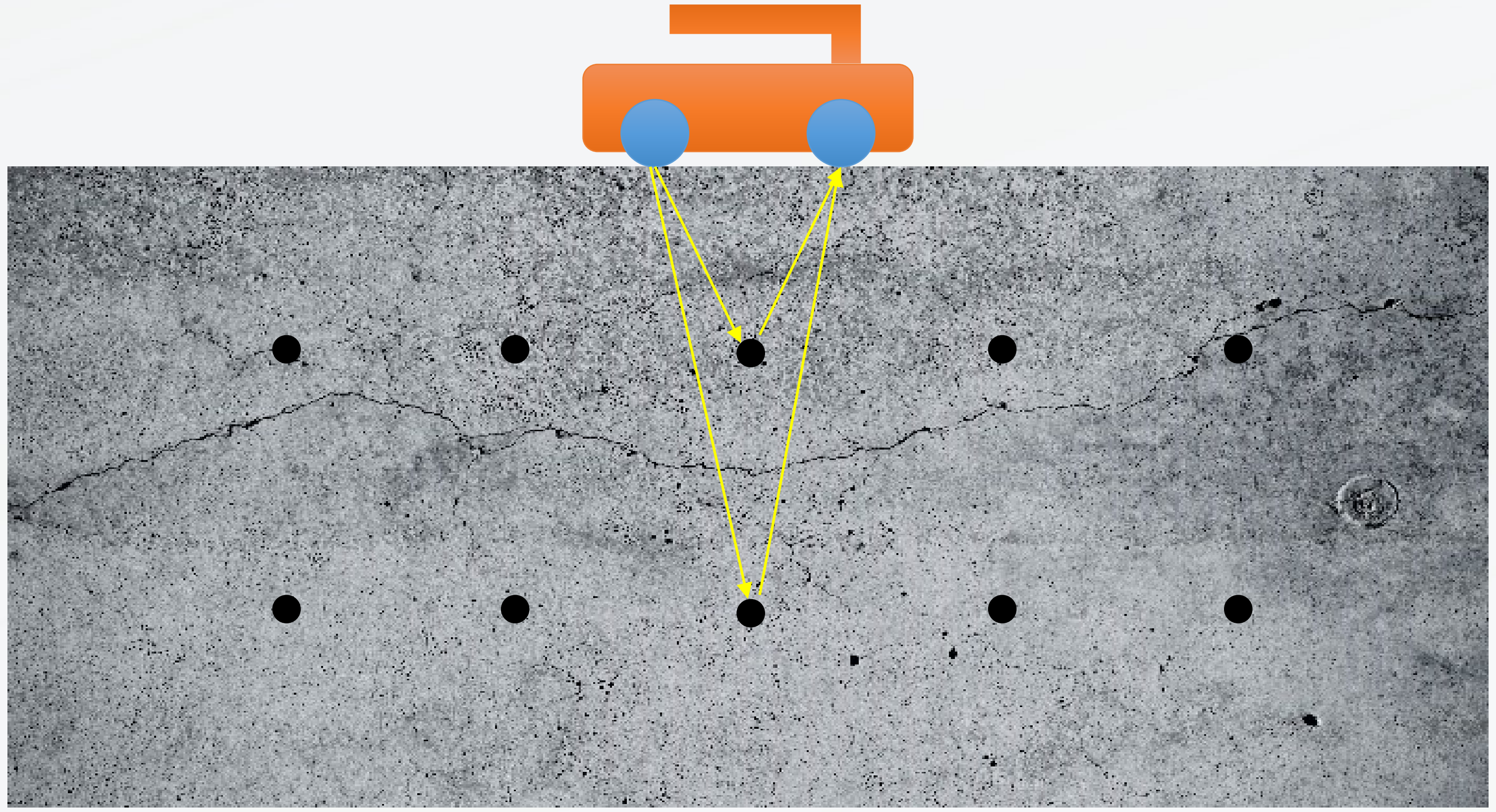

- GPR Antenna Frequency
- Signal Amplitude
- Relative Dielectric Constant

GPR – Relative Dielectric Permittivity (K or ε)

- GPR Wave Speed through Air

  c = 300,000 m/s (0.3 m/ns)

- GPR Wave Speed in other materials:

$$c' = \frac{c}{\sqrt{K}}$$

Material	Appx RDP	Appx Velocity (m/ns)
Air	1	0.3
Concrete	**7**	**0.12**
Asphalt	2-4	0.15
Steel	∞	
GFRP	**<5**	**0.13**

GPR – Reflection at Interface of Concrete-Rebar

- How much energy gets reflected?

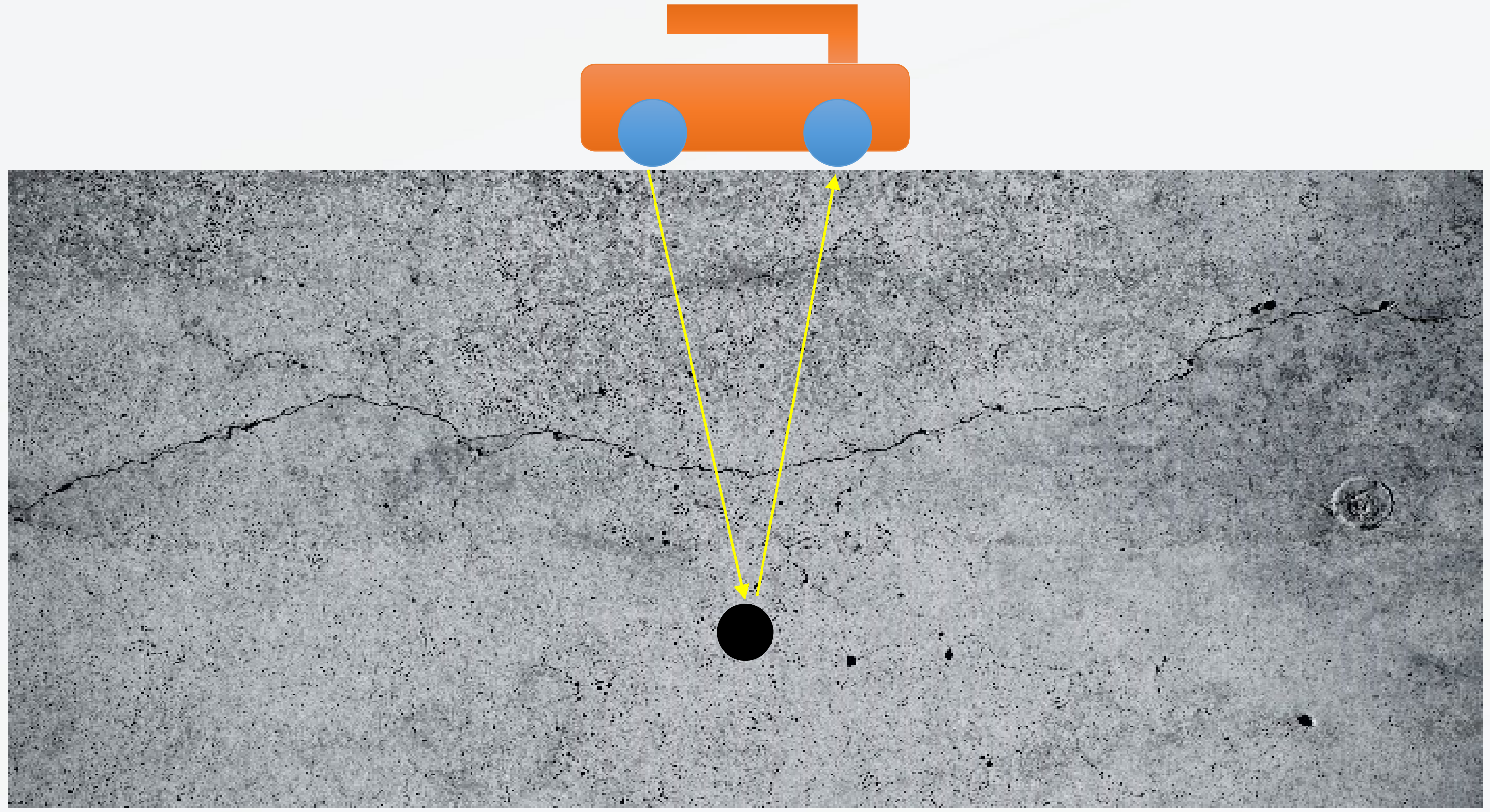

$$R = \frac{\sqrt{\varepsilon_1} - \sqrt{\varepsilon_2}}{\sqrt{\varepsilon_1} + \sqrt{\varepsilon_2}}$$

R: GPR Reflection Coefficient

$$-1 < R < 1$$

Reflected at the interface

transmitted through the interface

GPR – Reflection at Interface of Concrete-Rebar

- How much energy gets reflected?

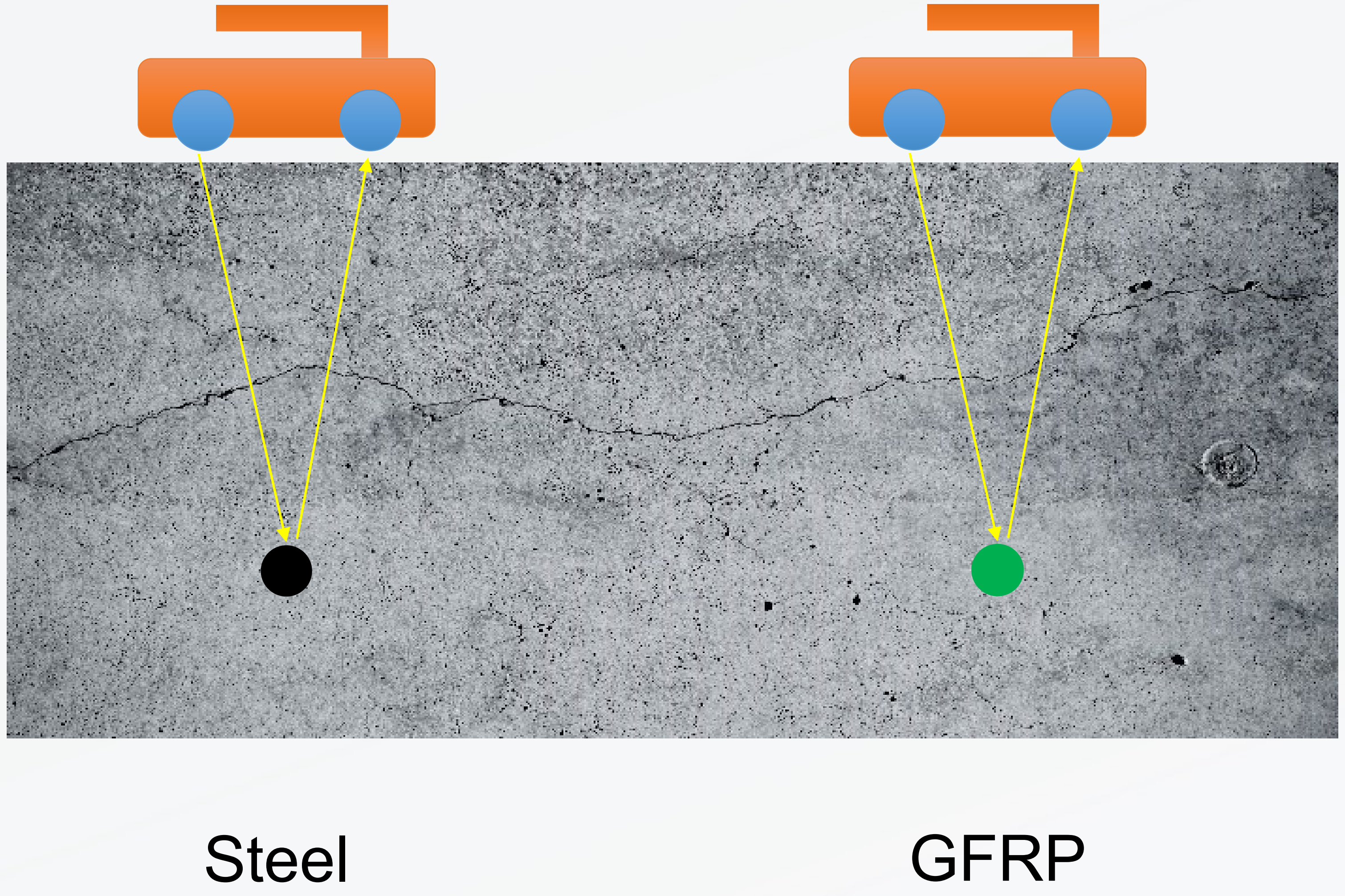

$$R_{concrete-steel} = \frac{\sqrt{7} - \sqrt{\infty}}{\sqrt{7} + \sqrt{\infty}} \sim \mathbf{100\%}$$

$$R_{concrete-GFRP} = \frac{\sqrt{7} - \sqrt{5}}{\sqrt{7} + \sqrt{5}} = \mathbf{8\%}$$

FPrimeC SOLUTIONS

Literature Review

applied sciences

MDPI

Article

Feasibility of Conventional Non-Destructive Testing Methods in Detecting Embedded FRP Reinforcements

Pranit Malla [1,*], Seyed Saman Khedmatgozar Dolati [1], Jesus D. Ortiz [2], Armin B. Mehrabi [1,*], Antonio Nanni [2] and Kien Dinh [3]

[1] Department of Civil and Environmental Engineering, Florida International University, Miami, FL 33174, USA; skhed004@fiu.edu
[2] Department of Civil and Architectural Engineering, University of Miami, Coral Gables, FL 33146, USA; jdo72@miami.edu (J.D.O.); nanni@miami.edu (A.N.)
[3] NDT Concrete LLC, Deltona, FL 32725, USA; kien@ndt-concrete.com
* Correspondence: pmall011@fiu.edu (P.M.); amehrabi@fiu.edu (A.B.M.)

Abstract: Fiber-Reinforced Polymer (FRP) bars/strands are the most promising alternative to their steel counterparts for reinforcing concrete elements due to their resistance to corrosion, lighter weight, higher strength and better durability. However, very limited research has been conducted in relation to non-destructive testing (NDT) methods that are applicable to damage detection in FRP bars or the detection of FRP reinforcements embedded in concrete. The ability to assess the condition of the relatively new and unique FRP reinforcements will increase the confidence of the construction industry in their use as a reliable substitute for steel reinforcements. This paper investigates the ability of two of the most commonly used NDT methods, Ground Penetrating Radar (GPR) and Phased Array Ultrasonic (PAU), in detecting FRP bars/strands embedded in concrete elements. GPR and PAU tests were performed on two slab specimens reinforced with GFRP (Glass-FRP) bars, the most commonly used FRP bar, with variations in their depth, size and configuration, and a slab specimen with different types of available FRP reinforcements. The results show that GPR devices can detect GFRP bars/strands and CFRP (Carbon-FRP) strands to some extent, and their detectability increases with the increase in their antenna center frequency. On the contrary, PAU is only capable of detecting GFRP and CFRP strands. The results of this paper also emphasize the need for further research and developments related to NDT applications to embedded FRP bars.

Keywords: fiber-reinforced polymer (FRP); ground penetrating radar (GPR); ultrasonic testing (UT); phased array ultrasonic (PAU); non-destructive testing (NDT); reinforced concrete

check for updates

Citation: Malla, P.; Khedmatgozar Dolati, S.S.; Ortiz, J.D.; Mehrabi, A.B.; Nanni, A.; Dinh, K. Feasibility of Conventional Non-Destructive Testing Methods in Detecting Embedded FRP Reinforcements.

- Major outcomes:
- **GPR can potentially detect GFRP bars**
- **Higher frequency GPR scanners perform better**
- **Larger GFRP bars are generally easier to detect**

Can GPR Detect GFRP Bars?

A Case Study

- L = 3 m (~ 10′)
- W = 1 m (3.3′)
- Thickness = 200 mm (8″)

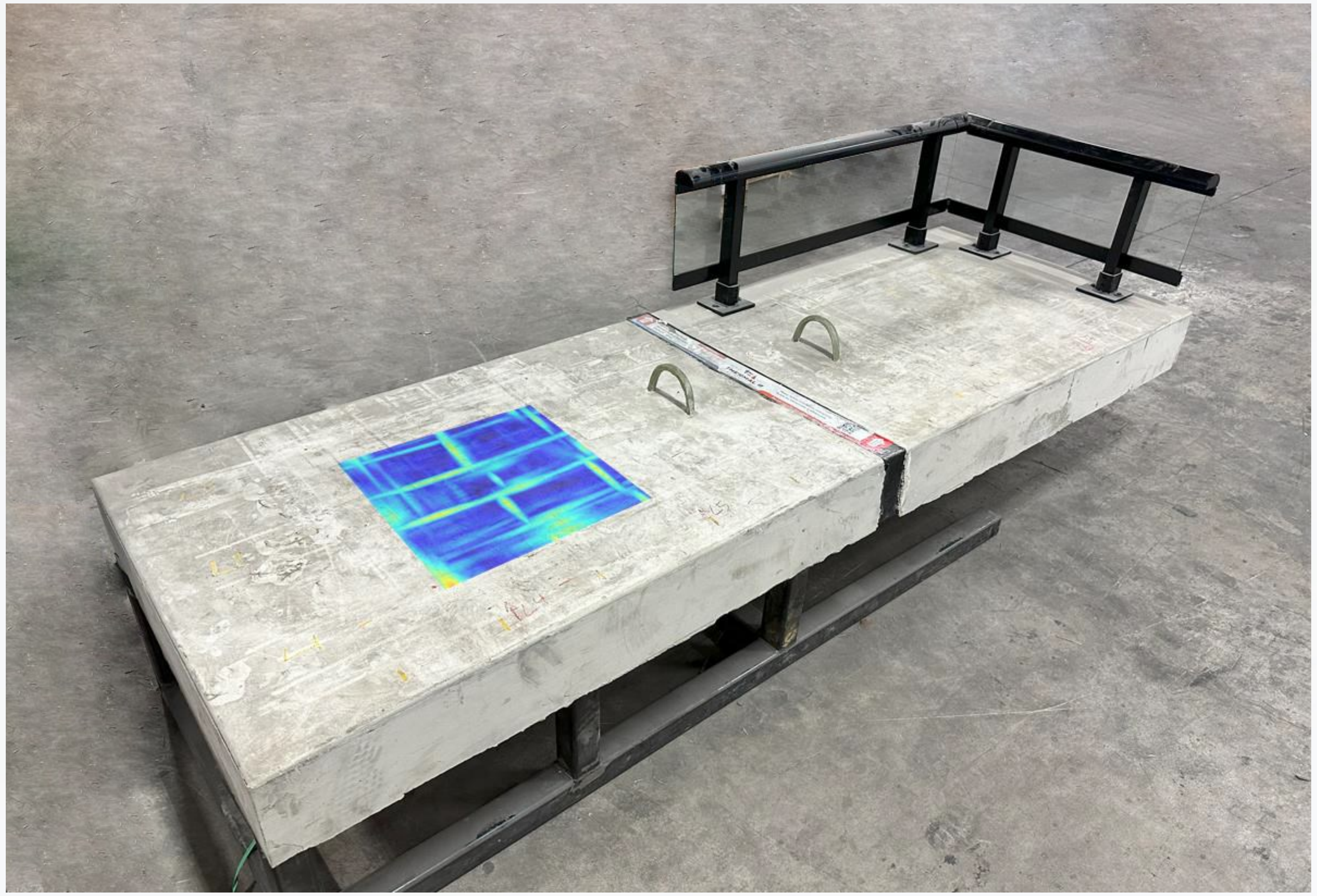

Description of Test Specimen

- Slab thickness: 200 mm
- 40 MPa Concrete
- 15M GFRP bars
- Cover thickness: 45 – 50 mm

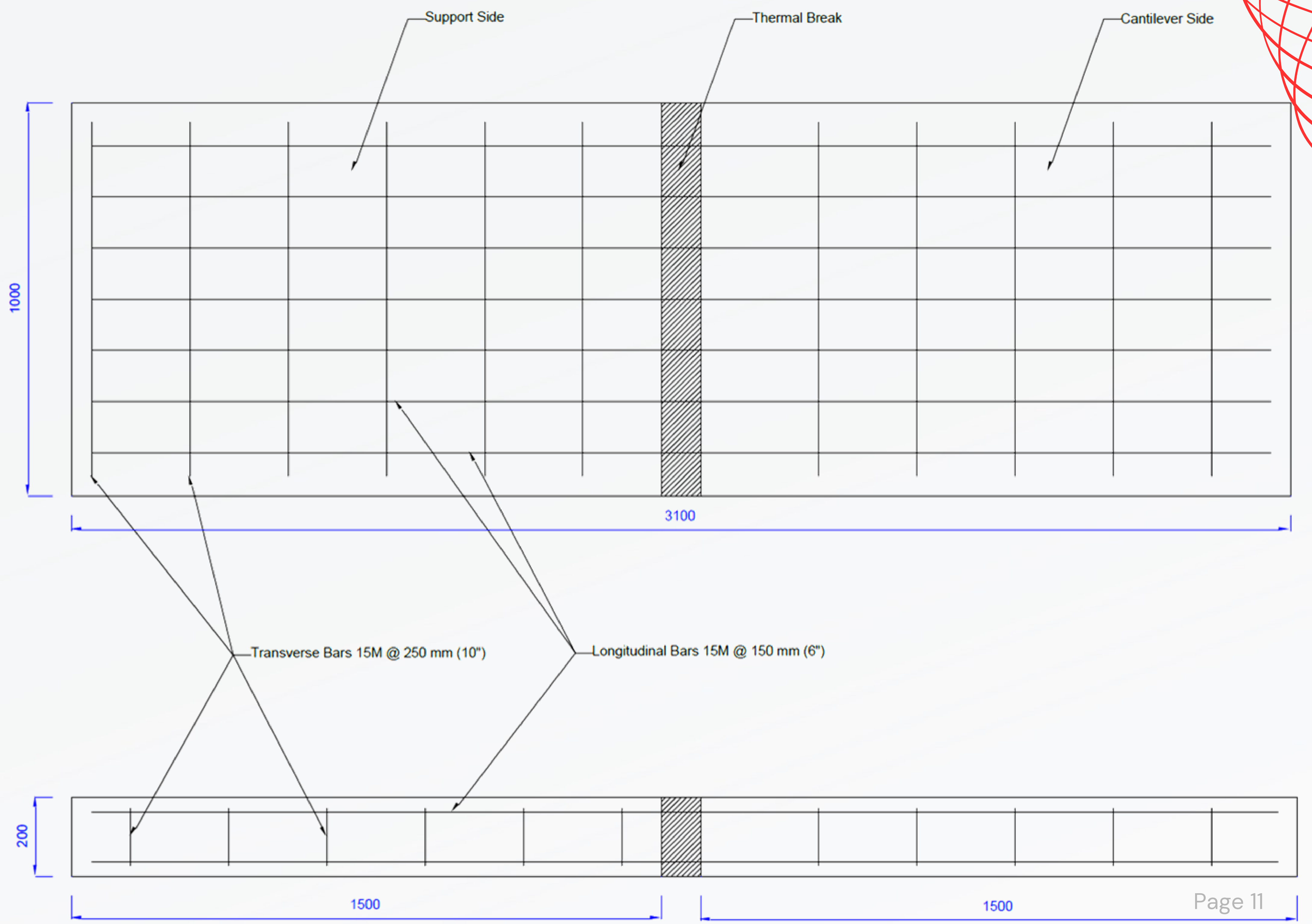

FPrimeC SOLUTIONS

Description of Test Specimen

GPR Scanners

1000 MHz

400 MHz to 6000 MHz (stepped frequency)

Line Scan and Grid Scan

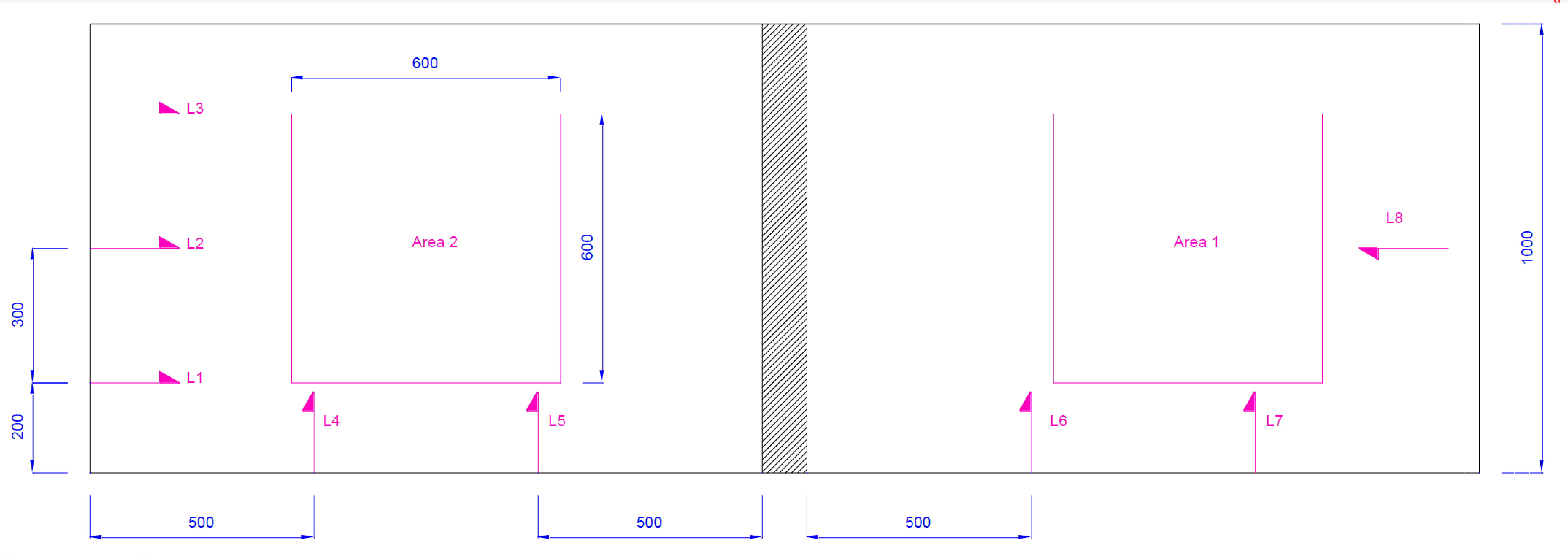

FPrimeC
SOLUTIONS

GPR Scans – Transverse Bars

1000 MHz

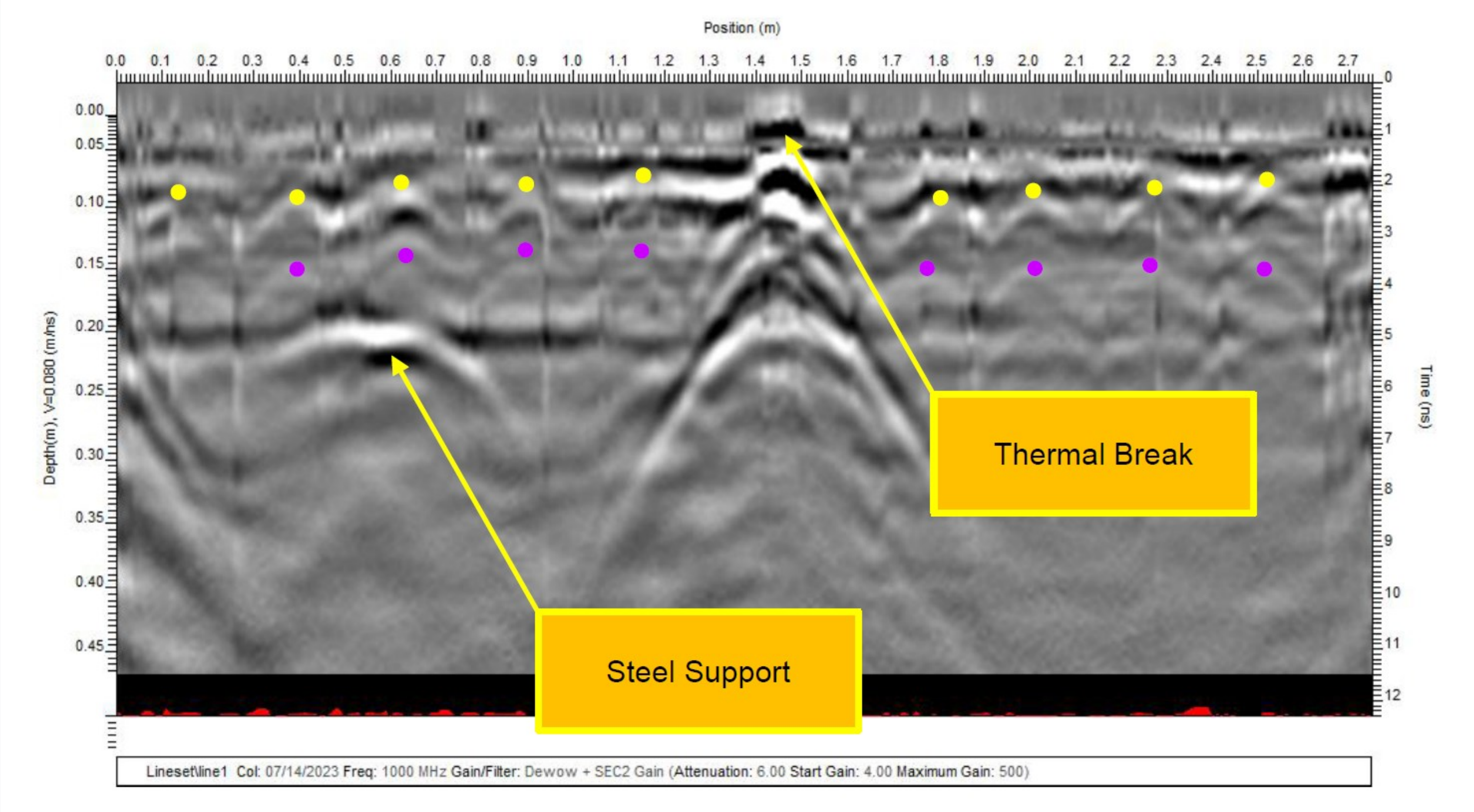

400 MHz to 6000 MHz (stepped frequency)

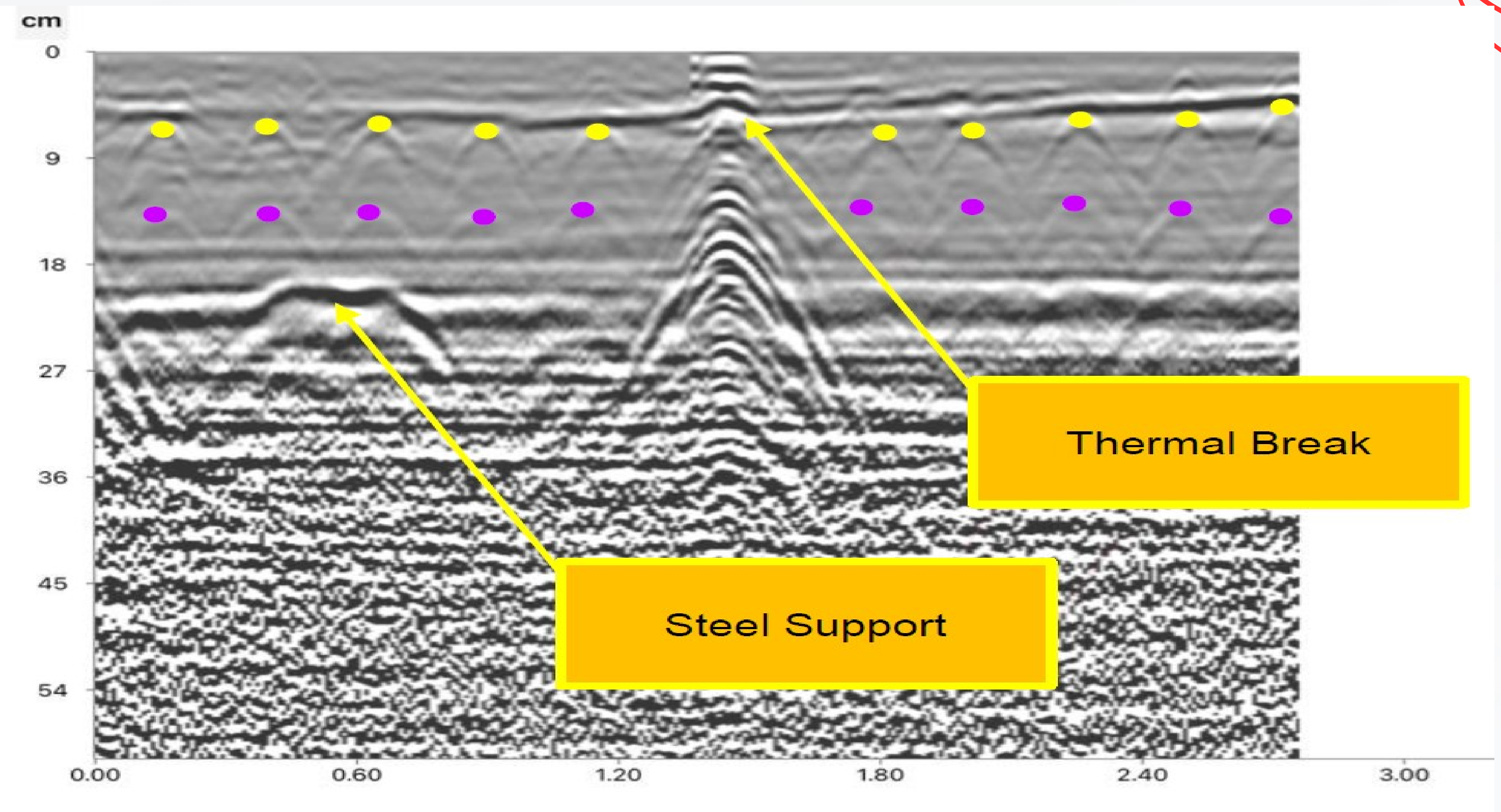

GPR Scans – Longitudinal Bars

1000 MHz

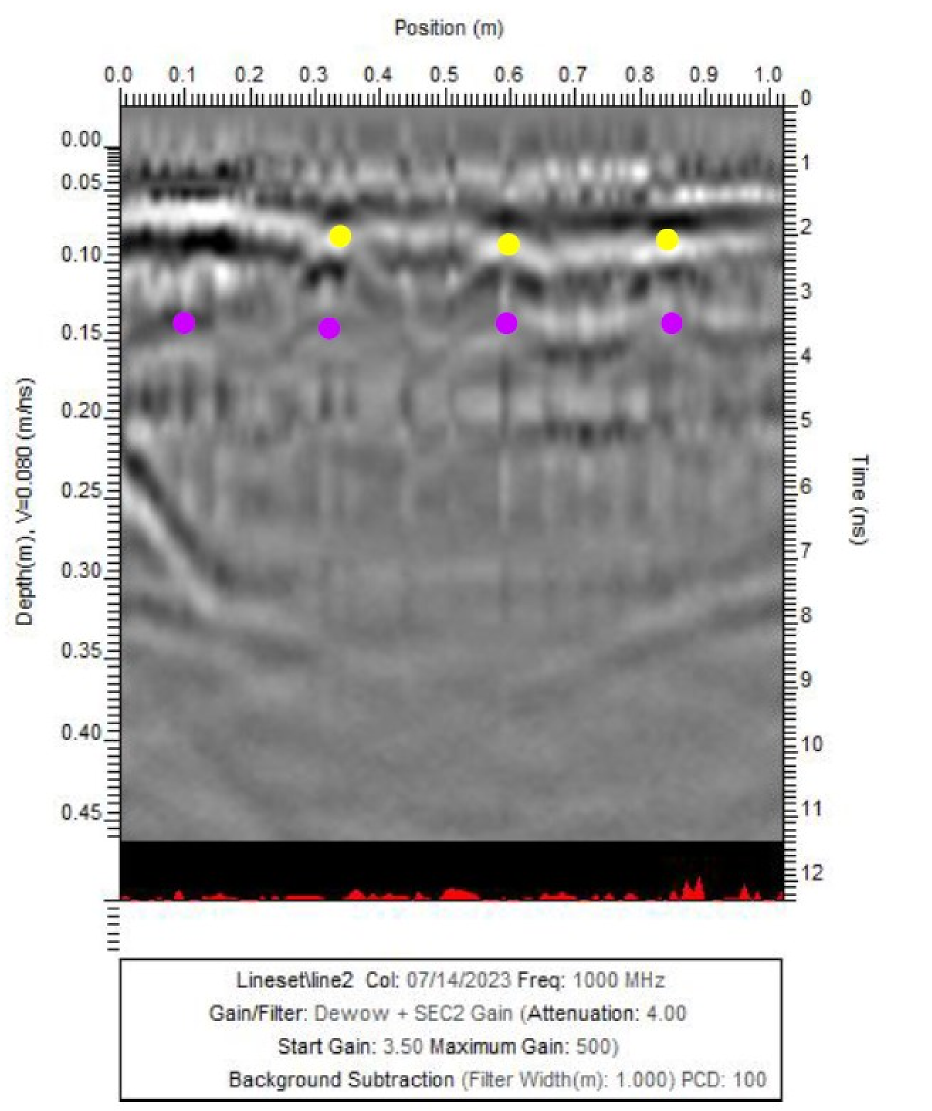

Figure A 2 – Line Scan 2.

400 MHz to 6000 MHz (stepped frequency)

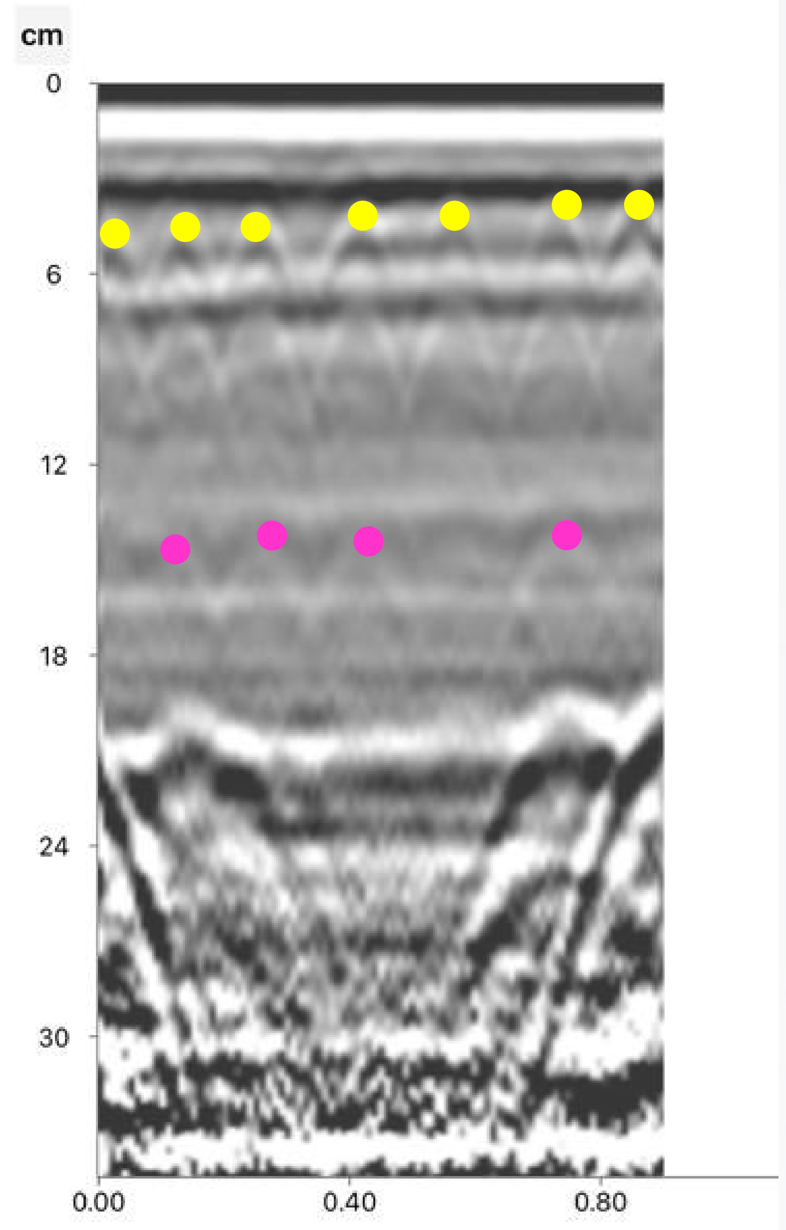

Depth Calibration - Hyperbola

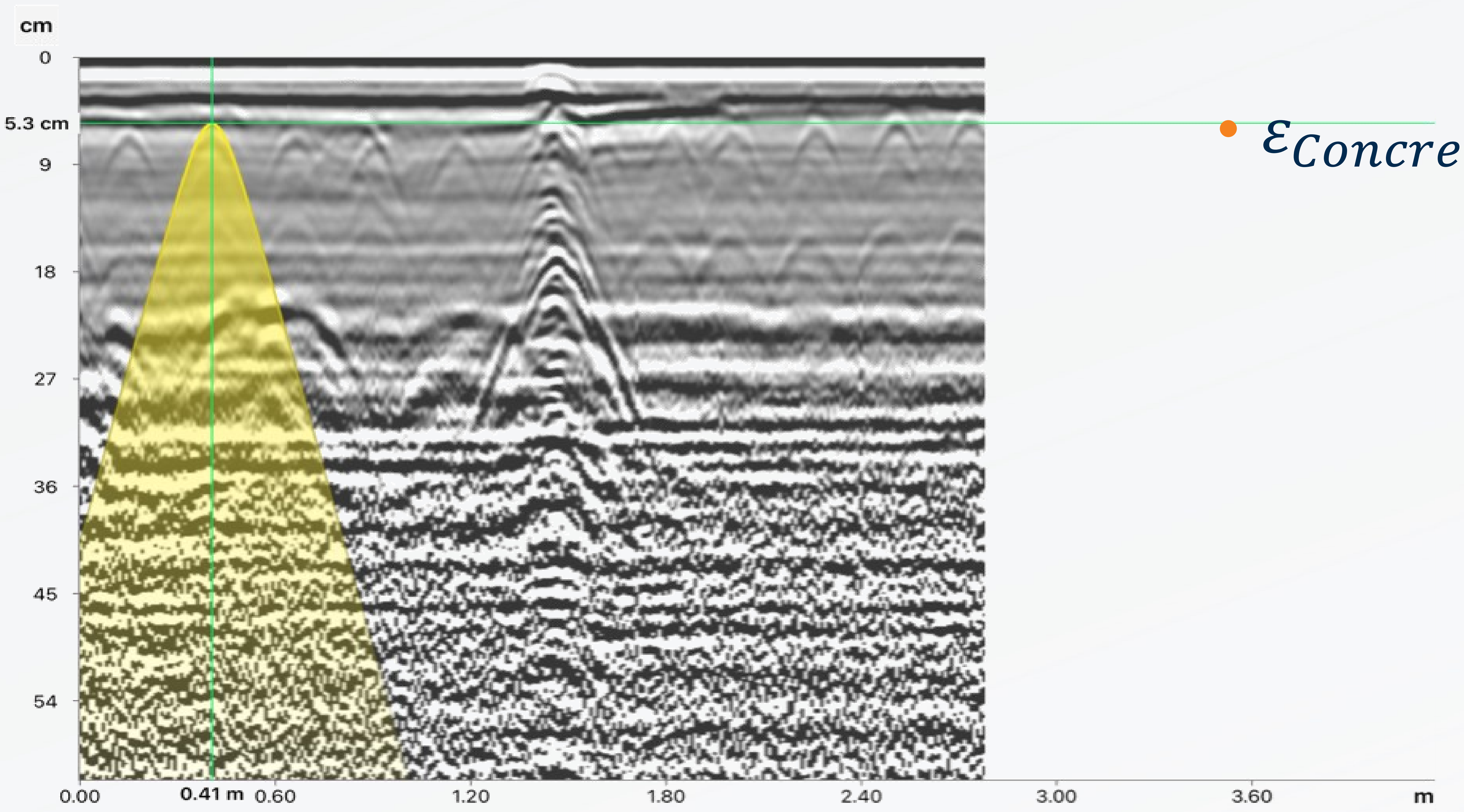

- $\varepsilon_{Concrete} = 7.9$

GPR Scans – Area Scan (Grid)

1000 MHz

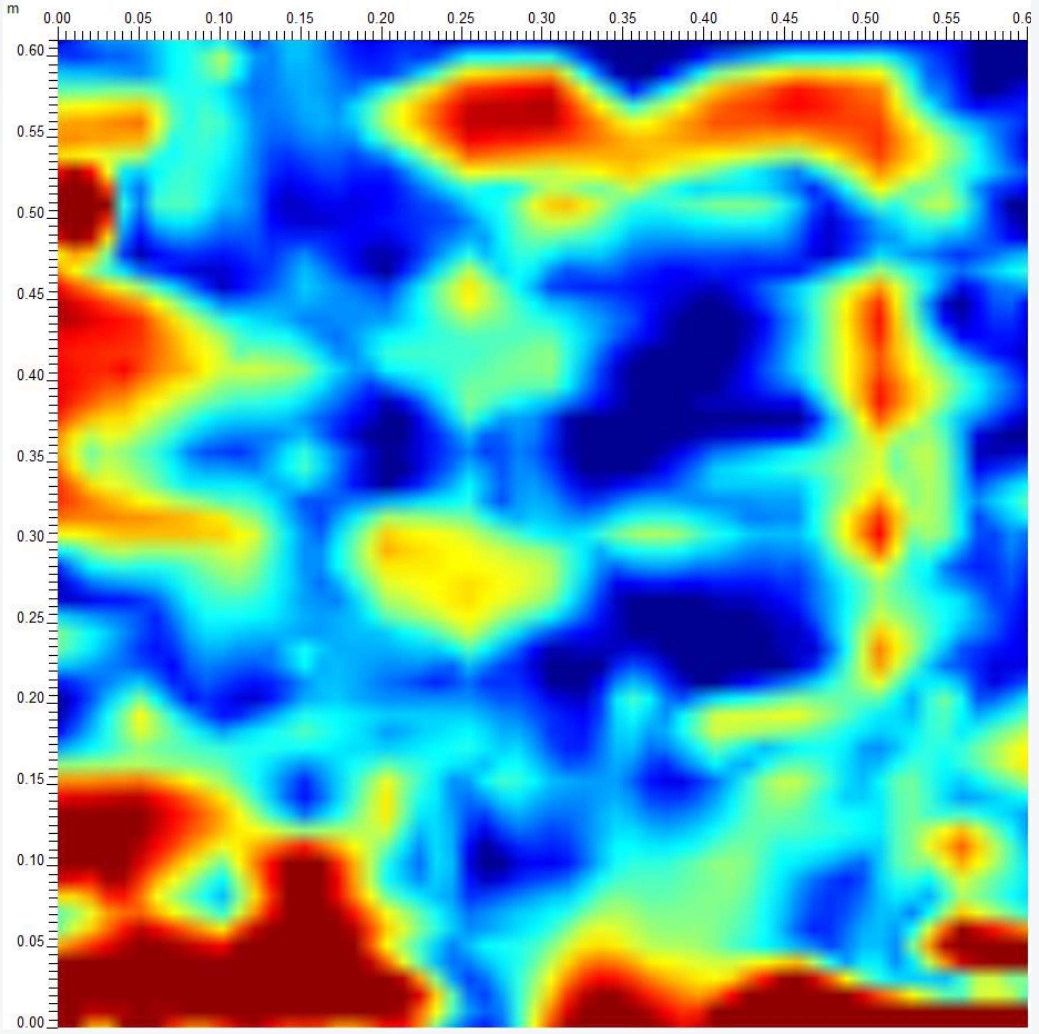

400 MHz to 6000 MHz (stepped frequency)

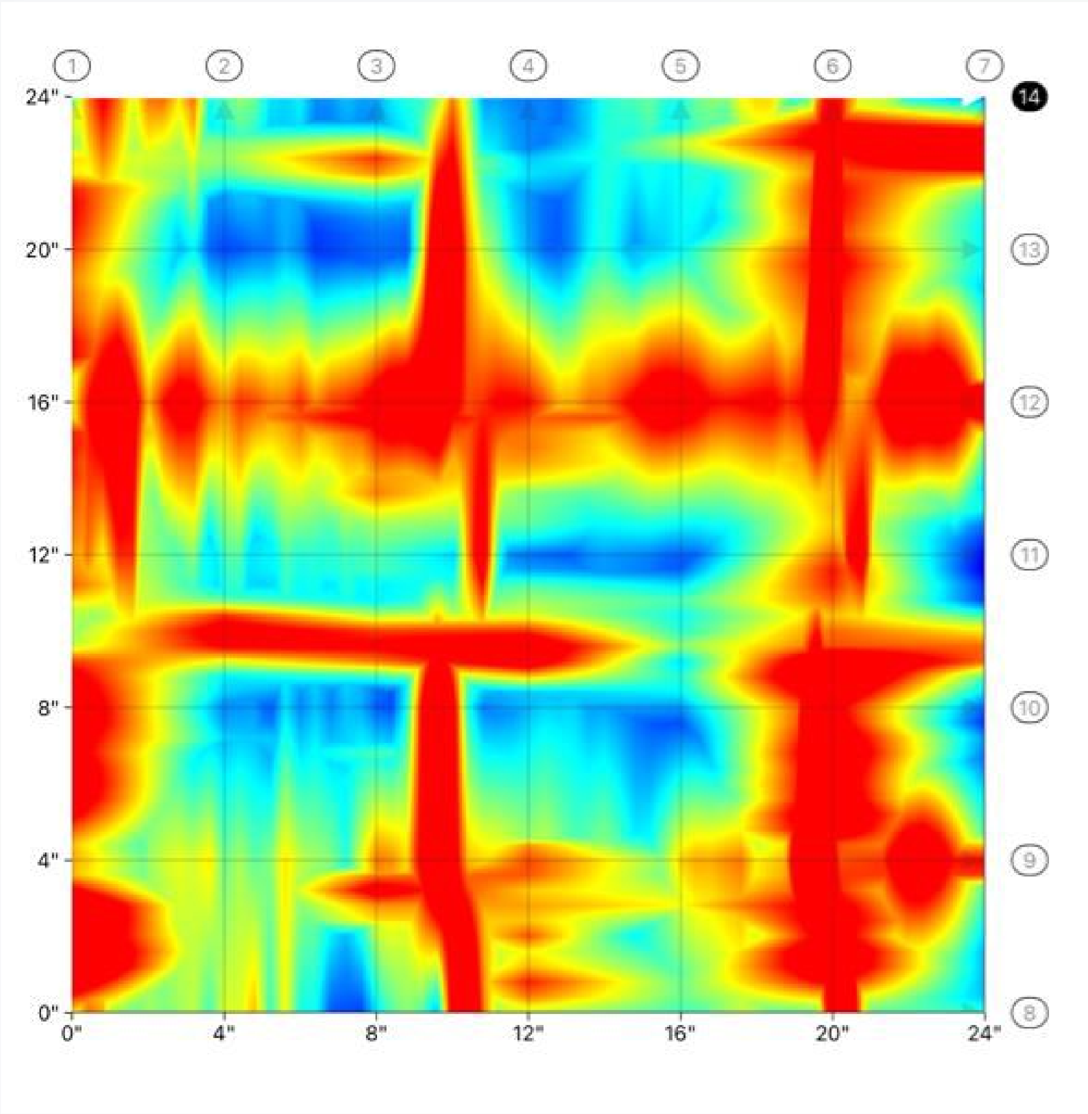

Other Parameters – Bar Size

- Rebar Size (#3, #4, #5, …)

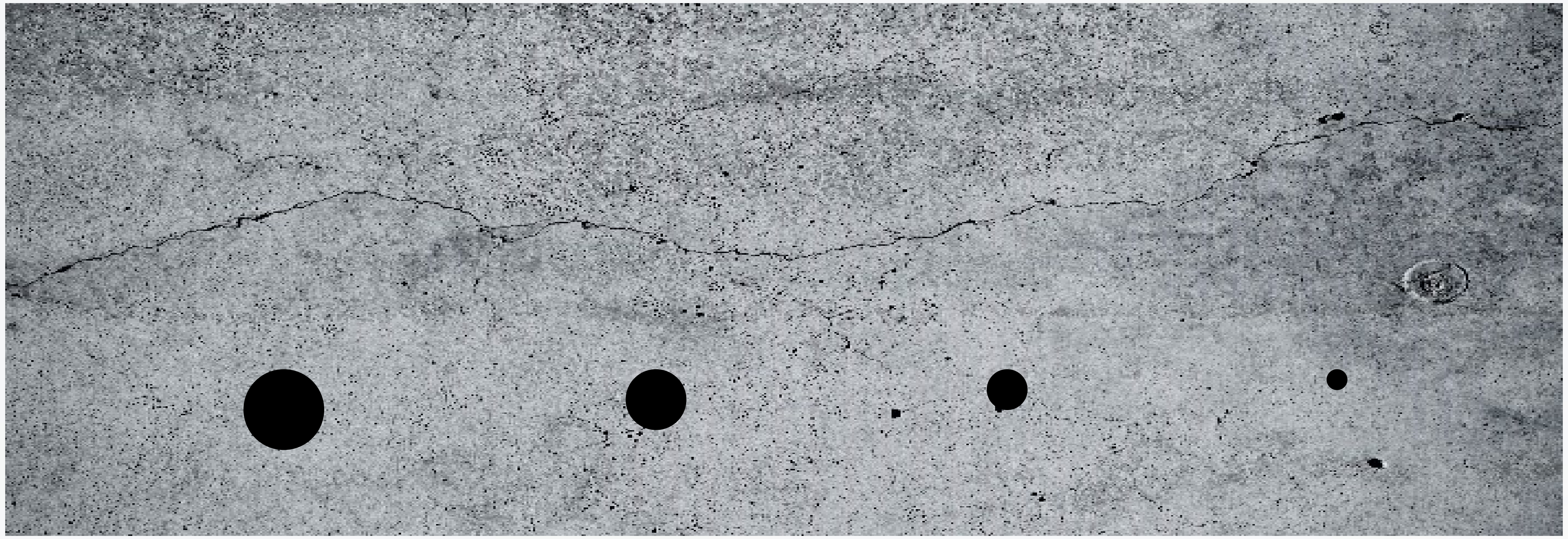

Easier, Better Resolution

Harder, Lower Resolution

Other Parameters – Bar Shape

- What causes the reflection ?
  - Difference in dielectric constant?
  - The geometry of the interface layer?

Key Takeaways

- GPR can potentially identify GFRP bars
- Detecting larger diameter bars is generally easier.
- Detecting near surface bars is generally easier.
- A higher frequency GPR antenna appears to deliver a better resolution

THANK YOU
FOR YOUR ATTENTION

FPrimeC
SOLUTIONS

5-80 West Beaver Creek Rd
Richmond Hill, ON, L4B 1H3
(647) 933-6633
info@frpimec.com

FOURTH INTERNATIONAL WORKSHOP ON FRP BARS FOR CONCRETE STRUCTURES

"Advances in concrete reinforcement"

August 8-9, 2024 - Toronto, Ontario

TENSILE PROPERTIES OF GFRP BARS SUBJECTED TO EXTREME COLD TEMPERATURES (DOWN TO -170℃)

Basil Ibrahim

Postdoctoral Fellow (Mitacs Scholar) – Pultrall VROD/UdeS

UNIVERSITÉ DE SHERBROOKE NSERC CRSNG UNIVERSITY OF MIAMI Center for Integration of Composites into Infrastructure FDOT

EXTREME COLD TEMPERATURES (DOWN TO -170°C)

- Storing substances like Liquefied Natural Gas (LNG), Liquid Nitrogen (LN2), and Liquid Oxygen (LOX) at temperatures as low as -170°C demands specialized equipment and materials.

EXTREME COLD TEMPERATURES (DOWN TO -170°C)

- **GFRP (Glass Fiber Reinforced Polymer) tanks or GFRP-reinforced concrete containers are used to contain liquids**
- **However, the mechanical properties of these bars need to be investigated under very low temperature to determine whether they can be used.**


AmTech – Tank Lining Systems


Orson Resins & Coatings Private Limited

EXTREME COLD TEMPERATURES (DOWN TO -170°C)

- In 2010, V-ROD GFRP bars from Pultrall were experimentally tested at the University of Sherbrooke for cold temperature applications.
- This project aimed to utilize these V-ROD bars in a project for Hydro-Quebec in Northern Quebec, where temperatures plummet to extreme sub-zero levels.

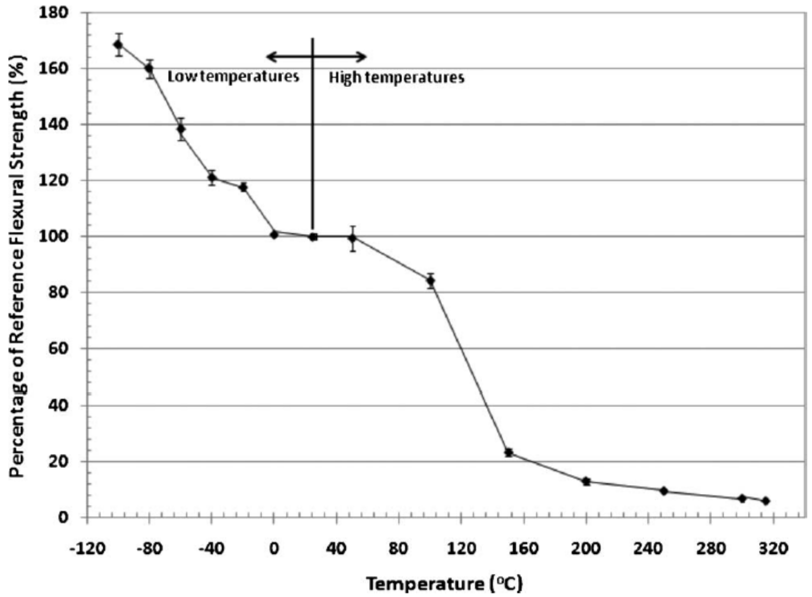

Robert, M., & Benmokrane, B. (2010). Behavior of GFRP reinforcing bars subjected to extreme temperatures. Journal of composites for construction, 14(4), 353-360.

EXTREME COLD TEMPERATURES (DOWN TO -170°C)

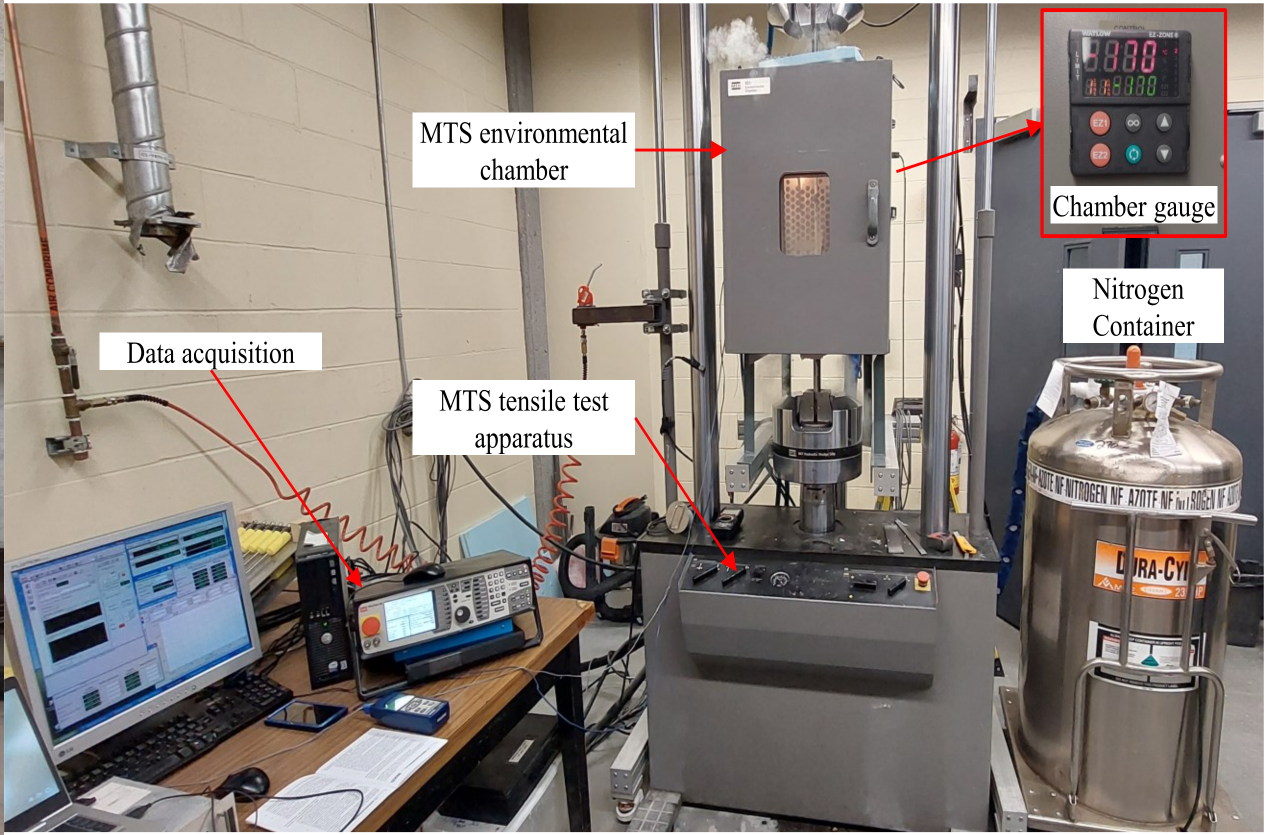

EXTREME COLD TEMPERATURES (DOWN TO -170°C)

Bar ID	Bar diameter d_b (mm)	Testing temperature (°C (°F))	$P_{u,\exp.}$ (kN)	$\sigma_{u,\exp.}$ (MPa)	E (GPa)	$\varepsilon_{\exp.}$ ($\mu\varepsilon$)
C3-1	9.5					
C3-2	9.5	-170 (-274)	115	1620	69.3	18,350
C3-3	9.5					
N3-1	9.5					
N3-2	9.5	25 (77)	97	1370	66.7	21,200
N3-3	9.5					
C4-1	12.7					
C4-2	12.7	-170 (-274)	184	1420	64.3	21,800
C4-3	12.7					
N4-1	12.7					
N4-2	12.7	25 (77)	150	1160	63.1	22,350
N4-3	12.7					

18.5%

22.7%

EXTREME COLD TEMPERATURES (DOWN TO -170°C)

SEM for GFRP bars after rupture at 25°C

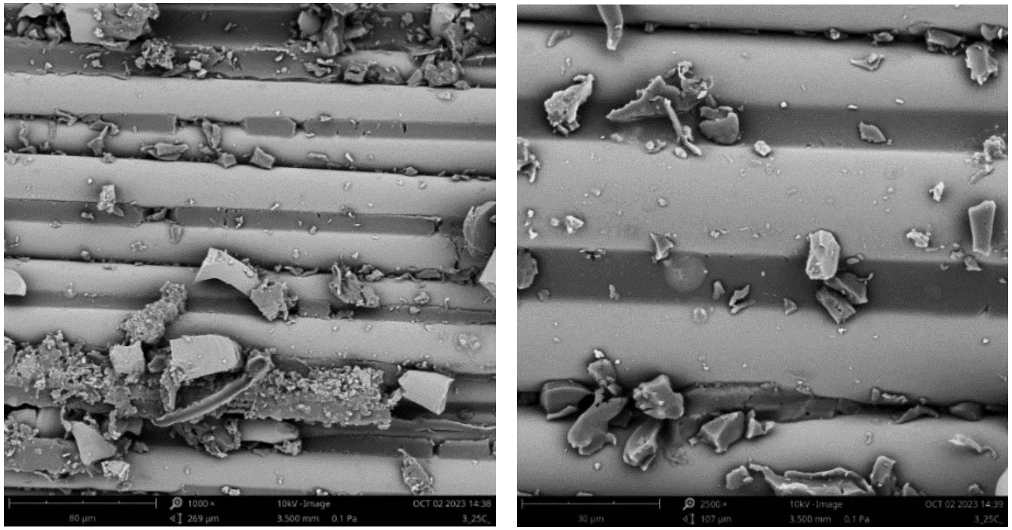

SEM for GFRP bars after rupture at -170°C

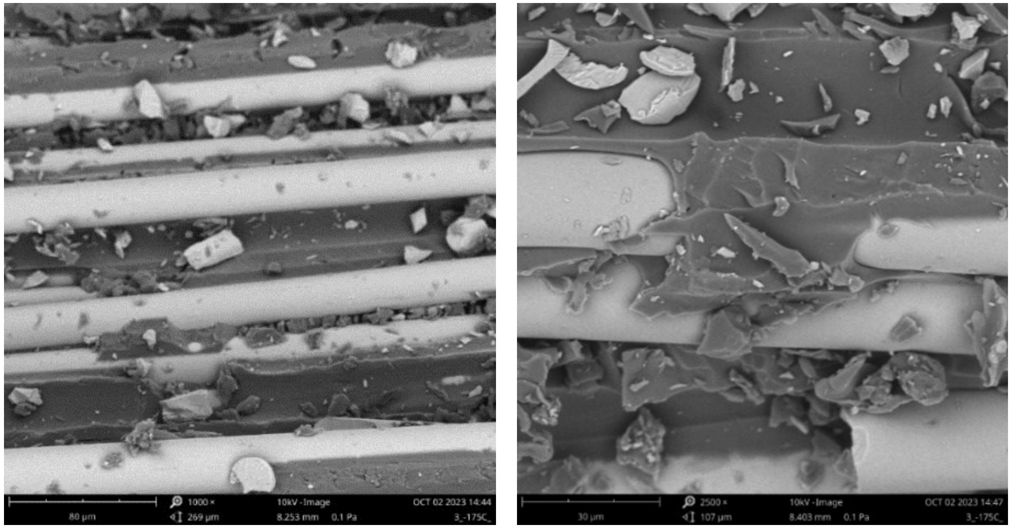

EXTREME COLD TEMPERATURES (DOWN TO -170℃)

- The extremely cold temperature enhances the properties of the resin matrix, resulting in increased stiffness by reducing the voids ratio.
- This properties enhancement contributes to an increased tensile strength of 18.2% for GFRP bar #3 and 22.4% for GFRP bar #4 when tested at -170℃, compared to their corresponding tested at a temperature of 25 ℃.
- No fiber debonding was observed in the SEM microstructural analysis at either extremely cold or room temperature, despite substantial thermal expansion differences between glass fibers and resin in FRP bars.
- GFRP can be efficiently utilized as internal reinforcing bars for cryogenic substances storage tanks.

EXPERIMENTAL TESTING FOR INDUSTRIAL APPLICATIONS

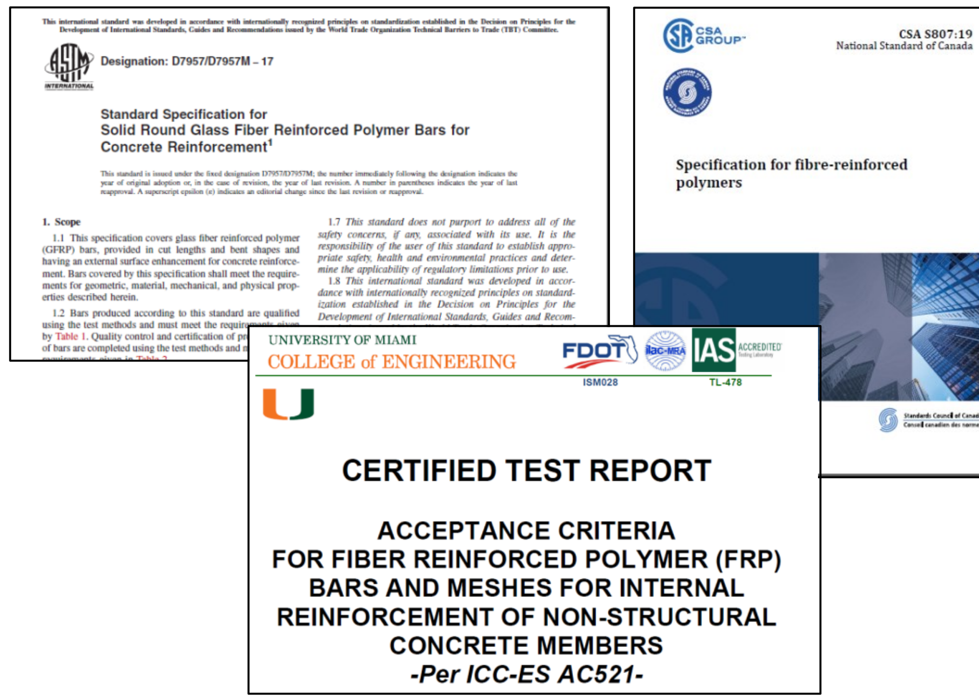

Designation: D7957/D7957M – 17

Standard Specification for
Solid Round Glass Fiber Reinforced Polymer Bars for
Concrete Reinforcement[1]

1. Scope

1.1 This specification covers glass fiber reinforced polymer (GFRP) bars, provided in cut lengths and bent shapes and having an external surface enhancement for concrete reinforcement. Bars covered by this specification shall meet the requirements for geometric, material, mechanical, and physical properties described herein.

1.7 This standard does not purport to address all of the safety concerns, if any, associated with its use. It is the responsibility of the user of this standard to establish appropriate safety, health and environmental practices and determine the applicability of regulatory limitations prior to use.

CSA S807:19
National Standard of Canada

Specification for fibre-reinforced polymers

UNIVERSITY OF MIAMI
COLLEGE of ENGINEERING

CERTIFIED TEST REPORT

ACCEPTANCE CRITERIA
FOR FIBER REINFORCED POLYMER (FRP)
BARS AND MESHES FOR INTERNAL
REINFORCEMENT OF NON-STRUCTURAL
CONCRETE MEMBERS
-Per ICC-ES AC521-

EXPERIMENTAL TESTING FOR INDUSTRIAL APPLICATIONS

University of Sherbrooke

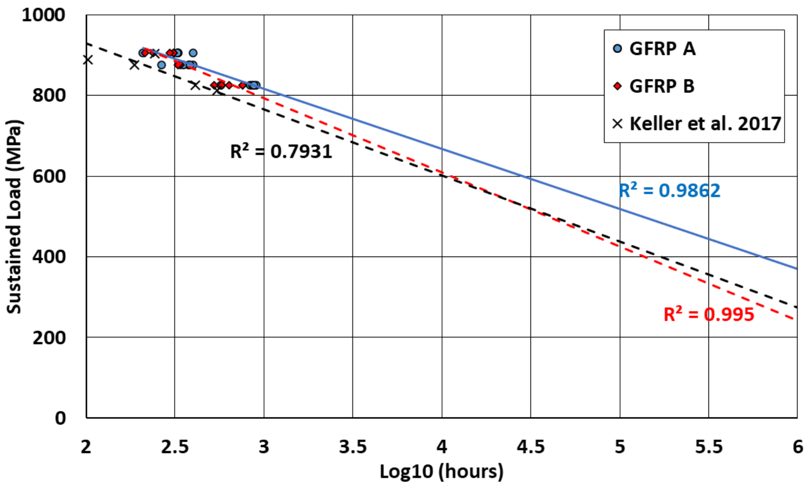

University of Toronto - Harper, C., & Sheikh, S. A. (2024). Glass Fiber-Reinforced Polymer Bars under Sustained Load and Alkaline Conditions. ACI Structural Journal, 121(4), 3-18.

NSERC CRSNG MIAMI FDOT

CURVILINEAR GFRP BARS FOR PCTL SEGMENTS

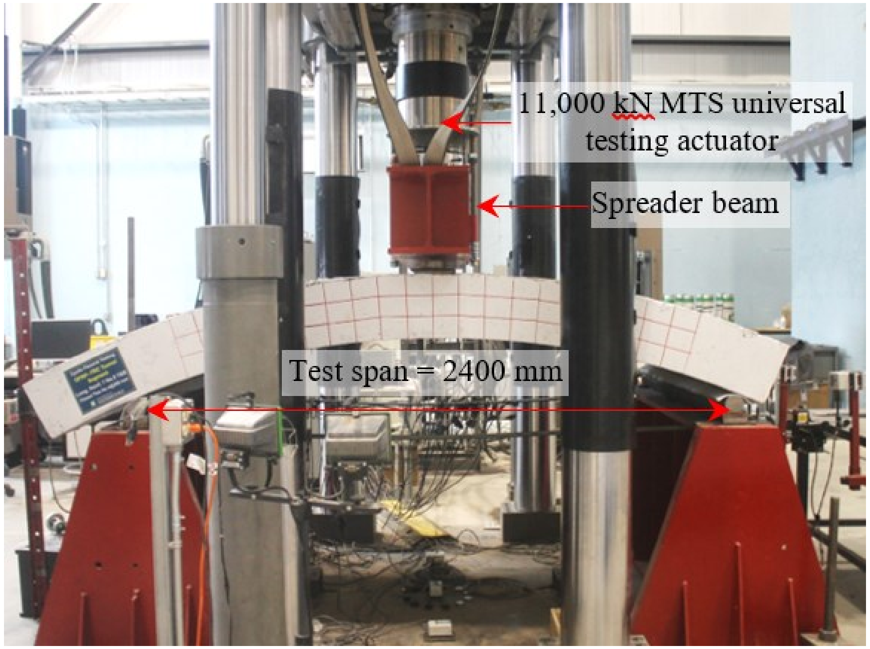

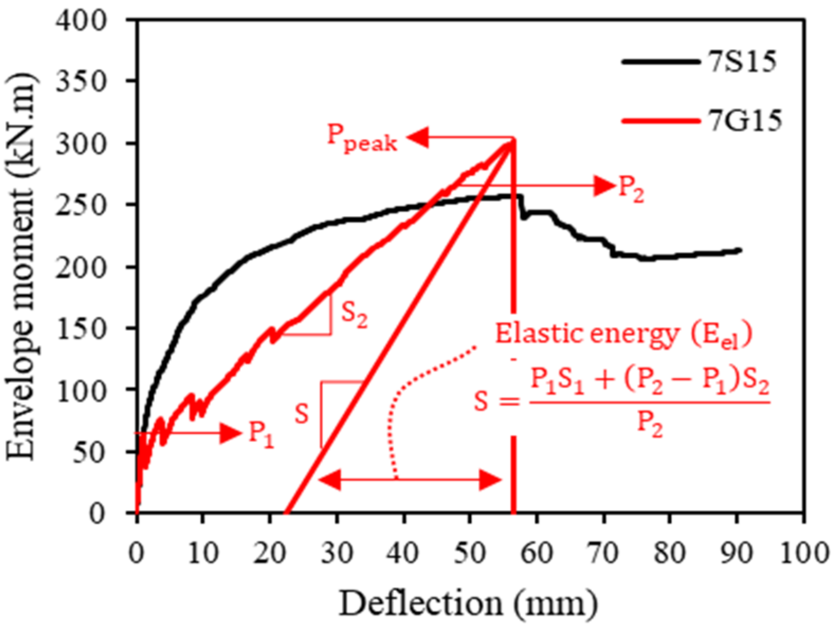

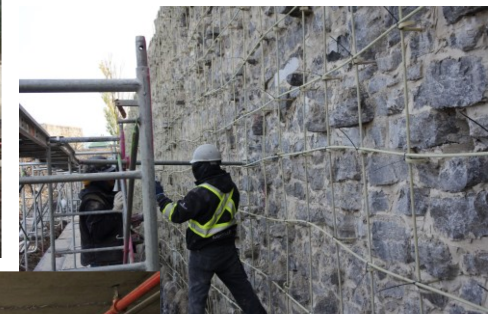

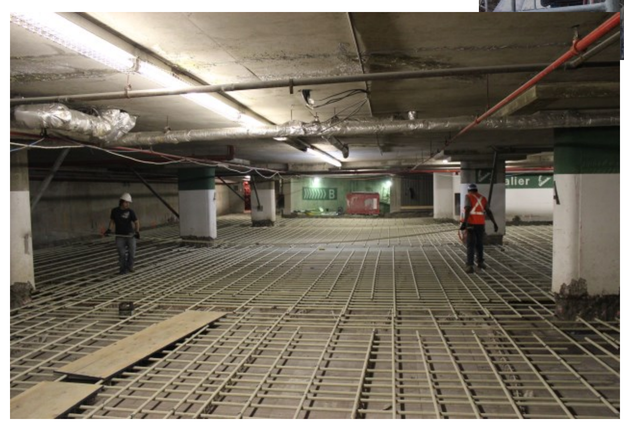

FOURTH INTERNATIONAL WORKSHOP ON FRP BARS FOR CONCRETE STRUCTURES

"Advances in concrete reinforcement"

August 8-9, 2024 - Toronto, Ontario

GFRP Reinforced Concrete Performance in Fire

Mark F. Green

Co-authors: Hamzeh Hajiloo and Bronwyn Chorlton

Queen's University and Carleton University

SPONSORED BY:

PULTRALL V-ROD FIBERGLASS Innovations

ALTAIR

MST BAR MAXIMUM STRENGTH GFRP

SFTec

ACMA AMERICAN COMPOSITES MANUFACTURERS ASSOCIATION FRP Rebar Manufacturers Council

UNIVERSITÉ DE SHERBROOKE

NSERC CRSNG

UNIVERSITY OF MIAMI

Center for Integration of Composites into Infrastructure

FDOT

Outline

- Research steps to identify the fire safety concerns
- Full scale fire resistance tests of GFRP reinforced concrete slabs
- Design approaches to mitigate fire effects on FRP reinforced concrete

Fire resistance of GFRP reinforced concrete

- GFRP reinforcing bars are resistant to corrosion and have high strength-to-weight ratios
- Concerns about GFRP material performance at high temperature
- Extensive research has been conducted to understand the behavior of GFRP-reinforced concrete members under fire conditions
- Design standards (e.g., ACI Code-440.11) have been updated to include guidelines for achieving fire safety

Challenges in Establishing Fire Resistance

- ASTM E119 was developed on the notion that steel reinforced members are designed for full-strength, however, GFRP-reinforced concrete members are designed for service loads
- Deflection limits and crack width criteria generally govern design with GFRP reinforcement
- ASTM E119 requires application of a superimposed load, usually based on strength only

CSA S806-12: Building structures with FRPs

- Provides a semi-empirical approach for determining the fire resistance of FRP reinforced concrete
- Based on minimum concrete cover
- *Annex R – Procedure for the determination of a fire-resistance rating for concrete slabs reinforced with FRP and concrete members strengthened with FRP*
- Reliant on the notion of a critical temperature at which the reinforcing bar loses 50% of its strength – taken as 250 °C (480 °F) for CFRP and 325 °C (620 °F) for GFRP bars

CSA S806-12 – Temperature of reinforcement

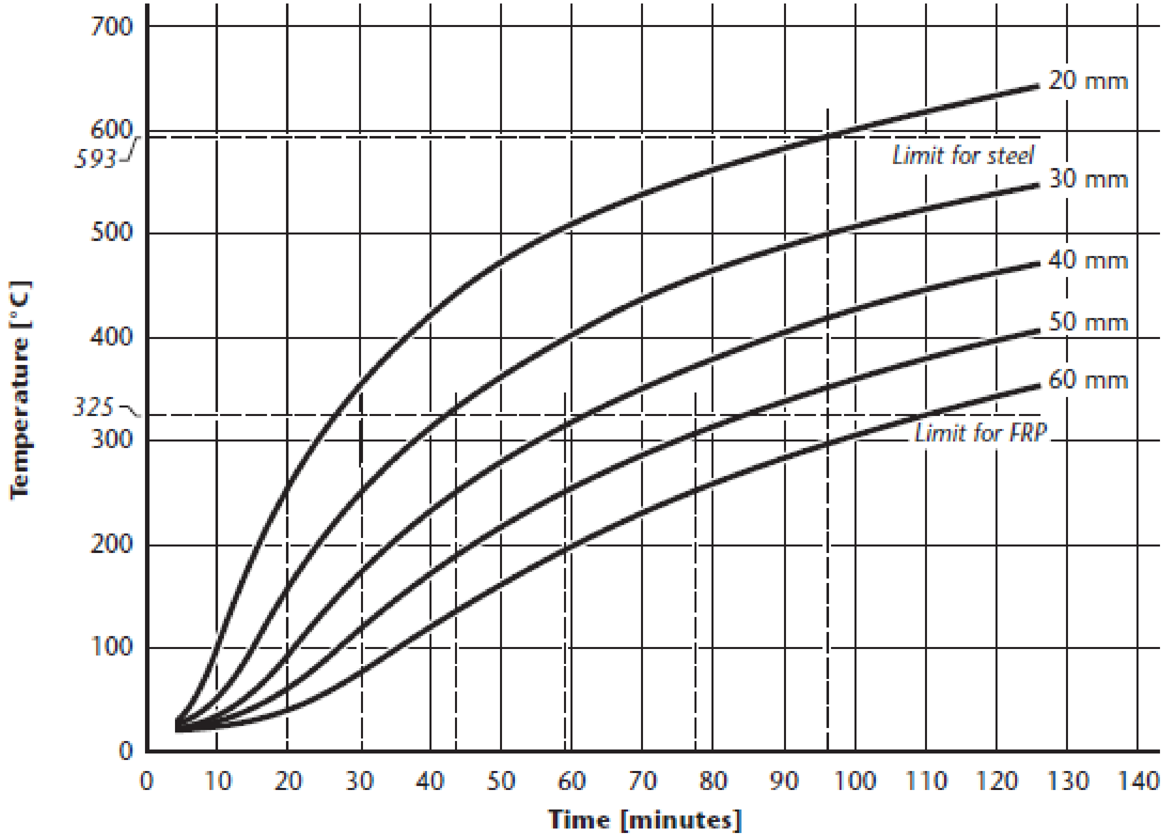

Note: *This figure is based on Kodur and Baingo* (1998).

Figure R.1
Fire resistance of 120 mm concrete slabs
(carbonate aggregate)
(See Clause R.1.)

The conditions at end zones of GFRP concrete slabs
End zone length 200 mm (8 in.) & 40 mm cover (1.5 in.)

- Three hours of fire resistance
- 600 °C (1100 °F) at the bottom of the bars in the exposed zone
- 100 °C at 75 mm (3 in.) and 350 °C at 150 mm (6 in.) from the end of the slab

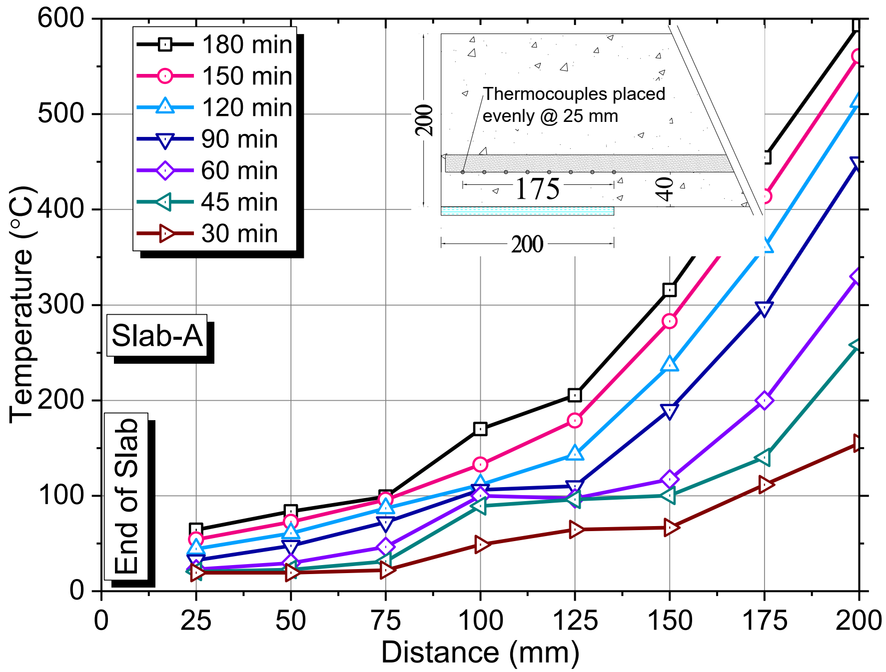

Temperature gradients in the unexposed zones

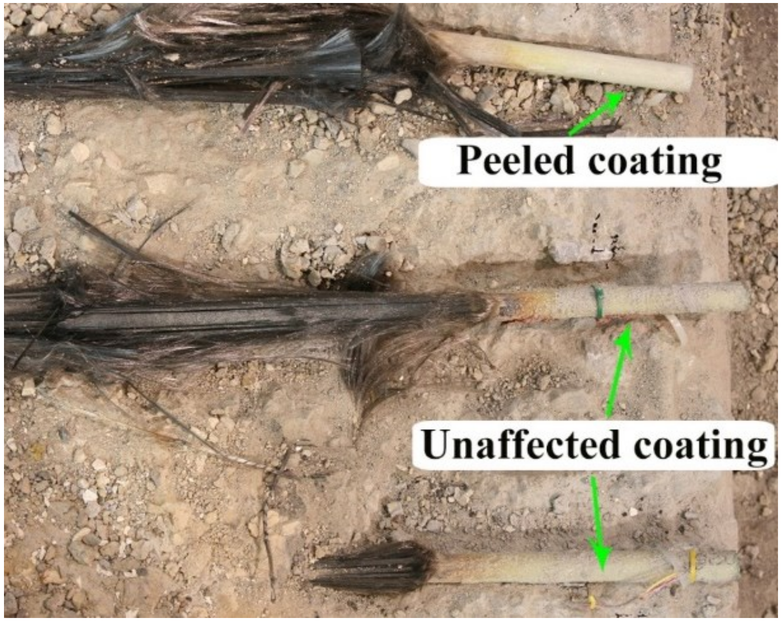

Condition of bars in the exposed and unexposed zones

ACI 440.11-22 guidelines for fire safety

1. Concrete cover
2. Unexposed length of FRP bars (embedment length)
3. FRP reinforcement layout (splices, cut-offs)
4. The tensile stress in FRP bars

Embedment into the support of at least 12 in. or $20d_b$ is conservative.

Table R20.5.1.3.1—Fire resistance rating provided by minimum cover for non-bond-critical GFRP reinforcement

	Fire resistance, h		
Specified cover, in.	Slabs and non-load-bearing walls	Beams	Columns and load-bearing walls
2	1.5	1	0.5
1-1/2	1	0.5	0.5
3/4	0.5	NA	Less than 0.5

Table from ACI 440.11-22

ACI 440.11-22 guidelines for fire safety

If adequate embedment is not possible, additional protection can be provided by using a haunch or drop panel or insulating the concrete.

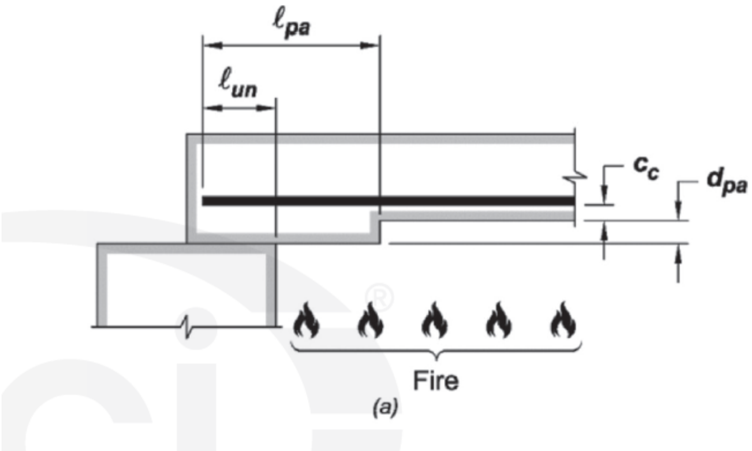

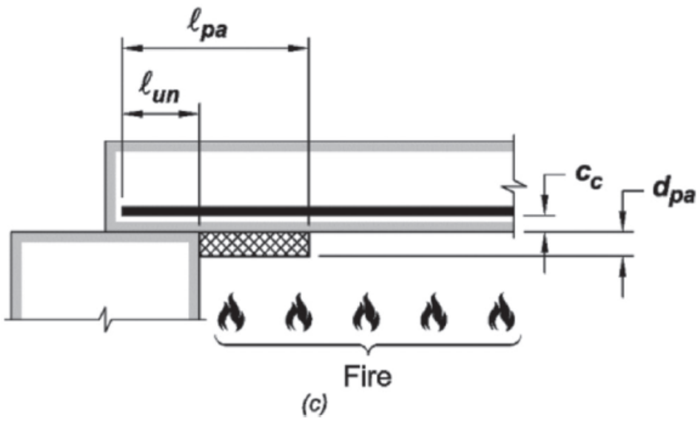

Protection of GFRP reinforcement near supports
(Figures from ACI 440.11-22)

Conclusions

Professional engineers who design GFRP-reinforced concrete must be aware of these guidelines and recommendations to achieve the desired fire ratings.

With proper design practices, GFRP-reinforced concrete members can be safely incorporated into reinforced concrete structures, ensuring both structural integrity and fire safety.

Acknowledgements

- NRC collaborators: Noureddine Benichou, Hossein Mostafaei, Mohamed Sultan
- Brahim Benmokrane, University of Sherbrooke
- Technical staff at NRC, Queen's, and the University of Sherbooke
- Funders: NSERC, MITACS, MTO
- Industry sponsors: Pultrall, BP Composites, MST Bar

Thank you. Questions?

More information:

ACI youtube channel

NEx youtube channel

NSERC CRSNG
MIAMI
FDOT

FOURTH INTERNATIONAL WORKSHOP ON FRP BARS FOR CONCRETE STRUCTURES

"Advances in concrete reinforcement"

August 8-9, 2024 - Toronto, Ontario

Developing Thermoplastic Rebar for Industry Use

Jacob Clark

University of Maine, Advanced Structures and Composites Center

SPONSORED BY:

PULTRALL V·ROD FIBERGLASS Innovations
ALTAIR
MST BAR MAXIMUM STRENGTH GFRP
SFTec
ACMA American Composites Manufacturers Association FRP Rebar Manufacturers Council
UNIVERSITÉ DE SHERBROOKE
NSERC CRSNG
UNIVERSITY OF MIAMI
Center for Integration of Composites into Infrastructure
FDOT

Roberto Lopez-Anido, Ph.D., P.E.
- Faculty Advisor

Bill Davids, Ph.D., P.E.
- Faculty Advisor

Andrew Schanck, Ph.D., P.E.
- Senior Research Engineer

Cody Sheltra, P.E.
- ERDC - Program Manager

James Bryce
- TIDC - Program Manger

STEEL FREE INFRASTRUCTRE

FIBER REINFORCED POLYMER REBAR

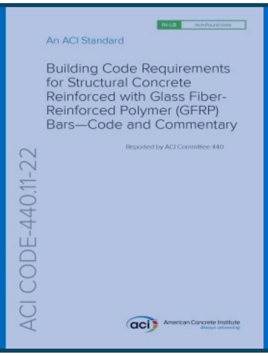

An ACI Standard

Building Code Requirements for Structural Concrete Reinforced with Glass Fiber-Reinforced Polymer (GFRP) Bars—Code and Commentary

Reported by ACI Committee 440

ACI CODE-440.11-22

American Concrete Institute

INDUSTRY ACCEPTANCE

FOURTH INTERNATIONAL WORKSHOP ON FRP BARS FOR CONCRETE STRUCTURES

"Advances in concrete reinforcement"

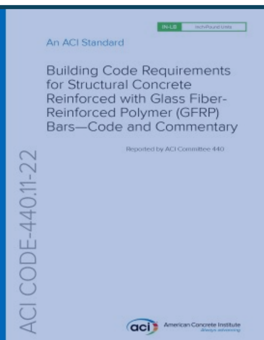
An ACI Standard

Building Code Requirements for Structural Concrete Reinforced with Glass Fiber-Reinforced Polymer (GFRP) Bars—Code and Commentary

Reported by ACI Committee 440

ACI CODE-440.11-22

American Concrete Institute

INDUSTRY ACCEPTANCE

Steel Free Infrastructure

- **FRP-Tube bridge filled with concrete**
- **Benefits:**
  - Steel free bridge solution for spans between 10m – 20m
  - 100-year design life
  - Easy to construct
- **Testing:**
  - Strength
  - Fatigue
  - Environmental
- **AASHTO Code Approval**
- **MaineDOT Confidence**
- **AIT established to license the technology**
- **28 Bridges in service, domestically and internationally**

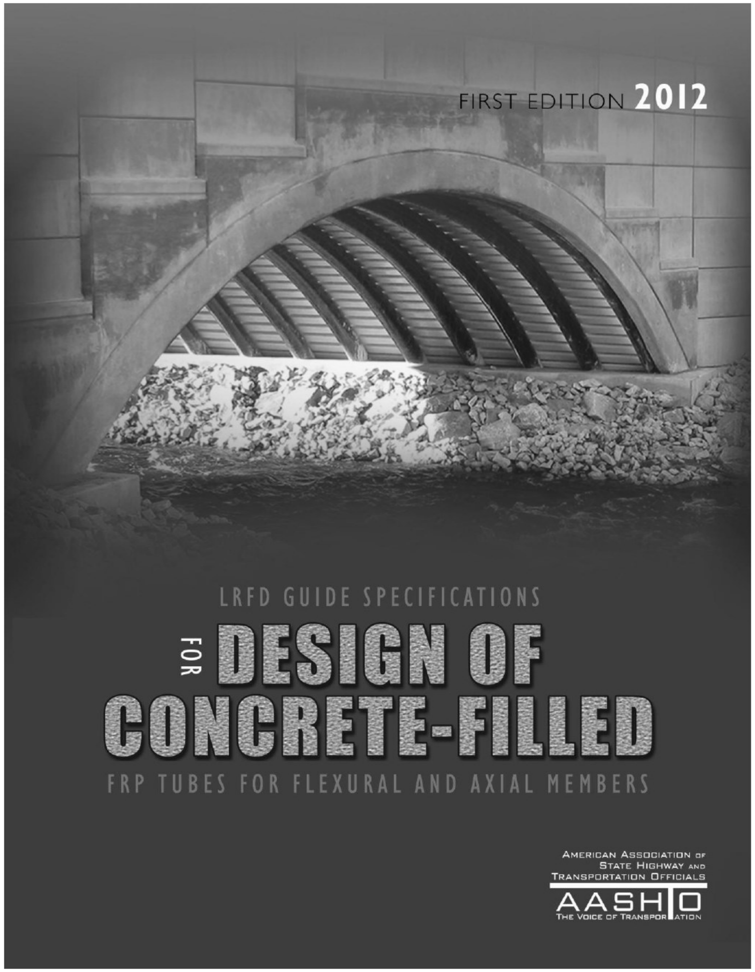

Continuing Development

- **Hybrid fiber composite tub girder**
- **Benefits:**
  - Spans up to 30m
  - 100-year design life
  - Light weight
- **Testing:**
  - Strength
  - Fatigue
  - Creep
- **5-year concept to deployment thanks to DOT confidence and AIT available to license to**
- **4 Bridges in service today, 2 more under contract**
- **Pursuing Codification**

STEEL FREE INFRASTRUCTRE

FIBER REINFORCED POLYMER REBAR

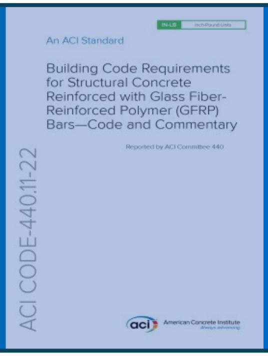

An ACI Standard

Building Code Requirements for Structural Concrete Reinforced with Glass Fiber-Reinforced Polymer (GFRP) Bars—Code and Commentary

Reported by ACI Committee 440

ACI CODE-440.11-22

American Concrete Institute

INDUSTRY ACCEPTANCE

Steel Rebar Alternative

- **FRP Rebar**
  - Highly corrosion resistant
  - High strength
  - Light weight
- **Limitations**
  - Cannot be field bent
  - Limited recycling options
- **Thermoplastic Rebar**
  - Can be reheated and shaped ✓
  - Can be recycled ✓
  - Requires design standard ?
  - Manufacturing challenges ?

https://materialsanalyticalgroup.com/2019/03/22/how-the-ph-of-concrete-is-related-to-corrosion-protection/

The Continuous Forming Machine (CFM)

- The CFM is a novel, non-reactive thermoplastic pultrusion process for prismatic members.

- Can pultrude up to 4m/min.
- Can use any commercially available resin and reinforcement combination
- Feedstock may use UD Tapes, Weaves, Prepreg Textiles, etc.
- Thermoplastic enables co-processing

Current Thermoplastic Rebar Research

- Optimizing CFM parameters
- Bond strength development
- Prototype tension testing
- Prototype beam testing
- Durability testing

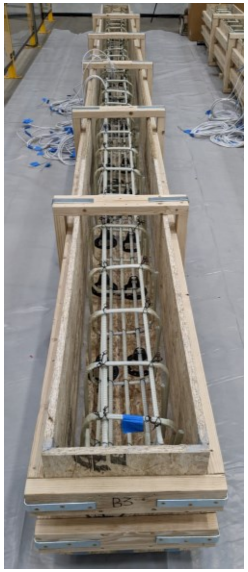

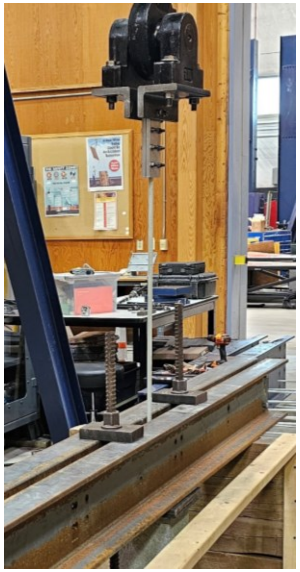

RC-Beam Testing and Modeling

- **Structural scale 6m beam tests with prototype rebar**
- **Predictable Results:**
  - AASHTO Strength Prediction within 3.4%
  - Finite Difference Model Strength Prediction within 4.9%
  - Good Force-Deflection Agreement

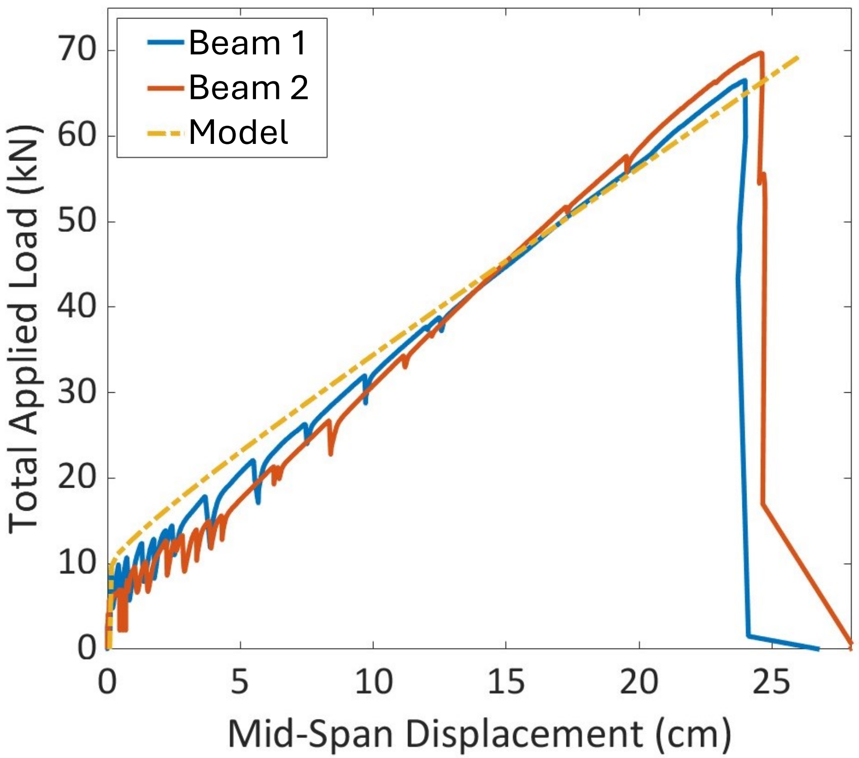

These initial tests demonstrate the feasibility of thermoplastic rebar made on the CFM.

Tension Testing Development

- Conventional FRP rebar testing is challenging.
- Thermoplastic rebar can be reshaped.
- Reshaping thermoplastic bar can enable the use of reusable grips.
- Initial results indicate tension results comparable to conventional methods.

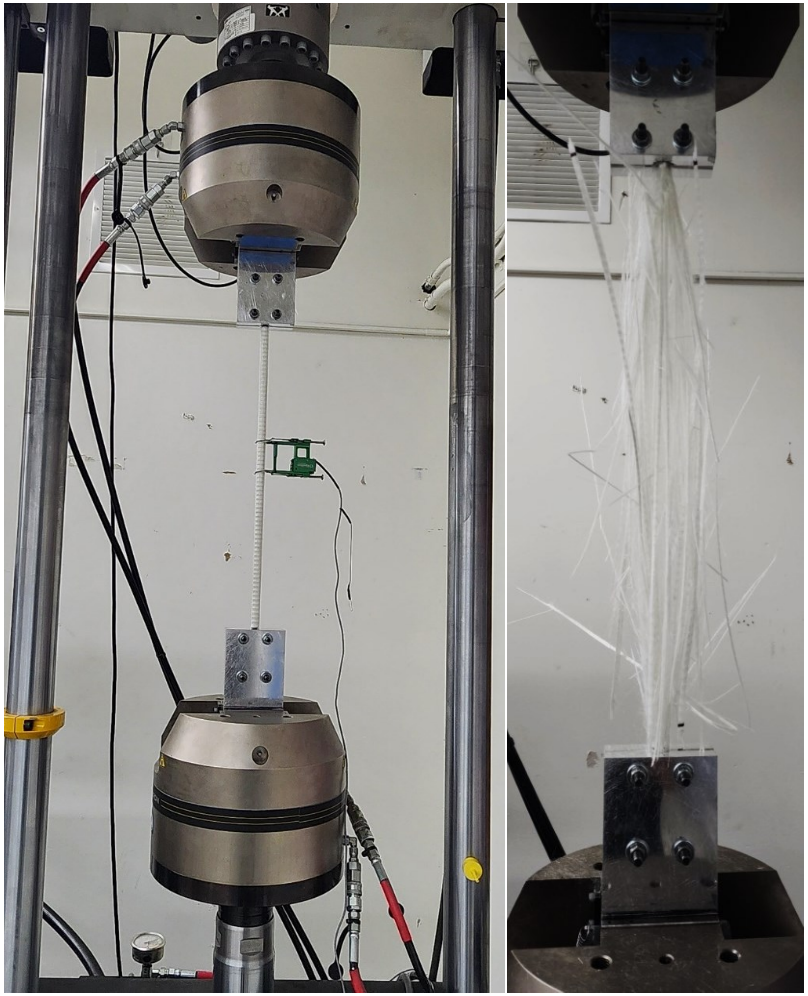

FOURTH INTERNATIONAL WORKSHOP ON FRP BARS FOR CONCRETE STRUCTURES

"Advances in concrete reinforcement"

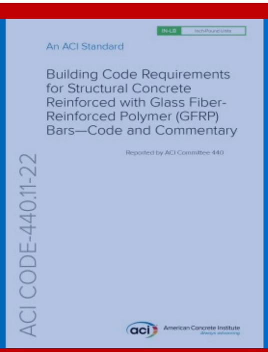
An ACI Standard

Building Code Requirements for Structural Concrete Reinforced with Glass Fiber-Reinforced Polymer (GFRP) Bars—Code and Commentary

Reported by ACI Committee 440

ACI CODE-440.11-22

American Concrete Institute

INDUSTRY ACCEPTANCE

MIAMI

Thermoplastics Research Questions

- **What are the long-term considerations of thermal cycling?**
  - Weather cycles
- **What are the effects of thermoforming?**
  - Field forming
  - Thermoforming surface deformations
- **What are the effects of extreme heat or cold?**
  - Fire resistance
  - Concrete curing

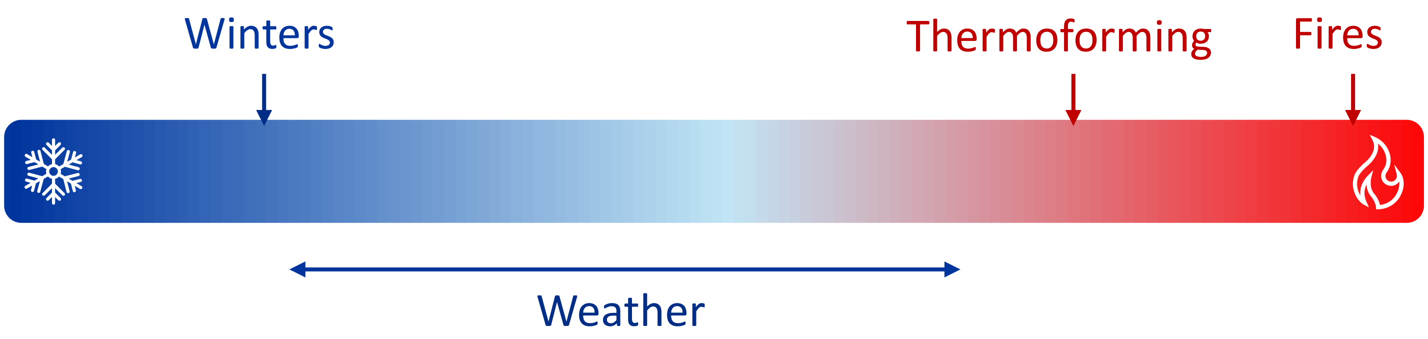

Future Work

- Material durability testing
- Continued development length testing
- Thermal-mechanical testing
- Tensile characterization of finalized bar
- RC testing / demonstration project
- Codification

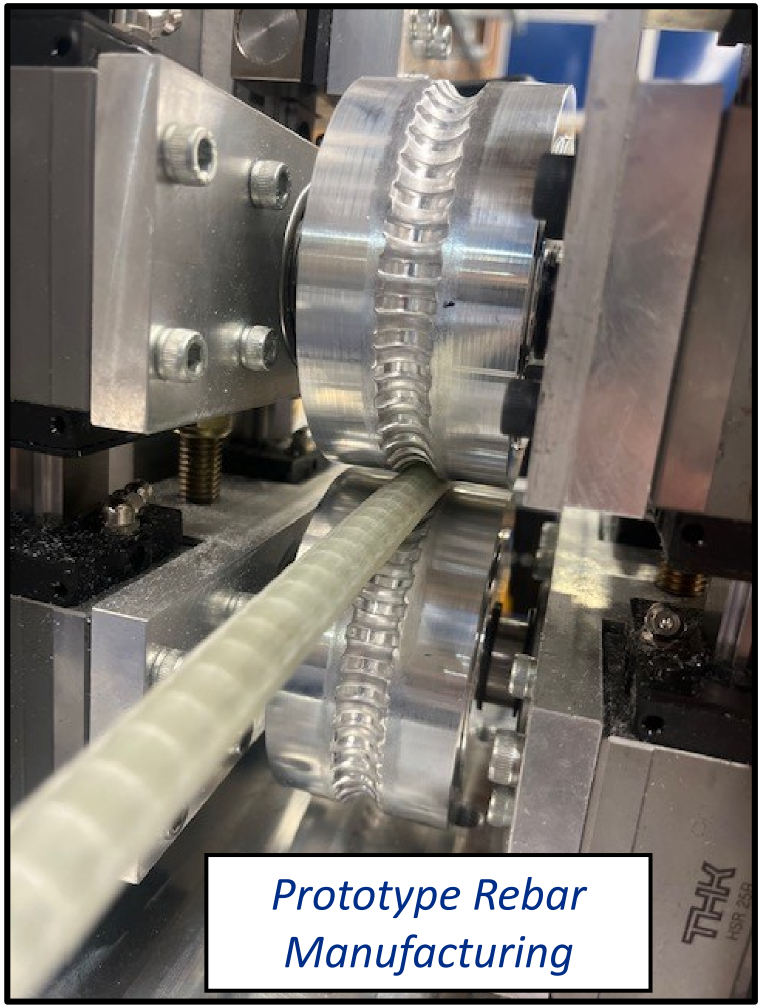

Prototype Rebar Manufacturing

Thank You

For Inquires:	
Rebar:	Jacob Clark Research Engineer jacob.clark@composites.maine.edu
CFM:	Cody Sheltra, P.E. R&D Program Manager cody.sheltra@composites.maine.edu
G-Beam:	Dr. William Davids, P.E. Professor of Civil and Environmental Engineering william.davids@maine.edu

Prototype Rebar Cage

FOURTH INTERNATIONAL WORKSHOP ON FRP BARS FOR CONCRETE STRUCTURES

"Advances in concrete reinforcement"

August 8-9, 2024 - Toronto, Ontario

Segmental Precast Concrete Decks Post-tensioned by GFRP Rods for Maritime Infrastructures

Shahrad Ebrahimzadeh

University of Southern Queensland

SPONSORED BY:

PULTRALL V-ROD FIBERGLASS innovations

ALTAIR

MST BAR MAXIMUM STRENGTH GFRP

SFTec

ACMA American Composites Manufacturers Association FRP Rebar Manufacturers Council

UNIVERSITÉ DE SHERBROOKE

NSERC CRSNG

UNIVERSITY OF MIAMI

Center for Integration of Composites into Infrastructure

FDOT

Crack on Concrete Surface accelerating the corrosion

Galvanic Corrosion in decks using in maritime infrastructures

Major need to assure the steel is replaced entirely with GFRP rebar in concrete members using in marine infrastructures

Testing on Concrete Pontoon Decks (Monolithic)

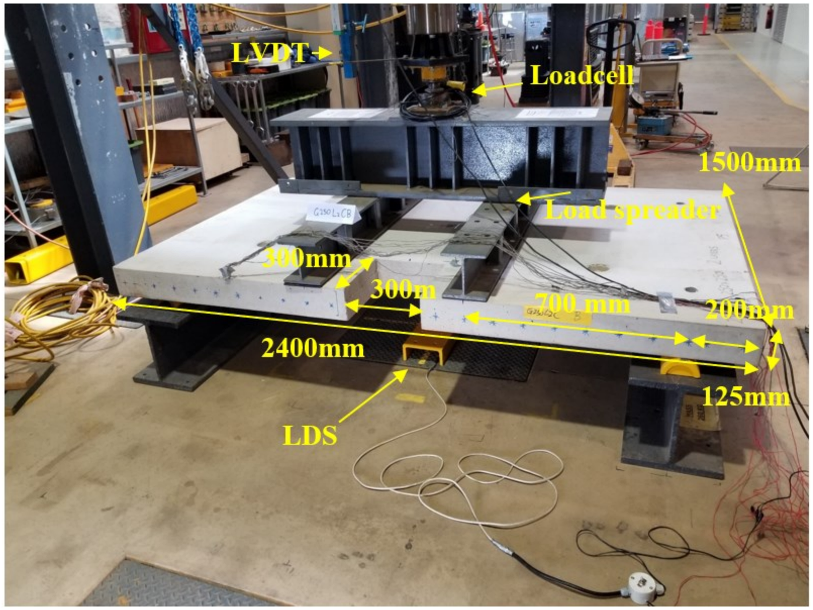

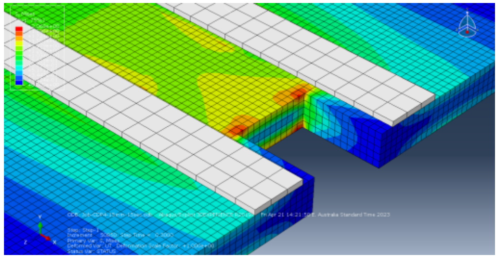

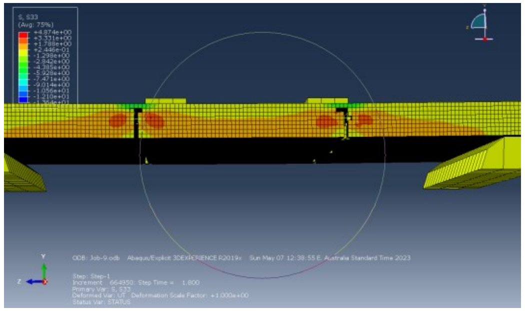

Cutout is needed to accommodate the pile

1- What is the effect of cutout?

2- What is the effect of the span-to-depth ratio with cutout?

3- What is the effect of the different loading scenarios on the slab with cutout?

4- What is the effect of the effective depth in a slab with cutout?

Structures 59 (2024) 105796

Contents lists available at ScienceDirect

Structures

journal homepage: www.elsevier.com/locate/structures

Flexural behaviour of GFRP-reinforced concrete pontoon decks under static four-point and uniform loads

Shahrad Ebrahimzadeh [a], Xian Yang [a], Allan Manalo [a], Omar Alajarmeh [a,*], Zaneta Senselova [a], Charles Dean Sorbello [b], Senarath Weerakoon [b], Brahim Benmokrane [c]

[a] Centre for Future Materials (CFM), School of Engineering, University of Southern Queensland, Toowoomba 4350, Australia
[b] Maritime Safety Queensland, Department of Transport and Main Roads, Brisbane, Qld 4000, Australia
[c] University of Sherbrooke, Sherbrooke, Quebec J1K 2R1, Canada

ARTICLE INFO

Keywords:
Cutout
Flexural behaviour
Four-point bending
GFRP bars
Reinforced concrete decks
Uniform distributed loading

ABSTRACT

Concrete pontoon decks are subject to flexural loading actions under concentrated and uniform loads caused by self-weight, live loads, and wave actions. This study investigated the structural behaviour of concrete pontoon decks reinforced with glass fiber-reinforced polymer (GFRP) bars under static four-point and uniform loading conditions. Five large-scale GFRP-reinforced concrete decks with a length of 2400 mm, width of 1500 mm, and thickness of 125 mm were tested to evaluate their moment capacity, strain behaviour, cracking propagation, and failure mechanism. The effects of the loading configurations, reinforcement arrangement, and cutout simulating the piles' location were evaluated. The edge cut-out initiated flexural-shear cracks, causing the pontoon decks to fail at an effective bending stress 10% lower than the solid decks. Decreasing the span-to-depth ratio from 5.6 to 4.0 increased the induced shear stress of a section and caused the deck to fail by shear compression. Uniform loading resulted in an even load distribution and minimized the stress concentration around the cutout. An increase in the effective depth improved all deck flexural characteristics. The equations in ACI 4401. R-15 and CSA S806–12 provided an accurate prediction for solid decks but overestimated the ultimate flexural strength of the GFRP-reinforced concrete decks with a cutout.

Nomenclature

a	Shear span
b	Width of rectangular cross-section
c	Distance from the extreme compression fiber to the neutral axis
d	Distance from the extreme compression fiber to the centroid of the tension reinforcement
d_v	Effective shear depth
E_c	Modulus of elasticity of concrete
E_f	Modulus of elasticity of FRP
E_{fv}	Modulus of elasticity of the FRP shear reinforcement
f'_c	Specified compressive strength
f_f	Stress in the FRP reinforcement under a specified load
f_{fu}	Design tensile strength of FRP, considering reductions for service environment
f_r	Modulus of rupture of concrete
I_g	Gross moment of inertia
k	Neutral-axis factor
K_{el}	Initial stiffness
V_c	Shear strength resistance provided by the concrete
y_t	Distance from the centroidal axis of the cross-section to the extreme fiber in tension
α_1	The ratio of the average stress of the equivalent rectangular stress block to f'_c
β_1	Factor taken as 0.85 for concrete strength up to 28 MPa. Above that, the factor was reduced at a rate of 0.05 for every 7 MPa to a minimum of 0.65
ε_{cu}	Ultimate strain in the concrete
λ	Factor to account for concrete density
ϕ_c	Resistance factor of the concrete
ρ_f	Reinforcement ratio

* Corresponding author.
E-mail address: omar.alajarmeh@usq.edu.au (O. Alajarmeh).

https://doi.org/10.1016/j.istruc.2023.105796
Received 20 August 2023; Received in revised form 30 November 2023; Accepted 19 December 2023
Available online 28 December 2023

Needs for initiatives

1- Financial aspect of 2022 Queensland – New South Wales flood : 7.7 Billion AUD (Queensland Reconstruction Authority-2022)

2- Localized damage observed in marine infrastructures

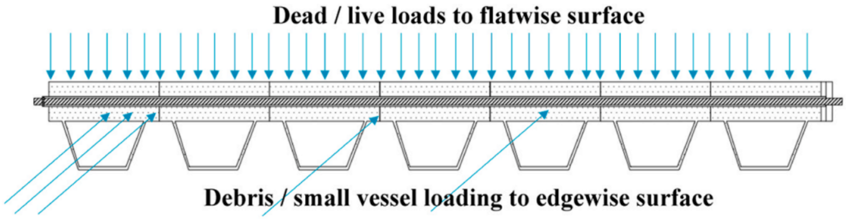

Different loading conditions

The segmental pontoon deck will be exposed to different loading configurations

Dead/live load - flatwise

Raging water- edgewise

1- load carrying capacity ?
2- Strain behaviour? (concrete / rod)
3- GFRP rod's axial load?
4- Joint opening behaviour?
5- Failure mechanism?
6- Prediction equation?
7- Numerical modelling?

Load directly on the joint

Result – Flexural loading (Flatwise - Edgewise)

Structures 65 (2024) 106712

Contents lists available at ScienceDirect

Structures

journal homepage: www.elsevier.com/locate/structures

Flexural behaviour of the segmental precast concrete decks post-tensioned by GFRP rods

Shahrad Ebrahimzadeh [a], Allan Manalo [a,*], Omar Alajarmeh [a], Xian Yang [a], Charles Dean Sorbello [b], Senarath Weerakoon [b], Reza Hassanli [c], Brahim Benmokrane [d]

[a] Centre for Future Materials (CFM), School of Civil Engineering and Surveying, University of Southern Queensland, Toowoomba 4350, Australia
[b] Maritime Safety Queensland, Department of Transport and Main Roads, Brisbane, QLD 4000, Australia
[c] UniSA STEM, University of South Australia, Mawson Lakes, SA 5095, Australia
[d] University of Sherbrooke, Department of Civil & Building Engineering, Sherbrooke, Quebec J1K 2R1, Canada

A R T I C L E I N F O

Keywords:
Segmental deck
Precast concrete
GFRP rebar
Flexural behaviour
Post-tensioned GFRP rod
Numerical analysis

A B S T R A C T

This paper introduces an innovative post-tensioned segmental concrete deck system internally reinforced and tied with GFRP reinforcements for application in pontoon decks and other deck structures in aggressive marine environments. Utilisation of the GFRP reinforcements in floating concrete structures is essential because of their non-corrosive characteristics. Six large-scale segmental decks following the specifications of Queensland maritime infrastructure were designed, manufactured, and tested to assess the reliability of the new construction system under static flexural loading in the flatwise and edgewise orientations. One segmental deck served as a reference with hand-tight post-tensioning, while the remaining specimens were connected by the GFRP rods with varying levels of post-tensioning. All decks were tested up to failure, allowing for an investigation of their flexural strength, load-strain behaviour, joint opening, and failure mechanism. The results showed that post-tensioning the GFRP rods improves the flexural performance of the segmental decks. The higher the level of post-tensioning, the higher the contact area between the segments at the joint is achieved. A numerical model was developed to understand the detailed mechanism of both flatwise and edgewise specimens. A strain reduction coefficient in the segmental concrete deck under flexure is introduced accounting for the joint presence to reliably calculate the stress in the post-tensioned internal GFRP rod when the concrete in the joint crushes. The system investigated can increase maritime and recreational infrastructure's construction efficiency and provide creative solutions in the GFRP-reinforced concrete structures in the building and construction industry.

1. Introduction

Steel corrosion in reinforced concrete structures presents a significant economic challenge costing around 4 % of a developed nation's gross domestic product [1]. In Australia, out-of-service, maintenance, and replacement activities for steel-corroded infrastructure cost the economy over AU$13 billion annually [2]. The Maritime Safety Queensland division of the Queensland Department of Transport and Main Roads in Australia allocates a minimum of AU$ 10 million annually to keep boating and maritime facilities [3]. Similarly, the Victorian and Australian governments have jointly committed AU$ 50 million to support the maintenance of the infrastructures on Great Ocean Road, a vital tourist route in Victoria that spans 240 kilometres and connects several key towns and coastal villages [4]. There is, therefore, a significant benefit in using non-corrosive and high-strength reinforcements such as glass fibre-reinforced polymer (GFRP) composite bars to achieve a cost-effective and low-maintenance concrete infrastructure especially those built near coastal and other harsh environmental conditions.

The use of GFRP bars as internal reinforcement, as opposed to traditional steel bars, has been successfully demonstrated in the construction and design of various concrete structures. Examples include pontoon decks [5,6], boating ramp planks and approach slabs [3,7], bridge barriers [8], concrete bridges [9], bridge foundations [10], marine docks [11], piles [12–14], seawalls [15], and concrete slabs [16]. Despite these advancements, many structures in coastal areas and aggressive environments worldwide have not yet benefited fully from the distinct advantages of GFRP bars/rods such as the high strength-to-weight ratio, non-corrosiveness and the ability to be

* Corresponding author.
E-mail address: omar.alajarmeh@unisq.edu.au (O. Alajarmeh).

https://doi.org/10.1016/j.istruc.2024.106712
Received 22 March 2024; Received in revised form 19 May 2024; Accepted 5 June 2024
Available online 12 June 2024

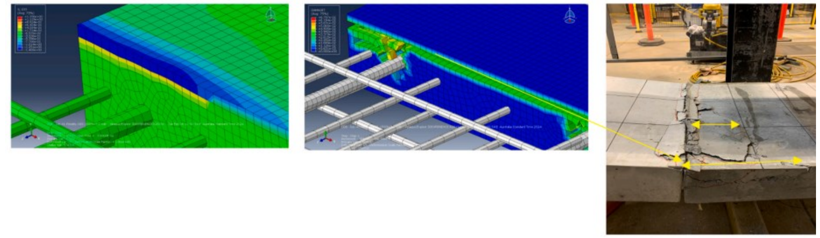

(a) F0 (S_{33} @ 1.1 kN & 3.25 mm) (b) F0 (DAMAGE @11.2 kN) (c) Ultimate failure F0

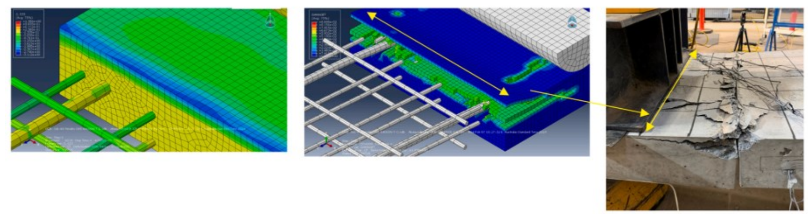

(d) F64 (S_{33} @1.2 kN & 0.4 mm) (e) F64 (DAMAGE @11.6 kN) (f) Ultimate failure-F64

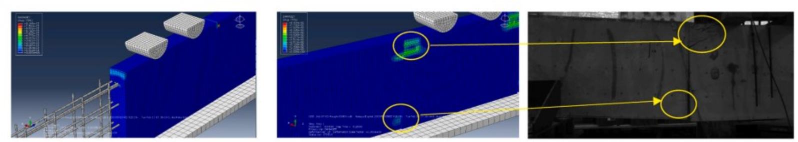

(a) E0-DAMAGE (@ joint opening) (b) E0-DAMAGE (@ 40-mm) (c) E0-Failure (@ 40-mm)

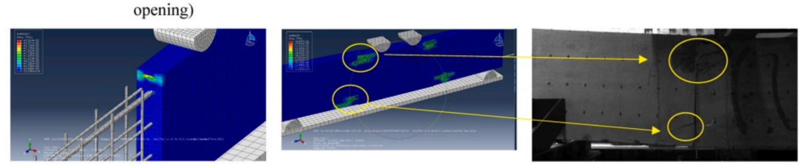

(d) E45-DAMAGE (@ joint opening) (e) E45-DAMAGE (@ 40-mm) (f) E45-Failure (@ 40-mm)

Immediate application in industry- boatramp

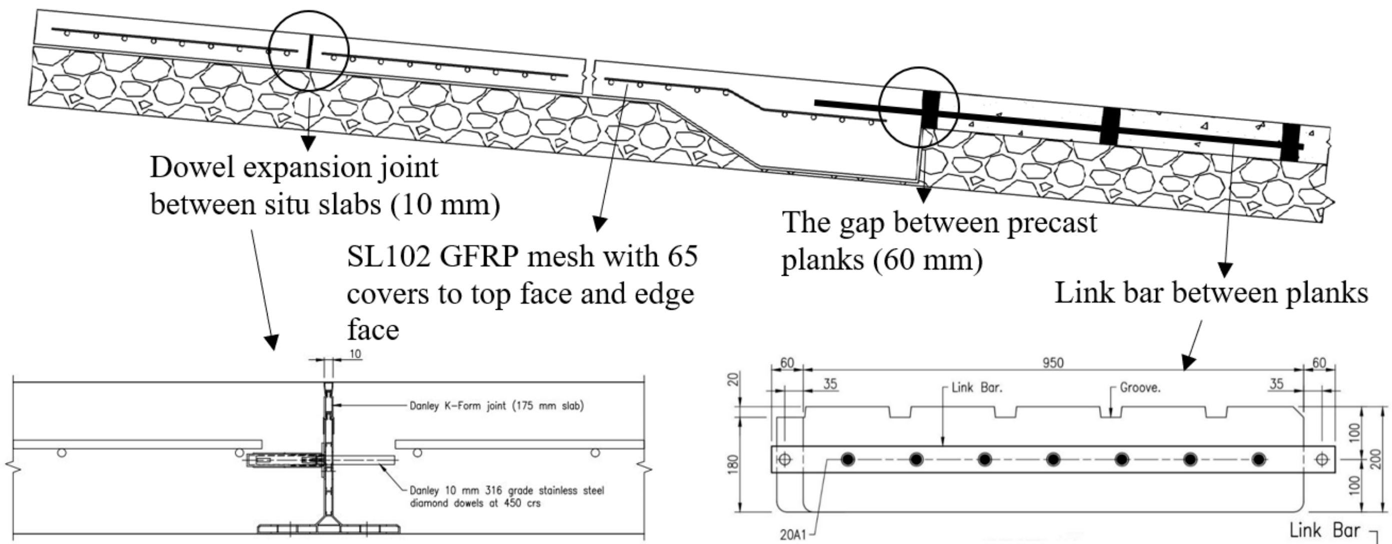

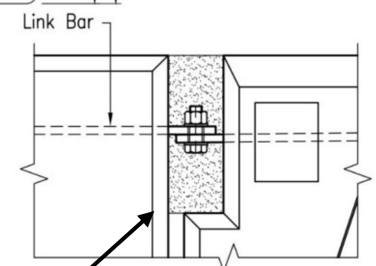

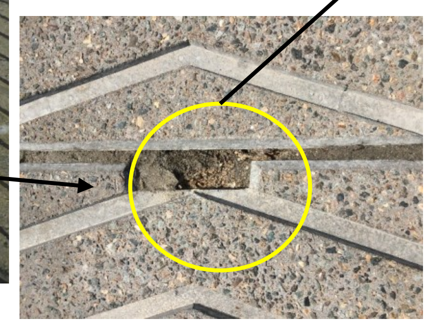

NSERC CRSNG
MIAMI
FDOT

New design for boat ramps


Image courtesy of Senarath Weerakoon and Charles Dean Sorbello (Maritime Safety Queensland)

Opportunities and need for further investigations

1- Precast segmental concrete provides faster construction speed, less environmental disturbance, repair capacity, easier transportation , and higher quality compared to in-situ

2- Using GFRP rod provides non-corrosiveness and applying the pre-tension load on rod enhance the stiffness and overall behaviour

3- Different loading types investigated

4- All decks systems in maritime structures and bridge constructions can potentially benefit the system

5- To promote the segmental precast concrete system for more industrial applications, more investigation is needed to understand different aspects of the precast concrete members with a pre-tensioned GFRP rod